이학박사 학위논문

애기장대 면역의 전사 및 후성유전학적 조절에 관한 연구

A study on the transcriptional and epigenetic regulation of immunity in *Arabidopsis*

2023년 2월

서울대학교 대학원

생명과학부

윤 세 훈

애기장대 면역의 전사 및 후성유전학적 조절에 관한 연구

A study on the transcriptional and epigenetic regulation of immunity in *Arabidopsis*

지도 교수 노 유 선

이 논문을 이학박사 학위논문으로 제출함

2023년 2월

서울대학교 대학원

생명과학부

윤 세 훈

윤세훈의 이학박사 학위논문을 인준함

2023년 1월

위 원 장 최 연 희 (인)

부위원장 노 유 선 (인)

위 원 이 일 하 (인)

위 원 전 종 성 (인)

위 원 이 유 리 (인)

A study on the transcriptional and epigenetic regulation of immunity in *Arabidopsis*

A dissertation submitted in partial fulfillment of the requirement for the degree of
DOCTOR OF PHILOSOPHY
to the Faculty of School of Biological Sciences
at
Seoul National University
by
Se-Hun Yun
Date approved: January, 2023

Yeonhee Choi _____ **(Chair)**

Yoo-Sun Noh _____ **(Supervisor)**

Ilha Lee _____

Jong-Seong Jeon _____

Yuree Lee _____

Abstract

A study on the transcriptional and epigenetic regulation of immunity in *Arabidopsis*

Se-Hun Yun

Department of Biological Sciences

The Graduate School

Seoul National University

Plants are continuously exposed to pathogen challenges during their lifetime due to being sessile. To defend themselves from various phytophathogens, plants have developed sophisticated innate and induced immunities. Recognition of invading pathogens by membrane-localized or intracellular receptors triggers a local immunity. Besides triggering local immunity, plants also establish a systemic immunity in the whole plant body to confer broad spectrum and long-lasting resistance to secondary infections. Salicylic acid (SA) is a phytohormone that regulates both local and systemic immunities. SA induces genome-wide transcriptional reprogrammings to trigger immunity against biotrophic and

hemibiotrophic pathogens within local tissues that are infected with pathogens. An increase in SA level in distal tissues which are not exposed to pathogen infection is involved in the establishment of systemic acquired resistance (SAR). Once SAR is established, plants are prepared to induce more rapid and robust immune responses upon secondary infection, a phenomenon called defense priming. In the processes of SA-induced transcriptional reprogramming and defense priming at the transcriptional level, epigenetic mechanisms that modulate chromatin structure and the accessibility of transcription factors to *cis*-elements are engaged. Growing evidence has indicated the importance of epigenetic regulation in plant immunity.

In this study, I address two topics on the transcriptional and epigenetic regulation of immunity in Arabidopsis. In the first part, I provide negative evidence on the transgenerational inheritance of defense priming. Previously, it was observed that defense priming in parental plants can be inherited into descendants. With the initial aim to elucidate the underlying epigenetic mechanism, I reassessed transgenerational inheritance of defense priming in a much stricter view. To clarify truly transgenerational defense priming, parental plants were repetitively infected with bacterial pathogens during either vegetative or reproductive stages. Irrespective of the existence of gametes in parental plants during the period of infection, the descendants did not show enhanced resistance to the bacterial pathogen. The same result was obtained when different methods for pathogen infection were used to vary the degree of pathogen stress. These results were contrary to the previous observations on the transgenerational inheritance of defense priming in Arabidopsis. Therefore, transgenerational defense priming in plants should be thoroughly reevaluated.

In the second part, I report genomic overview on the role of NONEXPRESSER OF PATHOGENESIS-RELATED GENES1 (NPR1) in SA-triggered immunity. The SA-triggered immunity is developed through transcriptional reprogramming. As NPR1 acts as both an SA receptor and a transcriptional co-activator, SA-induced transcriptional reprogramming is predominantly regulated by NPR1, the master regulator of SA-triggered immunity. Here, I identified genome-wide direct NPR1 targets specific to SA signal and investigated the biological and molecular functions involving NPR1 targets showing *NPR1*-dependent regulation. SA-dependent NPR1 targeting primarily induced the transcriptional activation of genes encoding various transcription factors, triggering transcriptional cascades required for SA-induced transcriptional reprogramming. Furthermore, I investigated the cooperative roles of NPR1 and its binding partners, HISTONE ACETYLTRANSFERASE OF THE CBP FAMILY1 (HAC1) and TGACG-motif binding transcription factors (TGAs), at the genome-wide level. I identified genome-wide HAC1 targets and hundreds of genes that are co-targeted by NPR1 and HAC1 in the presence of SA. NPR1 and HAC1 regulated SA-induced histone H3 acetylation and expression of a subset of the co-targets. In genomic regions targeted by NPR1, the TGACG motif was the most abundant DNA sequence and I demonstrated that TGA2 indeed binds to NPR1 targeting regions containing the TGACG motif, indicating NPR1 targeting at the genomic level is principally mediated by TGAs. Finally, I found that genes pre-targeted by NPR1 in the basal state are more rapidly and robustly induced upon SA signal compared to genes targeted by NPR1 only in the presence of SA. Thus, my study reveals a holistic view of the role of NPR1 and the cooperativity of NPR1, HAC1, and TGAs in SA-induced transcriptional reprogramming.

Keywords : Defense priming, Transgenerational epigenetic inheritance, SA-induced transcriptional reprogramming, NPR1, HAC1, TGAs

Student Number : 2013-20307

Table of Contents

List of Figures

Chapter I. General Introduction

Chapter II. Negative evidence on the transgenerational inheritance of defense priming in *Arabidopsis thaliana*

Chapter III. Genomic overview of salicylic acid-induced NPR1 targeting and transcriptional cascades in Arabidopsis

List of Tables

Chapter II. Negative evidence on the transgenerational inheritance of defense priming in *Arabidopsis thaliana*

Chapter III. Genomic overview of salicylic acid-induced NPR1 targeting and transcriptional cascades in Arabidopsis

Abbreviations

ChIP	Chromatin immunoprecipitation
ChIP-seq	ChIP-sequencing
CRC	Chromatin remodeling complex
ET	Ethylene
ETI	Effector-triggered immunity
HAC1	HISTONE ACETYLTRANSFERASE OF THE CBP FAMILY1
HR	Hypersensitive response
INA	2,6-dichloroisonicotinic acid
ISR	Induced systemic resistance
JA	Jasmonic acid
LncRNA	long-noncoding RNA
NLR	Nucleotide-binding domain, leucine-rich-repeat receptor
NPR1	NONEXPRESSER OF PATHOGENESIS-RELATED GENES1
PAMP	Pathogen associated molecular pattern
PR	*PATHOGENESIS-RELATED*
PRR	PAMP recognition receptor
Pst DC3000	*Pseudomonas syringae* pv *tomato* DC3000
PTI	PAMP-triggered immunity
ROS	Reactive oxygen species
SA	Salicylic acid
SAR	Systemic acquired resistance
TGAs	TGACG-motif binding proteins

Chapter I

General Introduction

1. Introduction

Plants are potential hosts for a wide range of pathogens and continuously confront diverse pathogen challenges during their lifetime. Unlike vertebrates, plants lack specialized cells and circulatory systems developed for immunity; however, plants do have a capacity to trigger innate immune responses. Phytopathogens have developed various strategies to enhance their invasion, survival, and proliferation within host plants, to which plants have responded by developing sophisticated immune strategies.

The innate immunity of plants relies on large numbers of receptors for the surveillance of pathogen attacks. Plant cells recognize pathogen invasions using cell-surface receptors that detect the conserved molecular structures present in pathogens, and intracellular receptors that sense specific molecules secreted by pathogens. Signals initiated from pathogen recognition are conveyed to hormone-mediated signaling pathways, which induce massive transcriptional reprogramming to turn on the expression of defense-related genes and repress growth-promoting genes. In addition to eliciting local immunity, plant cells exposed to pathogen challenges generate mobile signals that trigger a systemic immunity to enable the whole plant body to be prepared for subsequent pathogen challenges. Through this local and systemic immune signaling, plants convert their cells into an immune-equipped state, and thus operate a plastic rather than a permanently specified immune system.

2. Local immunity

In plants, local immunity is composed of a two-tiered innate immune response: pathogen associated molecular pattern (PAMP)-triggered immunity (PTI) and effector-triggered immunity (ETI) (Figure 1). PAMPs, such as flagellin, the bacterial elongation factor Tu, and chitin, are small molecular motifs that are conserved among a class of pathogens. PTI is induced when cell membrane–localized PAMP recognition receptors (PRRs) detect PAMPs. To suppress PTI and enhance their virulence, pathogens secrete effector molecules into host cells via the type III secretion system. ETI is induced when pathogen effectors are recognized by host intracellular receptors called disease resistance (R) proteins, which directly bind with the effectors or detect changes in host proteins induced by pathogen effectors.

Although PTI and ETI are differently triggered, these two immune responses eventually elicit various immune responses that are similar to each other, including calcium influx, reactive oxygen species (ROS) burst, callose deposition, stomatal closure, the production of antimicrobial secondary metabolites, the activation of mitogen-activated protein kinase (MAPK) cascades, and transcriptional reprogramming. The existence of an intricate crosstalk between PTI and ETI was recently described (Ngou et al., 2021; Pruitt et al., 2021; Yuan et al., 2021), which likely enables the two immune response pathways to coordinate and share various downstream events. Nonetheless, ETI is known to be activated more quickly and result in more robust immune responses than PTI. Furthermore, during ETI but not PTI, a programmed cell death called the hypersensitive response (HR)

is developed to restrict the growth and spread of pathogens (Figure 1).

2.1. Pathogen associated molecular pattern (PAMP)-triggered immunity (PTI)

PTI relies on PRRs that are localized in the plasma membrane. PRRs interact with co-receptors in a PAMP-induced manner to activate downstream signaling pathways (Figure 1); for example, FLAGELLIN-SENSITIVE2 (FLS2) and EF-TU RECEPTOR (EFR), which are receptors for bacterial flg22 and EF-Tu, respectively, interact with the co-receptor BRI1-ASSOCIATED KINASE1 (BAK1) (Chinchilla et al., 2007). The PAMP-induced interaction between BAK1 and FLS2 or EFR is facilitated by FERONIA (FER) acting as a scaffold protein (Stegmann et al., 2017). In its basal state, BAK1 is sequestered from FLS2 or EFR by directly binding with BAK1-INTERACTING RECEPTOR-LIKE KINASE2 (BIR2) and BIR3 (Halter et al., 2014; Imkampe et al., 2017).

Similar to FLS2 and EFR, LYSM-CONTAINING RECEPTOR-LIKE KINASE5 (LYK5), a well-known chitin receptor, requires the co-receptor CHITIN ELICITOR RECEPTOR KINASE1 (CERK1) to trigger antifungal immunity (Cao et al., 2014). Interestingly, bacterial elicitors also induce BAK1-mediated CERK1 phosphorylation, which results in enhanced antifungal immunity (Gong et al., 2019). This example suggests that bacterial pathogen–induced PRR complexes might prime the PRR complexes to function in antifungal immunity.

Signals initiated from PAMP-induced PRR complexes are conveyed to receptor-like cytoplasmic kinases (RLCKs), including BOTRYTIS-INDUCED KINASE1 (BIK1), through auto- and trans-phosphorylation events. After its

phosphorylation by BAK1, BIK1 directly phosphorylates the NADPH oxidase RESPIRATORY BURST OXIDASE HOMOLOGUE D (RbohD) to trigger a ROS burst (Li et al., 2014). Moreover, the BIK1-mediated phosphorylation of CYCLIC NUCLEOTIDE GATED CHANNEL4 (CNGC4) activates a heteromeric calcium channel composed of CNGC2 and CNGC4, resulting in a calcium influx into cytosol (Tian et al., 2019). In addition, PAMP-induced PRR complexes activate multiple downstream signaling pathways, including calcium-dependent kinases (CDKs) and MAPKs (Figure 1).

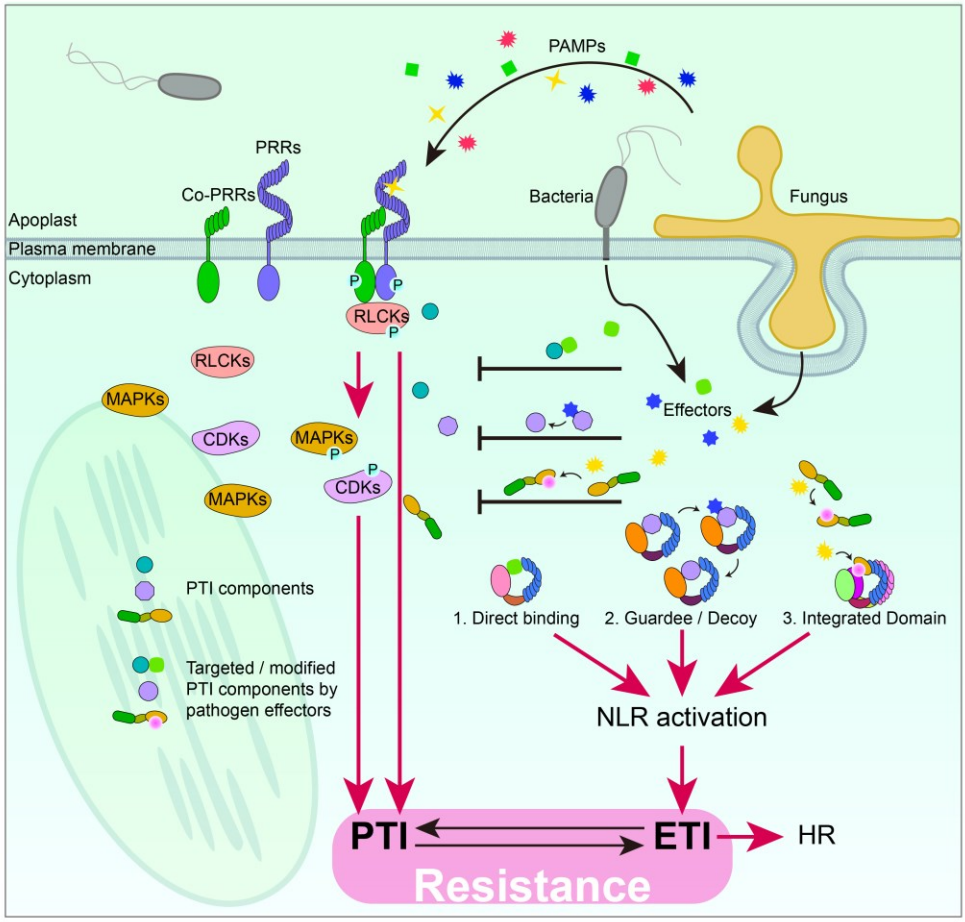
PAMPs
PRRs
Co-PRRs
Apoplast
Plasma membrane
Cytoplasm
Bacteria
Fungus
P
P
RLCKs
P
RLCKs
MAPKs
CDKs
MAPKs
P
P
CDKs
MAPKs
Effectors
PTI components
Targeted / modified
PTI components by
pathogen effectors
1. Direct binding
2. Guardee / Decoy
3. Integrated Domain
NLR activation
PTI
ETI
HR
Resistance

Figure 1. Schematic of pathogen associated molecular pattern (PAMP)-triggered immunity (PTI) and effector-triggered immunity (ETI) in Arabidopsis.

In PTI, PAMPs derived from invading pathogens are perceived by PAMP recognition receptors (PRRs) in the plasma membrane, which also leads to the interaction between PRRs and co-PRRs. Activated PRR complexes transmit signals through phosphorylation relays: receptor-like cytoplasmic kinases (RLCKs) are thought to relay PRR-derived signals to multiple downstream signaling pathways, including those involving mitogen-activated protein kinase (MAPK) cascades and calcium-dependent kinases (CDKs) are involved. To suppress PTI, phytopathogens secret effector molecules into host cells. Pathogen effectors bind to host proteins and can induce conformational changes or post-translational modifications; however, host nucleotide-binding domain leucine-rich-repeat receptors (NLRs) can specifically recognize pathogen effectors either directly or indirectly and disable their activity. In indirect perception mechanisms, NLRs interact with guardees or decoys to monitor the changes in their conformations or modifications caused by effectors. In some cases, NLRs contain integrated domains, which are subject to modulation by effectors. NLRs become activated when they sense the presence of effectors, triggering ETI. A programmed cell death called the hypersensitive response (HR) occurs only during ETI; however, PTI and ETI do exhibit substantial similarities in various immune responses. Intricate crosstalk between PTI and ETI is likely responsible for these similarities, and could enhance disease resistance.

2.2. Effector-triggered immunity (ETI)

ETI relies on intracellular receptors known as R proteins, most of which belong to a subfamily of nucleotide-binding domain leucine-rich-repeat receptors (NLRs) (Figure 1). Plant NLRs contain either Toll/interleukin-1 receptor (TIR) domain, a coiled-coil (CC) domain, or a resistance to powdery mildew8-like (RPW8) domain at the N-terminus, resulting in their division into three classes: TIR-type NLRs (TNLs), CC-type NLRs (CNLs), and RPW8-type NLRs (RNLs), respectively.

NLRs recognize effectors secreted from pathogens using a variety of strategies. Some NLRs physically interact with the effectors; however, more commonly NLRs sense conformational changes or post-translational modifications of host proteins that are induced by the targeting of pathogen effectors. The indirect perception mechanisms of pathogen effectors by plant NLRs have been described in guardee and decoy models (van der Hoorn and Kamoun, 2008), in which the guardee is a host protein playing a role in plant immunity and the decoy is a mimic of host protein targeted by the pathogen effector. Guardees or decoys are directly modified by pathogen effectors, and cognate NLRs recognize the changes of guardees or decoys to trigger ETI (Figure 1).

The guardee protein RESISTANCE TO *P. SYRINGAE* PV MACULICOLA1 (RPM1)-INTERACTING4 (RIN4) is itself a negative regulator of PTI (Kim et al., 2005), and is targeted by the pathogen effectors AvrRpt2, AvrRpm1, and AvrB. To monitor these effectors, RESISTANT TO *P. SYRINGAE*2 (RPS2) and RPM1, the CNL class members, interact with RIN4 in the plasma membrane. While RPM1 senses AvrRpm1- and AvrB-induced RIN4 phosphorylation, RPS2 senses the AvrRpt2-mediated reduction in RIN4 and

triggers the RPM1- or RPS2-dependent signaling pathways, respectively (Mackey et al., 2002; Axtell and Staskawicz, 2003).

PROBABLE SERINE/THREONINE-PROTEIN KINASE2 (PBL2) acts as a BIK1 decoy in ETI. BIK1 uridylylation by an effector AvrAC suppresses BIK1-mediated PTI (Feng et al., 2012), while by contrast PBL2 uridylylated by AvrAC forms a complex with HOPZ-ACTIVATED RESISTANCE1 (ZAR1) via interacting with RESISTANCE RELATED KINASE1 (RKS1) to trigger ZAR1-mediated ETI (Wang et al., 2015). ZAR1-mediated ETI is also induced when ZAR1 senses the HopZ1a-mediated acetylation of HOPZ-ETI-DEFICIENT1 (ZED1) acting as a decoy (Lewis et al., 2013). ZAR1 forms a pentameric funnel-shaped structure, called the ZAR1 resistosome, on the plasma membrane (Wang et al., 2019), which when activated functions as a calcium-permeable channel (Bi et al., 2021).

A subset of plant NLRs carry integrated domains that mimic the binding targets of pathogen effectors; for instance, RESISTANT TO *RALSTONIA SOLANACEARUM*1 (RRS1) contains an integrated WRKY domain to which the AvrRps4 and PopP2 effectors bind. RPS4 interacts with RRS1 to sense AvrRps4 targeting to the WRKY domain and the Pop2-mediated acetylation of the WRKY domain (Sarris et al., 2015). WRKY proteins are DNA-binding transcription factors acting in the regulation of defense genes; thus, the two NLRs (RPS4 and RRS1) with RRS1 as a helper NLR act as a pair to detect effectors that interfere with the functions of the WRKY transcription factors.

In addition to effector sensing, helper NLRs act downstream of NLR-mediated signaling pathways. N REQUIREMENT GENE1 (NRG1) functions

together with a heterodimer complex composed of ENHANCED DISEASE SUSCEPTIBILITY1 (EDS1) and SENESCENCE-ASSOCIATED GENE101 (SAG101) to trigger HR (Rietz et al., 2011), and ACTIVATED DISEASE RESISTANCE1 (ADR1) acts together with a heterodimer composed of EDS1 and PHYTOALEXIN-DEFICIENT4 (PAD4) to promote the biosynthesis of salicylic acid (SA), a key phytohormone in plant immunity (Dong et al., 2016). NRG1 and ADR1 associate with the EDS1/SAG101 and EDS1/PAD4 complex, respectively, following the activation of the TNL-mediated signaling pathways (Sun et al., 2021), which are converged on a lipase-like protein, EDS1 (Rietz et al., 2011).

Taken together, plant NLRs generally detect self-molecules perturbed by pathogen effectors rather than non-self-molecules, suggesting that plants with limited defense genes effectively sense diverse effectors sharing target molecules.

3. Systemic immunity

Besides local immunity at infection sites, plants trigger systemic immunity to protect the rest of the plant body from subsequent pathogen attack. This phenomenon is called systemic acquired resistance (SAR), and confers long-lasting and broad-spectrum resistance. It is established by a slightly increase in the levels of SA in uninfected tissues and is accompanied by the expression of the SA marker *PATHOGENESIS-RELATED* (*PR*) genes (Yalpani et al., 1991; Gaffney et al., 1993; Wildermuth et al., 2001). The establishment of SAR is severely impaired by mutations in *NONEXPRESSOR OF PATHOGENESIS-RELATED GENES1* (*NPR1*) (Cao et al., 1994), suggesting that NPR1 acts as an essential regulator of SAR. Even though both SA accumulation and SA-mediated signaling are required for SAR, SA itself is unlikely to act as a mobile signal (Vernooij et al., 1994; Ryals et al., 1995). The roles of SA and NPR1 in local immunity will be further explained later.

Instead of SA, methyl salicylate (MeSA) was once proposed to be a phloem-mobile signal that could induce the systemic immune response upon hydrolysis to active SA in systemic tissues, as well as being an airborne signal that can induce disease resistance in neighboring plants (Park et al., 2007). This molecule is unlikely to be the main systemic immunity signal however, as it was later reported that most MeSA accumulated in the pathogen-infected leaves is emitted into the atmosphere, and SAR is not affected by mutations in an SA methyltransferase gene (Attaran et al., 2009).

Recent studies have suggested that a new pathway involving pipecolic acid (Pip) → nitric oxide (NO) ↔ ROS → azelaic acid (AzA) → glycerol-3-phosphate (G3P) acts in parallel with the SA pathway for the establishment of SAR. Pip is increased both in the petiole exudates of infected and uninfected tissues upon pathogen infection, and an exogenous application of Pip induces SAR (Návarová et al., 2012). The Pip-mediated SAR is dependent on FLAVIN-DEPENDENT-MONOOXYGENASE1 (FMO1) catalyzing the conversion of Pip to N-hydroxypipecolic acid (NHP) (Hartmann et al., 2018). The *de novo* biosynthesis of Pip in uninfected but not in infected tissues is dependent on both SA and G3P, and Pip functions upstream of the NO/ROS-mediated signaling pathway in both uninfected and infected tissues (Wang et al., 2018). Following the Pip-induced accumulation of NO/ROS, several ROS act in an additive manner to induce AzA biosynthesis, which results in G3P biosynthesis (Wang et al., 2014). The biosynthesis of G3P is dependent on two lipid-transfer proteins, DEFECTIVE IN INDUCED RESISTANCE1 (DIR1) and AZELAIC ACID INDUCED1 (AZI1), which interact with each other (Yu et al., 2013a). G3P may act as a mobile signal to induce SAR, and its translocation to uninfected tissues is interdependent with DIR1 (Chanda et al., 2011).

Once systemic immunity is established, plants are primed to induce more rapid and robust immune responses upon subsequent pathogen challenges. Defense priming is a type of immune memory that plants adopt as an adaptive strategy to survive their continuous exposure to surrounding pathogens. It was reported that bacterial pathogen- or herbivore-induced defense priming could be inherited by subsequent generations (Luna et al., 2012; Rasmann et al., 2012; Slaughter et al.,

2012); however, Yun et al. recently reported that they did not find evidence of the transgenerational inheritance of defense priming using a variety of methods used for pathogen infection and several developmental stages of host plants undergoing repetitive pathogen challenges (Yun et al., 2022). Thus, the transgenerational effect of defense priming should be more carefully reassessed in the context of the underlying molecular mechanisms.

Systemic immunity is also activated by beneficial microorganisms such as mycorrhizal fungi and plant growth–promoting rhizobacteria. This phenomenon is termed induced systemic resistance (ISR) to be distinguished from SAR. While SAR is dependent on SA-mediated signaling, ISR is dependent on jasmonic acid (JA)/ethylene (ET)-mediated signaling.

4. Phytohormone-mediated signaling pathways

Initiated from pathogen recognition, defense signals are transmitted in the form of phytohormones for signal amplification and transcriptional reprogramming. JA, ET, and SA are key hormones that play central roles in plant immunity. JA and ET are essential for defense against necrotrophic pathogens and herbivores, which destroy host cells to obtain nutrients and cause wounding to host plants, respectively. On the contrary, SA is responsible for defense against biotrophic pathogens, which derive nutrients from living host cells, and hemibiotrophic pathogens, which display an initial biotrophic phase before moving to a necrotrophic phase.

It has been documented that JA- and ET-mediated signaling pathways are synergistic, whereas the JA/ET- and SA-mediated signaling pathways are mutually antagonistic (Li et al., 2019); however, recent findings showed that the JA/ET- and SA-mediated signaling pathways are not always antagonistic. For instance, an exogeneous treatment of the ethylene precursor 1-aminocyclopropane-1-carboxylic acid (ACC) enhanced the SA-induced expression of *PR1*, and this effect was not shown in the *ethylene insensitive2-1* (*ein2-1*) mutant (De vos et al., 2006). By analyzing gene expression levels, another study reported that the synergistic effect of SA and JA is revealed when both hormones are applied at low concentrations, whereas an antagonistic effect is observed at high concentrations (Mur et al., 2006). It was also reported that during ETI involving SA-mediated signaling, the JA-responsive genes required for *de novo* JA biosynthesis are induced in an NPR3 and NPR4-dependent manner, and the increased JA levels contribute to HR induction (Liu et al., 2016). Mine et al. showed that a co-treatment with flg22 and methyl

jasmonic acid (MeJA) enhanced resistance to a biotrophic pathogen in a *delayed dehiscence2* (*dde2*) *pad4* double mutant to a greater extent than the flg22 treatment alone (Mine et al., 2017). Collectively, hormone-mediated signaling pathways in plant immunity are coordinated by a variety of crosstalks, constituting a complex signaling network.

4.1. Jasmonic acid (JA)-mediated signaling pathway

JA is biosynthesized in the chloroplasts and peroxisomes via the octadecanoid pathway involving several enzymatic steps. The biosynthesis of JA is initiated in the chloroplasts, where α-linoleic acid is converted into oxophytodienoic acid (OPDA). The export of OPDA into the cytosol is facilitated by JASSY proteins localized on the outer membrane of the chloroplasts (Guan et al., 2019). After their import into the peroxisome, OPDA is reduced by OPDA REDUCTASE3 (OPR3) and then converted into JA through three cycles of β-oxidation (Schaller et al., 2000) (Figure 2).

CORONATINE-INSENSITIVE1 (COI1) acts as a receptor for the bioactive form of JA, jasmonoyl-L-isoleucine (JA-Ile), and is the F-box subunit of the SKP1-CULLIN1-F-BOX-TYPE (SCF) ubiquitin ligase complex SCF^{COI1} (Katsir et al., 2008; Yan et al., 2009). JA-Ile mediates the binding of COI1 to the JASMONATE ZIM-DOMAIN (JAZ) proteins (repressors of JA-responsive genes) and thus results in the 26S proteasome–mediated degradation of JAZs (Chini et al., 2007; Thines et al., 2007) (Figure 2).

In their basal state, JAZs suppress the function of the transcriptional

activators of the JA-responsive genes by forming a transcriptional co-repressor complex with NOVEL INTERACTOR OF JAZ (NINJA), TOPLESS (TPL), and the TPL-RELATED PROTEINS (TPRs) (Pauwels et al., 2010). MYC2 is a binding target of the JAZs and acts as a key transcriptional activator of the JA-induced genes (Kazan and Manners, 2013); thus, the JA-induced degradation of JAZs causes the release of MYC2 from its suppression, leading to the transcriptional activation of the JA-responsive genes (Figure 2). This MYC2 branch of JA-mediated immunity is known to be induced by herbivores and mechanical wounding.

On the contrary, the ERF branch of JA-mediated immunity is induced by necrotrophic pathogens. The ERF branch is dependent on the OCTADECANOID-RESPONSIVE ARABIDOPSIS AP2/ERF59 (ORA59) and ETHYLENE RESPONSE FACTOR1 (ERF1) transcription factors. *ORA59* and *ERF1* expression is activated by ETHYLENE INSENSITIVE3 (EIN3) and EIN3 LIKE1 (EIL1), with which the JAZs interact to suppress their activities (Zhu et al., 2011). Thus, the JA-triggered degradation of JAZs results in the EIN3/EIL1-induced transcriptional activation of *ORA59* and *ERF1* (Figure 2). The ERF branch shows a synergistic interaction with ET-mediated signaling but an antagonistic interaction with the MYC2 branch. The antagonistic interaction between the ERF and MYC2 branches is fulfilled in such a way that EIN3 and MYC2 mutually inhibit their transcriptional activities by binding to each other (Song et al., 2014).

4.2. Ethylene (ET)-mediated signaling pathway

The gaseous hormone ET is produced in a two-step enzymatic reaction. In *Arabidopsis thaliana*, multiple ET receptors including ETYLENE RESPONSE1 (ETR1), ETHYLENE RESPONSE SENSOR1 (ERS1), ETR2, ERS2, and EIN4 have been identified. All of these ET receptors are localized in the membrane of the endoplasmic reticulum (ER).

Upon ET perception, the fragment generated by EIN2 cleavage at the C-terminus (EIN2-C) is translocated into the nucleus. By contrast, under normal conditions, CONSTITUTIVE TRIPLE RESPONSE1 (CTR1)-mediated EIN2 phosphorylation not only prevents the cleavage but also promotes EIN2 degradation (Ju et al., 2012; Qiao et al., 2012). When generated by ET signaling, the EIN2-C directly binds to the 3′ untranslated regions (UTRs) of the *EIN3-BINDING F BOX PROTEIN1* (*EBF1*) and *EBF2* transcripts to repress their translation (Li et al., 2015; Merchante et al., 2015). While the two F-box proteins, EBF1 and EBF2, mediate the degradation of EIN3/EIL1, which are essential transcription factors required for ET-induced gene expression under normal conditions (Potuschak et al., 2003), EIN3 and EIL1 become stabilized by ET signaling and trigger the ET responses by inducing the expression of numerous ET-responsive genes (Figure 2).

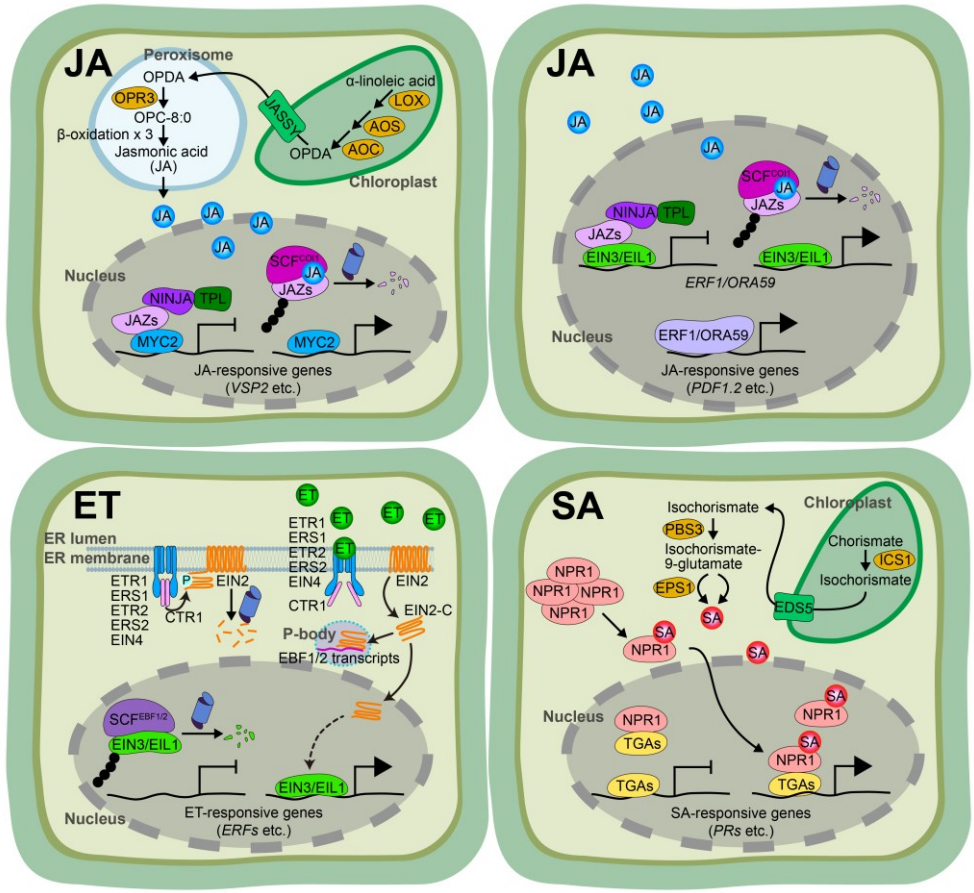
JA
Peroxisome
OPDA
OPR3
OPC-8:0
β-oxidation x 3
Jasmonic acid
(JA)
JASSY
α-linoleic acid
LOX
AOS
OPDA
AOC
Chloroplast
JA
Nucleus
SCFCOI1
JA
JAZs
NINJA
TPL
JAZs
MYC2
MYC2
JA-responsive genes
(VSP2 etc.)
JA
JA
JA
JA
JA
SCFCOI1
JA
JAZs
NINJA
TPL
JAZs
EIN3/EIL1
EIN3/EIL1
ERF1/ORA59
Nucleus
ERF1/ORA59
JA-responsive genes
(PDF1.2 etc.)
ET
ER lumen
ER membrane
ETR1
ERS1
ETR2
ERS2
EIN4
P
EIN2
CTR1
ET
ET
ET
ET
ETR1
ERS1
ETR2
ERS2
EIN4
CTR1
EIN2
EIN2-C
P-body
EBF1/2 transcripts
SCFEBF1/2
EIN3/EIL1
Nucleus
EIN3/EIL1
ET-responsive genes
(ERFs etc.)
SA
Isochorismate
PBS3
Isochorismate-
9-glutamate
Chloroplast
Chorismate
ICS1
Isochorismate
NPR1
NPR1
NPR1
NPR1
EPS1
SA
EDS5
SA
NPR1
SA
Nucleus
NPR1
TGAs
SA
NPR1
SA
NPR1
TGAs
TGAs
SA-responsive genes
(PRs etc.)

Figure 2. Phytohormone-mediated signaling pathways leading to transcriptional reprogramming and immunity in Arabidopsis.

For jasmonic acid (JA) biosynthesis, α-linoleic acid is first converted to oxophytodienoic acid (OPDA) by a series of reactions catalyzed by various enzymes, including LIPOXYGENASE (LOX), ALLENE OXIDE SYNTHASE (AOS), and ALLENE OXIDE CYCLASE (AOC), in the chloroplasts. OPDA is then exported through JASSY from the chloroplast to the cytoplasm and subsequently imported into the peroxisome. Within the peroxisome, OPDA is reduced by OPDA REDUCTASE3 (OPR3), and the reduced product is shortened through three cycles of β-oxidation to generate JA. JA is perceived by CORONATINE-INSENSITIVE1 (COI1), which comprises the F-box subunit of the SKP1-CULLIN1-F-BOX-TYPE (SCF) ubiquitin ligase complex SCF^{COI1}. This complex mediates the degradation of the JASMONATE ZIM-DOMAIN (JAZ) proteins through 26S proteasome. In the absence of JA, JAZs interact with MYC2 to suppress its transcriptional activity by forming a co-repressor complex with NOVEL INTERACTOR OF JAZ (NINJA) and TOPLESS (TPL). The JA-induced degradation of the JAZs enables MYC2 to induce the transcriptional activation of the JA-responsive genes, including *VEGETATIVE STORAGE PROTEIN2* (*VSP2*). The JAZs also repress the transcription of *ETHYLENE RESPONSE FACTOR1* (*ERF1*) and *OCTADECANOID-RESPONSIVE ARABIDOPSIS AP2* (*ORA59*) by interacting with ETHYLENE INSENSITIVE3 (EIN3) and EIN3 LIKE1 (EIL1). Upon JA-induced degradation of the JAZs, EIN3 and EIL1 induce the transcription of *ERF1* and *ORA59*, resulting in the subsequent expression of JA-responsive genes including *PLANT DEFENSIN1.2* (*PDF1.2*).

In the absence of ethylene (ET), CONSTITUTIVE TRIPLE RESPONSE1 (CTR1) interacts with multiple ET receptors, including ETYLENE RESPONSE1 (ETR1), ETHYLENE RESPONSE SENSOR1 (ERS1), ETR2, ERS2, and EIN4, and directly phosphorylates the C-terminal domain of EIN2 within the membrane of the endoplasmic reticulum (ER). EIN2 phosphorylation by CTR1 prevents the cleavage of the EIN2-C fragment but facilitates the degradation of EIN2 through the 26S proteasome. In addition, EIN3 and EIL1 are degraded by the $SCF^{EBF1/2}$ in the absence of ET in the nucleus. When ET receptors in the ER membrane perceive ET, the kinase activity of CTR1 becomes inactivated. As a result, EIN2-C is cleaved, binds with the *EBF1/2* transcripts, and targets them to the cytoplasmic processing body (P-body) for their translational repression. As a result, EIN3 and EIL1 are released from $SCF^{EBF1/2}$-mediated degradation upon ET signaling. EIN2-C is also translocated into the nucleus and activates the transcription of the ET-responsive genes, including the *ERF*s, through the activity of the undegraded EIN3 and EIL1.

Salicylic acid (SA) is biosynthesized through the isochorismate pathway upon pathogen infection. In the chloroplasts, chorismate is converted to isochorismate by ISOCHORISMATE SYNTHASE1 (ICS1). Isochorismate is then exported from the chloroplast to the cytoplasm by ENHANCED DISEASE SUSCEPTIBILITY5 (EDS5). Next, AVRPPHB SUSCEPTIBLE3 (PBS3) conjugates glutamate to isochorismate, generating isochorismate-9-glutamate. Finally, isochorismate-9-glutamate is converted into SA by ENHANCED PSEUDOMONAS SUSCEPTIBLITY1 (EPS1) or through spontaneous decay. SA induces the conversion of oligomeric NONEXPRESSOR OF PATHOGENESIS-

RELATED GENES1 (NPR1) proteins into their monomeric form. The monomerized NPR1 proteins are then translocated into the nucleus. Although NPR1 forms a complex with TGACG motif-binding transcription factors (TGAs) even in the absence of SA, the TGAs but not the NPR1–TGA complex are targeted to and repress the transcription of the SA-responsive genes, including the *PR*s. When NPR1 perceives SA via its direct binding, the NPR1–TGA complex is targeted to and activates the transcription of the SA-responsive genes.

4.3. Salicylic acid (SA)-mediated signaling pathway

Two SA biosynthetic pathways have been identified in plants, one involving ISOCHORISMATE SYNTHASE1 (ICS1) and the other involving PHENYLALANINE AMMONIA-LYASE (PAL) (Lefevere et al., 2020). In Arabidopsis, SA is mainly biosynthesized through the isochorismate pathway involving ICS1 upon pathogen infection, whereas the PAL pathway only has a minor effect on SA-mediated immunity.

ICS1 catalyzes the conversion of chorismate to isochorismate in the chloroplast. The expression of *ICS1* is activated by two transcriptional activators, CALMODULIN BINDING PROTEIN 60-LIKE G (CBP60g) and its homolog SYSTEMIC ACQUIRED RESISTANCE DEFICIENT1 (SARD1) (Zhang et al., 2010). EDS5 was proposed to export isochorismate from the chloroplasts into the cytoplasm on the basis that *EDS5* encodes a multidrug and toxin extrusion (MATE) transporter protein and SA accumulation is compromised in an *eds5* mutant (Nawrath et al., 2002). After export from plastids, isochorismate is conjugated to glutamate by AVRPPHB SUSCEPTIBLE3 (PBS3), after which isochorismate-9-glutamate decays into SA either spontaneously or facilitated by ENHANCED PSEUDOMONAS SUSCEPTIBLITY1 (EPS1) (Torrens-Spence et al., 2019) (Figure 2). SA is directly perceived by NPR1 (Wu et al., 2012; Ding et al., 2018) and its homologs, NPR3 and NPR4 (Fu et al., 2012; Ding et al., 2018).

4.3.1. NONEXPRESSER OF PATHOGENESIS-RELATED GENES1 (NPR1) in SA-mediated immunity

NPR1 is a *bona fide* SA receptor (Wu et al., 2012; Ding et al., 2018) (Figure 2). The direct binding of SA induces a conformational change in the NPR1 protein, resulting in the release of the C-terminal transactivation domain from the inhibitory effect of the N-terminal BTB/POZ domain (Wu et al., 2012). Mutations in *NPR1* cause failures in the development of SA-triggered immunity and impairments in SA- and pathogen-induced *PR* gene expression (Cao et al., 1994; Delaney et al., 1995; Cao et al., 1997; Shah et al., 1997). In addition, SA-induced transcriptional reprogramming is impaired in *npr1* mutants. According to microarray-based and RNA sequencing-based analyses, *npr1* mutations affect the expression of 99% of the benzothiadiazole S-methylester (called BTH; a functional SA analog)-inducible genes (Wang et al., 2006) and 71% of the 2,6-dichloroisonicotinic acid (called INA; a functional SA analog)-inducible genes (Jin et al., 2018), respectively; therefore, NPR1 acts as the master transcriptional regulator in the transmission of SA signals to transcriptional reprogramming.

The mechanism by which NPR1 regulates SA-mediated changes in gene expression has been extensively studied. An SA-triggered redox change induces NPR1 monomerization, and the monomeric NPR1 is translocated from the cytoplasm to activate the *PR* genes (Mou et al., 2003) by interacting with TGACG motif-binding transcription factors (TGAs) at the *PR* promoters (Zhang et al., 1999; Zhou et al., 2000; Després et al., 2003; Shearer et al., 2009) (Figure 2). Based on cryo-electron microscopy and crystal structure analyses, it was recently proposed that the SA-induced structural change of NPR1 facilitates the recruitment

of an unknown regulator for transcriptional activation (Kumar et al., 2022), suggesting that NPR1 might require other transcriptional activators for SA-induced gene expression. Indeed, a recent study demonstrated that NPR1 forms a transcriptional co-activator complex with CBP/p300-family histone acetyltransferases, HISTONE ACETYLTRANSFERASE OF THE CBP FAMILY1 (HAC1) and HAC5 (HAC1/5), as well as TGAs, and that the HAC-NPR1-TGA complex mediates histone H3 acetylation in the *PR1* promoter and its transcriptional activation upon SA signaling (Jin et al., 2018).

The SMALL UBIQUITIN-LIKE MODIFIER3 (SUMO3)-mediated sumoylation of NPR1 has been known to be a mechanism for NPR1 turnover (Saleh et al., 2015). This protein modification is induced by SA accumulation but inhibited by NPR1 phosphorylation at Ser55/Ser59 under normal conditions. The SA-induced NPR1 sumoylation promotes NPR1 phosphorylation at Ser11/Ser15, and the Ser11/Ser15 phosphorylation in turn enhances the NPR1 sumoylation and NPR1 activity. The SUMO3-mediated NPR1 sumoylation also facilitates proteasome-mediated NPR1 degradation; thus, it was proposed that the proteasome-mediated turnover of active NPR1 might facilitate NPR1-induced gene expression through a promoter-refreshing mechanism (Spoel et al., 2009).

4.3.2. NPR3 and NPR4 in SA-mediated immunity

The transcriptional co-activator role of NPR1 is suppressed by its homologs, NPR3 and NPR4 (NPR3/4). NPR3/4 act as SA receptors with affinities to SA that differ from that of NPR1, but also function as adaptors for the Cullin3 ubiquitin E3 ligase

which mediates the turnover of NPR1 protein in an SA concentration–dependent manner (Fu et al., 2012). Moreover, functionally redundant NPR3/4 target several genes that are also SA-dependent NPR1 targets and repress their expression in the basal state (Ding et al., 2018). NPR3/4 also induce the transcriptional activation of the JA-responsive genes required for *de novo* JA biosynthesis during ETI-induced SA accumulation by directly mediating the degradation of JAZ repressors, resulting in enhanced ETI and HR that are associated with SA-triggered immunity (Liu et al., 2016).

5. Epigenetic regulation of plant immunity

When attacked by pathogens, plants induce a massive transcriptional reprogramming to elicit an effective immune response. As eukaryotic DNA is organized into chromatin, changes in chromatin structure are prerequisites for massive transcriptional reprogramming. Chromatin structure is regulated by epigenetic mechanisms, including DNA methylation, histone modification, chromatin remodeling, and non-coding RNAs. These epigenetic mechanisms enable plants to differentially use the genetic information in their DNA and adapt to and survive various pathogen challenges.

5.1. Role of DNA methylations

The methylation of the fifth position of the pyrimidine ring of cytosine (5-methylcytosine) is the most abundant type of DNA methylation in plants, animals, and yeast. Whereas DNA methylation in animals mostly occurs at CG dinucleotides, DNA methylation in plants is deposited in three different cytosine sequence contexts: CG, CHG, and CHH (where H is A, T, or C). The genome-wide DNA methylation level has an impact on pathogen resistance in plants. Both the *methyltransferase1* (*met1*) single and *domains rearranged methylase1* (*drm1*) *drm2 chromomethylase3* (*cmt3*) triple mutants, which have reduced genome-wide CG and CHG/CHH methylation levels, respectively, were more resistant to a bacterial pathogen known to induce SA-mediated immunity (Dowen et al., 2012). In addition, several mutants defective in the RNA-directed DNA methylation pathway,

including *nuclear rna polymerase e1* (*nrpe1*), *nuclear RNA polymerase d2* (*nrpd2*), *rna-dependent rna polymerase2* (*rdr2*), *defective in rna-dependent dna methylation1* (*drd1*), *argonaute4* (*ago4*), and the double *drm1 drm2* mutant, were more susceptible to necrotrophic pathogens known to induce JA-mediated immunity (López et al., 2011). Some mutants defective in DNA methylation, including *decreased dna methylation1* (*ddm1*), *nrpe1*, *drd1*, and *cmt3*, displayed enhanced resistance to a biotrophic pathogen, while exhibiting diminished resistance to a necrotrophic pathogen (López Sánchez et al., 2016). Contrasting phenotypes to the above were observed in the *repressor of silencing1* (*ros1*) mutant, which has genome-wide hyper DNA methylation (López Sánchez et al., 2016).

DNA methylation is dynamically altered in response to infection by virulent and avirulent pathogens, and the SA content changes with a context-specific pattern (Dowen et al., 2012). More recently, it was reported that rapid DNA demethylation, which is dependent on ROS1, DEMETER-LIKE PROTEIN2 (DML2), and DML3, is induced by flg22 and the *ros1 dml2 dml3* triple mutant exhibits compromised flg22-triggered immunity (Huang et al., 2022). A pathogen attack induced DNA hypomethylation at centromeric and pericentromeric regions (Pavet et al., 2006), while the SA-induced hypomethylation at several transposable elements was positively correlated with the derepression of these transposable elements (Dowen et al., 2012). Thus, it has therefore been hypothesized that DNA methylation levels at transposons or other repetitive sequences near or within defense genes might affect the expression of these genes. The TNL-encoding gene *RESISTANCE METHYLATED GENE1* (*RMG1*) contains two helitron-related repeats in its promoter. Consistent with this hypothesis, the DNA methylation level

at the repeat proximal to the transcriptional start site was increased in all cytosine contexts, and both the basal and flg22-induced transcript levels of *RMG1* were compromised in a *ros1* mutant (Yu et al., 2013b).

5.2. Role of histone modifications

Eukaryotic DNA is wrapped around a histone octamer, forming a nucleosome, which is the basal repeating unit of chromatin. A histone octamer consists of two copies of the histone proteins H2A, H2B, H3, and H4. In addition, the histone H1 protein acts as a linker, and this linker activity is essential for higher-order chromatin organization. The N-terminal tail of each nucleosome histone protein protrudes from the nucleosome core, enabling histone modifiers easy access to the histone tails and post-translational modifications. The covalent modification of histones can affect the chromatin structure by altering the electric charge and structure of the histone tails. In addition, each covalent histone modification catalyzed by specific 'writers' can provide a binding platform for modification-specific 'readers', which eventually recruit 'effectors' that affect chromatin structure and transcription. Histone modifications therefore influence plant immunity mainly through regulating transcriptional output. Now, there is considerable evidence that numerous defense genes are regulated by histone modifications as written below.

The acetylation of lysine residues within histones is regulated by the opposing activities of histone acetyl transferases (HATs) and histone deacetylases (HDACs). Several HATs and HDACs have roles in the regulation of plant

immunity via their histone acetyltransferase and deacetylase activities, respectively. HISTONE ACETYLTRANSFERASE OF THE GNAT FAMILY1 (HAG1), a member of the GNAT family HATs, regulates the histone H3 lysine 14 (H3K14) acetylation levels in the 5′ and 3′ ends of its target genes, which is associated with the downregulation of genes acting in SA-mediated immunity and the upregulation of genes acting as inhibitors of SA biosynthesis (Kim et al., 2020). Another GNAT-family member, ELONGATA3 (ELO3), also known as ELONGATOR PROTEIN3 (ELP3) or HAG3, is the catalytic subunit of an elongator complex. The HAT activity of ELO3 was found to be required for SA-mediated immunity (Defraia et al., 2013); however, it remains unclear whether ELO3 directly targets and acetylates histones at SA-responsive gene loci to induce their transcription.

Both *HAC1* and *HAC5* (*HAC1*/*5*), members of the CBP/p300 family HATs, have positive roles in SA-mediated immunity with functional redundancy and *HAC1* dominance. Dozens of SA-responsive genes, including *PR* genes, were induced in the presence of SA through HAC1/5-dependent histone H3 acetylation, and a subset of those genes were co-regulated by NPR1 (Jin et al., 2018). Furthermore, to induce the expression of the JA-responsive genes, HAC1 acetylated H3K9 at their promoters by forming a complex with MEDIATOR SUBUNIT25 (MED25) and MYC2 (An et al., 2017). Notably, HAC1 interacted with NPR1 and MYC2, which play essential roles in SA- and JA-mediated immunity, respectively, suggesting that HAC1 might be a central regulator of multiple immunity pathways in Arabidopsis.

HISTONE DEACETYLASE19 (HDA19) and HDA6, members of the REDUCED POTASSIUM DEFICIENCY3 (RPD3)/HISTONE DEACETYLASE1

(HDA1) family, function as positive regulators in JA-mediated immunity (Zhou et al., 2005; Wu et al., 2008), but as negative regulators in SA-mediated immunity (Choi et al., 2012; Wang et al., 2017). In the regulation of JA-responsive genes, the opposing activities of HDA6 and HAG1 jointly maintain the acetylation homeostasis of a co-repressor, TOPLESS (TPL) (An et al., 2022). The *HDA6* transcript level is increased in response to JA, thus facilitating TPL deacetylation which suppresses the TPL-dependent repression of JA-induced genes. This case therefore indicates that antagonistic activities of histone modifiers control the expression of defense genes through the modification of a non-histone protein.

In addition to HATs and HDACs, several histone methyltransferases and demethylases are known to be involved in the regulation of defense genes. A histone methyltransferase ARABIDOPSIS HOMOLOG OF TRITHORAX1 (ATX1) is targeted to *WRKY70* in response to bacterial pathogens and deposits H3K4 trimethylation (H3K4me3) to activate the expression of the target gene (Alvarez-Venegas et al., 2007). Another histone methyltransferase, SET DOMAIN GROUP8 (SDG8), affects both SA- and JA/ET-mediated immunity by regulating the H3K36me3-associated transcription of defense genes; for example, the H3K36me3-associated transcription of a gene encoding an RPS4-like R protein is dependent on SDG8 (Palma et al., 2010). SDG8 also positively regulates both H3K36me3 enrichment and the transcription of SA- or JA/ET-responsive marker genes upon pathogen infection or exogenous hormone treatment (Berr et al., 2010; Zhang et al., 2020). An H3K4 methyltransferase, SDG25, plays a positive role in the regulation of genes encoding TNLs (Xia et al., 2013). Mutations in the *JUMONJI DOMAIN-CONTAINING PROTEIN14* (*JMJ14*) or *JMJ27* histone

demethylase gene cause a reduced disease resistance to a bacterial pathogen associated with SA-mediated immunity (Dutta et al., 2017; Li et al., 2020).

5.3. Role of chromatin remodeling complexes (CRCs)

Chromatin-remodeling complexes (CRCs) are large and multi-component complexes that affect the position and/or composition of the nucleosomes. CRCs contain an ATPase/helicase subunit of the SWITCHING DEFECTIVE2/SUCROSE NON-FERMENTING2 (SWI2/SNF2) family, and energy derived from ATP hydrolysis allows the CRCs to modify nucleosomes. The SWI2/SNF2-family CRCs are evolutionarily conserved and categorized into four subfamilies: SWI/SNF, IMITATION SWITCH (ISWI), CHROMODOMAIN HELICASE DNA-BINDING (CHD), and INOSITOL REQUIRING 80 (INO80). In comparison with other epigenetic mechanisms, little is known about the role of CRCs in plant immunity.

The SWI2/SNF2-RELATED1 (SWR1) complex belonging to the INO subfamily catalyzes the replacement of canonical H2A with the H2A.Z variant. PHOTOPERIOD-INDEPENDENT EARLY FLOWERING1 (PIE1) is the catalytic subunit of the SWR1 complex. Mutations in both *PIE1* and the genes encoding the subunits of the SWR1 complex and H2A.Z affects plant immunity. In the *pie1*, *sef*, and *hta9 hta11* mutants, the basal transcript levels of SA-responsive genes and basal resistance to biotrophic pathogens were increased (March-Diaz et al., 2008); however, by contrast, a more recent study showed that basal resistance to biotrophic pathogens was reduced in the mutants of genes encoding the SWR1

complex, including *pie1*, *swc6*, and *hta9 hta11* (Berriri et al., 2016). The same study also reported that ETI and JA/ET-mediated immunity were compromised in the *pie1* and *swc6* mutants (Berriri et al., 2016). A SWI/SNF subfamily member, SPLAYED (SYD), is required for the resistance against necrotrophic but not biotrophic pathogens, and targets several marker genes of JA/ET-mediated immunity to induce their transcription (Walley et al., 2008).

5.4. Role of long-noncoding RNA (lncRNAs)

LncRNAs are transcripts with more than 200 nucleotides and no protein-coding capacity. LncRNAs are pervasively transcribed from various genomic regions, including intergenic sequences, enhancers, introns, and some regions of protein-coding sequences in either sense or antisense orientations. This heterogeneity makes lncRNAs versatile regulators that are involved in diverse biological processes using a variety of molecular mechanisms. LncRNAs may regulate genes in *cis* and/or *trans*; *cis*-acting lncRNAs regulate the expression of genes located at or near their own loci of transcription, while *trans*-acting lncRNAs regulate the expression of genes at distant loci. LncRNAs may act as scaffolds for the assembly of RNA–protein complexes or sometimes recruit epigenetic or transcriptional factors to specific loci through their sequence complementarity to DNA or RNA. Recently, lncRNAs have emerged as important regulators of plant immunity.

The *ELF18-INDUCED LONG NONCODING RNA1* (*ELENA1*) recruits MED19a to the *PR1* promoter and induces its expression upon PAMP treatment, thereby acting as a positive regulator in PAMP-triggered SA-induced immunity

(Seo et al., 2017). More recently, ELENA1 was reported to evict FIBRILLARIN2 (FIB2) from MED19a on the *PR1* promoter, resulting in *PR1* derepression (Seo et al., 2019).

A lncRNA, *SALICYLIC ACID BIOGENESIS CONTROLLER1* (*SABC1*), balances immunity and growth by regulating SA biosynthesis (Liu et al., 2022). Under normal conditions, *SABC1* suppresses immunity and promotes growth by recruiting POLYCOMB REPRESSIVE COMPLEX2 (PRC2) to *NAC3* to repress its transcription via H3K27me3 deposition; however, upon pathogen infection, the transcript level of *SABC1* in decreased, resulting in the transcriptional activation of *NAC3* and the subsequent derepression of immunity and growth inhibition.

6. Concluding remarks

The co-evolutionary arms race between plants and phytopathogens has resulted in various types of virulence factors in phytopathogens and pathogen-receptors in plants. Research over the past few decades has revealed that plants and phytopathogens use a variety of strategies for successful pathogen recognition and enhanced virulence, respectively; however, our understanding of the underlying molecular mechanisms is limited to only a few plant receptors and pathogen effectors (Kourelis and van der Hoorn, 2018; Xin et al., 2018). Recent studies that have described the existence of intricate crosstalks between PTI and ETI further show the complexity of the plant immune responses against pathogens (Ngou et al., 2021; Pruitt et al., 2021; Yuan et al., 2021). Although PTI and ETI share various downstream events, the mechanisms by which ETI activates the more rapid and robust immune responses than PTI and the reason why HR is specific to ETI signaling should be answered in greater detail.

Crosstalks in plant immunity are also found among the phytohormone-mediated signaling pathways. It was proposed that the JA- and ET-mediated signaling pathways are synergistic, whereas the SA- and JA/ET-mediated signaling pathways are antagonistic to each other (Li et al., 2019); however, evidence from recent studies has indicated that the SA- and JA/ET-mediated signaling pathways are not necessarily antagonistic (De vos et al., 2006; Mur et al., 2006; Liu et al., 2016; Mine et al., 2017). Considering that the SA- and JA/ET-triggered immune responses are responsible for defense against different types of pathogens, the activation of one of the immunity pathways by a type of pathogen may make host

plants vulnerable to other types of pathogens which trigger the other immunity pathway. To avoid this risk, plants might balance and orchestrate various signaling pathways through crosstalks to achieve an optimal immunity to defend against potential attacks as well as responding to immediate attacks.

Based on nature of plant immunity, which is operated through cell-fate transitions from normal to immune-equipped cells, massive transcriptional reprogramming is necessary and fundamental in plant immunity. Therefore, epigenetic mechanisms and regulators that enable transcriptional reprogramming are to be important in plant immunity also. However, given that epigenetic regulators usually have multiple and broad targets and participate in various biological processes, pleiotropic effects from the misexpression of epigenetic regulators are to be expected and considered when the role of epigenetic components in immunity is assessed. For this reason, the molecular mechanisms as well as phenotypic effects of the epigenetic components must be elucidated in detail. As one epigenetic component–related aspect, it would be of interest to identify new epigenetic partners targeting the master transcriptional regulators of plant immunity, including NPR1, MYC2, and EIN3/EIL1 involved in SA-, JA- and ET-triggered immunity, respectively, and reveal their underlying regulatory molecular mechanisms.

Studies of systemic immunity in plants are of great value due to their major application potentials for enhancing this immune response. Despite extensive studies to identify the mobile signals that establish systemic immunity, *bona fide* mobile signals are yet to be confirmed. In addition to identifying the mobile signals, future studies on systemic immunity should address how the mobile signals are

generated in local tissues and perceived in systemic tissues. Systemic immunity enables plants to prime an enhanced resistance against broad-spectrum pathogens, and is likely to occur at the physiological, metabolic, and transcriptional levels. Epigenetic mechanisms, including DNA methylations and histone modifications, may provide mechanisms for defense priming at the transcriptional level. In this regard, it would be of interest to elucidate how an initial exposure to a pathogen is memorized at the transcriptional level through epigenetic mechanisms.

Chapter II

Negative evidence on the transgenerational inheritance of defense priming in *Arabidopsis thaliana*

This chapter was published as "Yun, S.-H., Noh, B. and Noh, Y.-S. (2022) Negative evidence on the transgenerational inheritance of defense priming in *Arabidopsis thaliana*. *BMB Reports*. **55(7)**: 342-347".

1. Abstract

Defense priming allows plants to enhance their immune responses to subsequent pathogen challenges. Recent reports suggested that acquired resistances in parental generation can be inherited into descendants. Although epigenetic mechanisms are plausible tools enabling the transmission of information or phenotypic traits induced by environmental cues across generations, the mechanism for the transgenerational inheritance of defense priming in plants has yet to be elucidated. With the initial aim to elucidate an epigenetic mechanism for the defense priming in plants, I reassessed the transgenerational inheritance of plant defense, however, could not observe any evidence supporting it. By using the same dipping method with previous reports, Arabidopsis was exposed repeatedly to *Pseudomonas syringae* pv *tomato* DC3000 (*Pst* DC3000) during vegetative or reproductive stages. Irrespective of the developmental stages of parental plants that received pathogen infection, the descendants did not exhibit primed resistance phenotypes, defense marker gene (*PR1*) expression, or elevated histone acetylation within *PR1* chromatin. In assays using the pressure-infiltration method for infection, I obtained the same results as above. Thus, my results suggest that the previous observations on the transgenerational inheritance of defense priming in plants should be more extensively and carefully reassessed.

2. Introduction

Epigenetic inheritance is the transmission of a trait that reflects mitotically and/or meiotically stable changes in gene expression without alteration of DNA sequence. In eukaryotes, chromatin modifications such as post-translational modification of histones and cytosine methylation on DNA are dynamically regulated by developmental or environmental cues, and these marks can give rise to epigenetic memory of transcriptional state (D'Urso and Brickner, 2014). Progressively, epigenetic information derived from environmental stimuli can be transmitted across generations enabling progeny to adapt to their surrounding environment (Heard and Martienssen, 2014).

Plants continuously withstand many environmental challenges and in the process adapt to various biotic and abiotic stresses through plastic responses. Against various pathogenic threats, plants develop sophisticated defense responses. As the first layer of plant defense, pathogen-associated molecular pattern (PAMP)-triggered immunity (PTI) is established when plants recognize highly conserved PAMPs by pattern-recognition receptors (PRRs; Pieterse et al., 2009; Macho and Zipfel, 2014), whereas the second layer of plant defense, effector-triggered immunity (ETI), involves highly variable resistance (R) proteins recognizing effector molecules secreted by pathogens (Pieterse et al., 2009; Kourelis and van der Hoorn, 2018).

In addition to the local defense mechanisms at the infection sites, plants also induce defense priming systemically even in uninfected tissues, which allows more rapid and robust responses to secondary pathogen attacks. This systemic

acquired resistance (SAR) depends on salicylic acid (SA) responses and confers long-lasting and broad-spectrum resistance against subsequent infections (Pieterse et al., 2009). It was reported that in the primed state, histone H3 lysine 9 and lysine 12 acetylation (H3K9K12Ac) and H3K4 di- and tri-methylation (H3K4me2/me3) levels are increased at some defense-gene loci compared to the non-primed state (Singh et al., 2014). However, the role of epigenetic modification of chromatin in SAR is not yet clear.

Recently, a few studies have reported that environmentally induced disease resistance in parents is transmitted to subsequent generations such that progenies obtain beneficial traits for responding to adverse environmental conditions. The priming state induced by SA-analog treatment or *Pst* DC3000 *avrRpt2* infection was transferred to the next generation, whereas the descendants that went through a stress-free generation returned to a non-primed state (Slaughter et al., 2012). On the other hand, Luna et al. (Luna et al., 2012) reported that the transgenerational effect of pathogen resistance obtained from repetitive *Pst* DC3000 infection was maintained over one stress-free generation. Induced resistance in parental plants by caterpillar herbivory, application of methyl jasmonate, or mechanical damage was also reported to be passed on to two subsequent generations (Rasmann et al., 2012). Transcriptional defense responses are routinely associated with epigenetic modifications. Although epigenetic modifications may serve as an epigenetic memory of transcriptional state (D'Urso and Brickner, 2014), their role as heritable materials responsible for the transgenerational inheritance of defense priming and environment-induced traits is yet to be demonstrated. Nonetheless, cytosine methylation on DNA has been

considered a favorable candidate (Luna et al., 2012; Rasmann et al., 2012; Lopez Sanchez et al., 2016) due to its maintenance mechanism through cell division.

With an initial aim to elucidate an epigenetic mechanism for the transgenerational defense priming in Arabidopsis, I set up experimental schemes following the previous reports and tested transgenerational effects first. However, I could not obtain any evidence proving that defense priming is inherited across generations. Defense priming that was known to be induced by repetitive pathogen infection in parental plants was not transmitted to descendants regardless of the existence of gametes during the period of infection. Considering subtle differences in experimental conditions, the degree of pathogen stress perceived in parental plants was thought to be a candidate factor affecting the transmittance of induced resistance to progenies. Nonetheless, I claim that the heritability of defense priming across generations should be evaluated in a much stricter view, especially after considering plant-unique later differentiation of germline-cell lineages and meristem-derived organ development.

3. Materials and methods

3.1. Plant materials, growth conditions, and pathogen infection

Arabidopsis thaliana Columbia-0 ecotype (Col-0) was used in all experiments. Parental plants were grown under 12-hr light/ 12-hr dark (12L/12D) photoperiod at 22℃. For syringe-infiltrations, 3-week (w)-old plants were infiltrated with 10^8 colony forming units (CFU)/ml of *Pst* DC3000 or *Pst* DC3000 *avrRpt2* (OD_{600} = 0.2). 10 mM $MgCl_2$ was used for mock treatment. This was repeated a total of five times with 3-day (d) intervals. For infection by dipping, 3-week (w)- or 5-w-old plants were dipped with *Pst* DC3000 suspension containing 10 mM $MgCl_2$ and 0.01% silwet L-77 (LEHLE SEEDS VIS-02). This was repeated a total of five times with 3-d intervals: The first three dippings were performed with *Pst* DC3000 suspensions at OD_{600} = 0.2 (10^8 CFU/ml), whereas the following two with *Pst* DC3000 at OD_{600} = 2.0 (10^9 CFU/ml). For mock treatment, 10 mM $MgCl_2$ containing 0.01% silwet L-77 was used. N1 and P1 plants in the next generation were grown for 4 w under 12L/12D at 22℃ for pathogen-resistance test and RT-qPCR analyses after pathogen infection. For 2,6-dichloroisonicotinic acid (INA) treatment, 0.3 mM INA was sprayed onto 2-w-old plants grown under 16L/8D on Murashige & Skoog (MS) media or onto 4-w-old plants grown under 12L/12D in soil and used for RT-qPCR analyses or chromatin immunoprecipitation (ChIP) assays. All plants were grown under 100 μE m^{-2} sec^{-1} cool white fluorescence light.

3.2. Pathogen resistance test

Pst DC3000 was grown at 28℃ in King's B medium supplemented with 60 mg/L rifampicin and 50 mg/L kanamycin. Pathogen inoculation was performed as described previously (Katagiri et al., 2002; Choi et al., 2012). Briefly, leaves of 4-week (w)-old plants were pressure-infiltrated with 5×10^5 CFU/ml (OD_{600} = 0.001) of *Pst* DC3000 using a needless syringe. Three inoculated leaf discs per plant were collected and homogenized in sterile H_2O at 0 or 3 days post-infection (dpi). Leaf extracts were serially diluted and plated on King's B medium. Bacteria were cultured at 28℃, and CFU was counted after 2 d.

3.3. RNA extraction and RT-qPCR analysis

Total RNA was extracted using TRI reagent (Molecular Research Center TR118) from 2-w-old seedlings excluding roots or from leaves of 4-w-old plants. Reverse transcription (RT) was performed with RevertAid reverse transcriptase (Thermo Scientific EP0442) using 3 μg of total RNA. Real-time quantitative PCR (qPCR) was performed using SYBR Green PreMIX (Enzynomics RT500) on the Rotor-Gene Q (QIAGEN). The sequences of primers used for RT-qPCR assays are listed in Table 1.

3.4. Chromatin immunoprecipitation (ChIP) assay

ChIP assays were performed as previously described (Choi et al., 2012). The antibody used for ChIP was α-H3Ac (Millipore 06-599). The amount of

immunoprecipitated chromatin was measured by qPCR with primers listed in Table 2. The $2^{-\Delta\Delta CT}$ method (Livak and Schmittgen, 2001) was used to determine the relative amounts of amplified products in samples. The value of each fragment was normalized to the respective input DNA (DNA isolated from chromatin that was cross-linked and fragmented under the same conditions as the immunoprecipitated DNA) and to *Ubiquitin 10* (*UBQ10*) to obtain H3Ac enrichment.

Table 1. Primers used for RT-qPCR analyses.

Gene	Name	Sequence
UBQ10	qUBQ-F	5'-GGCCTTGTATAATCCCTGATGAATAAG-3'
	qUBQ-R	5'-AAAGAGATAACAGGAACGGAAACATAGT-3'
PR1	qPR1-F	5'-GCCGTGAACATGTGGGTTAG-3'
	qPR1-R	5'-GGCACATCCGAGTCTCACTG-3'

Table 2. Primers used for ChIP assays.

Locus	Name	Sequence
UBQ10	ChIP-F	5'- TTGCCAATTTTCAGCTCCAC-3'
	ChIP-R	5'- TGACTCGTCGACAACCACAA-3'
PR1-P2	P2-F	5'-ATGGGTGATCTATTGACTGTTT-3'
	P6-R	5'-ATCACTCTTGCCTATGGCTG-3'
PR1-P3	P3-F	5'-GCCAAACTGTCCGATACGATT-3'
	P7-R	5'-TGTCATTCAGTTGTTTTGTGTTTTT-3'
PR1-P4	P8-F	5'-ACGTGAGATCTATAGTTAAC-3'
	P5-R	5'- CGATTAAAAATCGAGAATAGCCAG-3'
PR1-P5	qRT-F	5'- GCCGTGAACATGTGGGTTAG-3'
	qRT-R	5'- GGCACATCCGAGTCTCACTG-3'

4. Results

4.1. Experimental design to assess transgenerational defense priming in *Arabidopsis thaliana*

I used the standard ecotype of Arabidopsis thaliana, Columbia-0 (Col-0) accession, throughout this study. Parental Col-0 plants were either classified as N0 or P0 depending on the type of experimental treatments (Figure 3). Plants were treated with 10 mM $MgCl_2$ (for N0) or *Pseudomonas syringae* pv *tomato* DC3000 (*Pst* DC3000) suspension in 10 mM $MgCl_2$ (for P0) a total of five times with 3-day (d) intervals by syringe infiltration (Slaughter et al., 2012) or dipping (Luna et al., 2012). To clarify true transgenerational defense priming from effects directly or indirectly given to gametes by the pathogen during dipping procedure, the infection by dipping was performed at two different developmental stages, prior to and after the onset of flowering (bolting) (Figure 3). N1 and P1 plants were generated by self-pollinating N0 and P0 plants, respectively, and used for analyzing pathogen-resistance, *PR1*-expression, and H3Ac levels at the *PR1* locus (Figure 3).

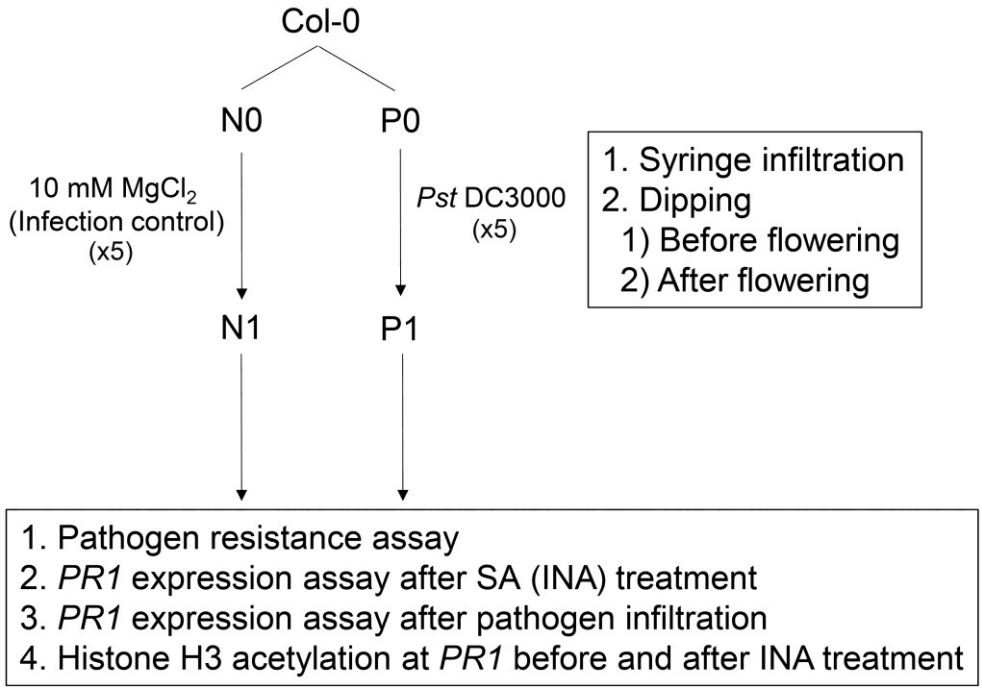

Figure 3. Schematic diagram of the experimental design for this study.

Parental plants, P0 plants, and their infection control N0 plants are all Col-0 ecotypes. P0 plants were inoculated with *Pst* DC3000 by two different methods, syringe-infiltration and dipping, a total of five times with 3-day (d) intervals for both methods. N0 plants were treated with 10 mM $MgCl_2$ in the same manner as with P0 plants. Dipping was performed before or after flowering. N1 and P1 plants in the next generation were produced from self-crossed N0 and P0 plants, respectively, and used for assays on defense priming.

4.2. Defense priming in parental plants was not inherited to descendants when parental plants were infected with bacterial pathogen before flowering

To explore if defense priming in parental plants can be transmitted to their descendants, the leaves of N0 and P0 plants were pressure-infiltrated as described in the Materials and Methods section and Figure 3. P0, but not N0, leaves showed an obvious disease symptom, which became severer as the number of infections increased (Figure 4A), indicating that pathogen infection was successful. N1 and P1 plants, which are the descendants of N0 and P0, respectively, were obtained and tested for their resistance to *Pst* DC3000. At 3 days post-infection (dpi), I found no significant differences in phenotypic disease symptoms in leaves (Figure 4B) or in bacterial cell growth (Figure 4C) between the N1 and P1 plants. As defense priming was previously reported to be associated with the priming of SA-responsive genes at the molecular level (Conrath et al., 2015), I studied the effect of pathogen infection to parental plants on the priming of defense-gene expression in descendants using *PR1*, a well-known SA-response marker gene. *PR1* transcript levels increased substantially after the treatment of 2,6-dichloroisonicotinic acid (INA; synthetic SA analog) after 12 hours (hr), indicating that INA was properly treated (Figure 4D). However, the basal levels and the levels of *PR1* transcript after INA treatment were not significantly different between the N1 and P1 plants (Figure 4D). Furthermore, when avirulent *Pst* DC3000 *avrRpt2* was used for P0 infection and subsequent P1 preparation, the induction pattern of *PR1* by INA in the P1 plants was not different from that of the N1 plants (Figure 5). To more directly address the transgenerational defense priming at the molecular level, I also analyzed *PR1* expression after pathogen infection. Consistent with the results of

leaf disease symptoms and bacterial cell growth, *PR1* transcript levels in the N1 and P1 plants were not significantly different from each other at both 1 dpi and 2 dpi, although the levels were clearly increased after pathogen infection (Figure 4E). Thus, all the results from the infiltration studies indicated that the experience of parental plants with bacterial-pathogen infection did not affect the defense priming of descendants.

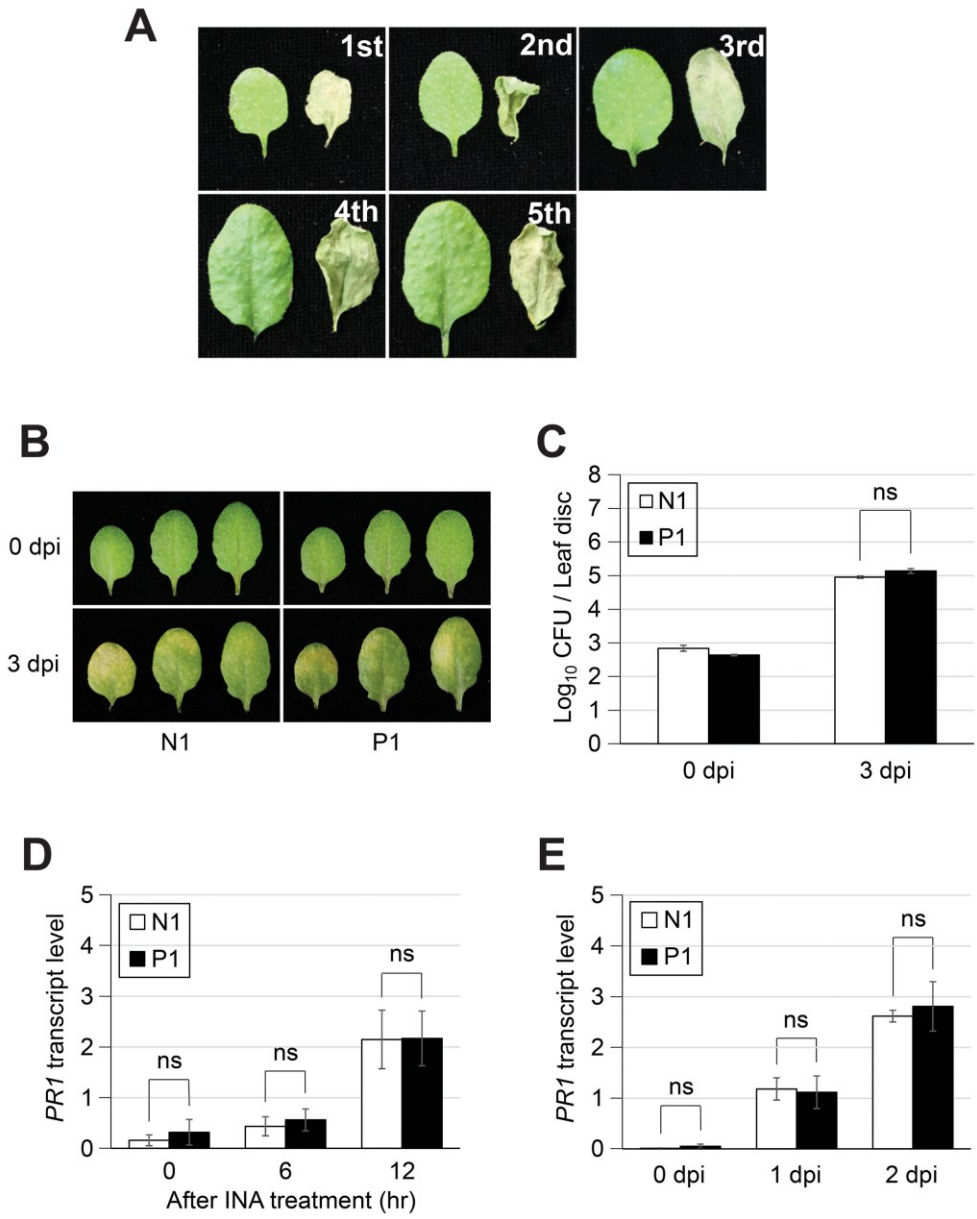
A
1st
2nd
3rd
4th
5th
B
0 dpi
3 dpi
N1
P1
C
Log10 CFU / Leaf disc
N1
P1
ns
0 dpi
3 dpi
D
PR1 transcript level
N1
P1
ns
ns
ns
0
6
12
After INA treatment (hr)
E
PR1 transcript level
N1
P1
ns
ns
ns
0 dpi
1 dpi
2 dpi

Figure 4. Assays to test transgenerational defense priming in the descendants of plants infected with *Pst* DC3000 by syringe-infiltration.

(**A**) Representative leaves of 3-week (w)-old N0 (left) and P0 (right) plants pressure-infiltrated with 10 mM $MgCl_2$ (N0) or *Pst* DC3000 suspension (P0). Infiltration was performed five times with 3-d intervals and the pictures were taken after 24 hr of each infiltration.

(**B**) Representative leaves of N1 and P1 plants at 0 and 3 days post-infection (dpi).

(**C**) Assays for bacterial cell growth using N1 and P1 plants at 0 and 3 dpi. Values are the means ± SE of three biological replicates. 'ns' means a statistically no significant difference in a Student's t-test.

(**D, E**) RT-qPCR analyses of *PR1* transcript levels in N1 and P1 plants after INA treatment (D) or *Pst* DC3000 infection (E). Means ± SE of three biological replicates are shown after normalization to Ubiquitin 10 (UBQ10).

Plants were grown on soil for 4 w under 12L/12D (B, C, E) or on MS media for 2 w under 16L/8D (D) and were treated with *Pst* DC3000 suspension at OD_{600} = 0.001 (B, C, E) or 0.3 mM INA (D).

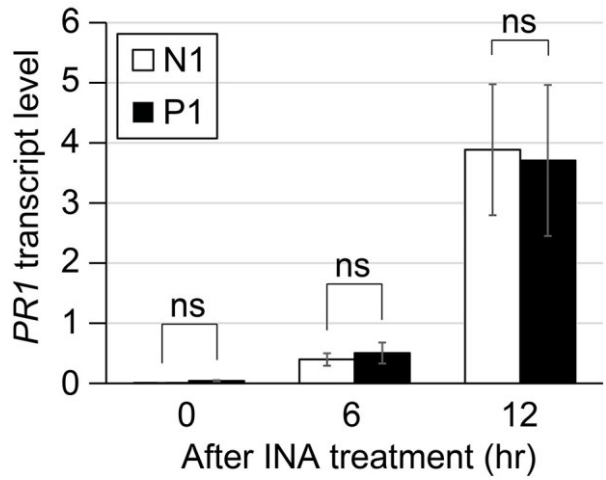

Figure 5. Assays to test transgenerational defense priming in the descendants of plants infected with *Pst* DC3000 *avrRpt2* by syringe-infiltration.

RTqPCR analyses of *PR1* transcript levels in N1 and P1 plants after INA treatment. Means ± SE of three biological replicates are shown after normalization to *UBQ10*. 'ns' means a statistically no significant difference in a Student's t-test.

4.3. Defense priming in parental plants was not inherited to descendants when parental plants were infected with bacterial pathogen after flowering

The results from my infiltration study described above were not consistent with a previous study (Luna et al., 2012) which reported a transgenerational defense priming after parental plant infection with *Pst* DC3000. Differences in experiments between the two studies were in the methods of inoculation (syringe-infiltration in my study vs. dipping in Luna et al. (Luna et al., 2012)) and the developmental stages of plants at infection time. Although I completed repeated infections before the onset of flowering, Luna et al. (Luna et al., 2012) infected parental plants by dipping across flowering stages; from before-flowering to after-flowering stages during the repeated dipping procedure. Therefore, I suspected a possibility that the defense priming observed in the next generation might have been resulted from the infection of the gametophytes of the parental generation. To address this possibility, first, I started an infection by dipping using 3-week (w)-old parental plants that were at vegetative stage and repeated dipping four-more times with 3-d intervals between the repeats. As shown in Figure 6A, there was no sign of bolting or flowering even at 3 d after the final infection by dipping, eliminating any chances of pathogen-inducing effects on reproductive cells. Similar to the results from the pressure-infiltration study (Figure 4), the N1 and P1 plants did not show distinguishable phenotypic susceptibilities (Figure 6B) nor significant differences in bacterial cell growth (Figure 6C) after *Pst* DC3000 infection. Although the transcript levels of *PR1* were elevated, the N1 and P1 plants did not show significantly different *PR1* induction patterns or amplitudes upon INA treatment (Figure 6D) and pathogen infection (Figure 6E). The parental plants were then

infected by dipping after bolting (Figure 7A). Surprisingly, the N1 and P1 descendants of these infected parental plants were not distinguishable in their pathogen resistance as represented by phenotypic susceptibility (Figure 7B), bacterial cell growth (Figure 7C), and *PR1* induction patterns after either INA treatment (Figure 7D) or pathogen infection (Figure 7E). Luna et al. (Luna et al., 2012) reported that the effect of repetitive pathogen attack in the parental generation could be transmitted to the next generation through increased H3Ac within the chromatin of defense genes including *PR1*. Therefore, I examined H3Ac levels within *PR1* chromatin in the N1 and P1 plants by chromatin immunoprecipitation (ChIP) assay (Figure 7F). In consistence with the transcriptional induction of *PR1* (Figure 7D) and previous reports (Choi et al., 2012; Jin et al., 2018), INA treatments increased H3Ac levels in several regions of the *PR1* locus (Figure 7F). However, H3Ac levels between the N1 and P1 plants were not significantly different at basal as well as induced states in all *PR1* regions tested. Thus, all my results from the pressure-infiltration (Figure 4) and dip-infection studies before (Figure 6) or after flowering (Figure 7) consistently demonstrate that repeated pathogen stress on plants did not result in transgenerational defense priming in the subsequent generation.

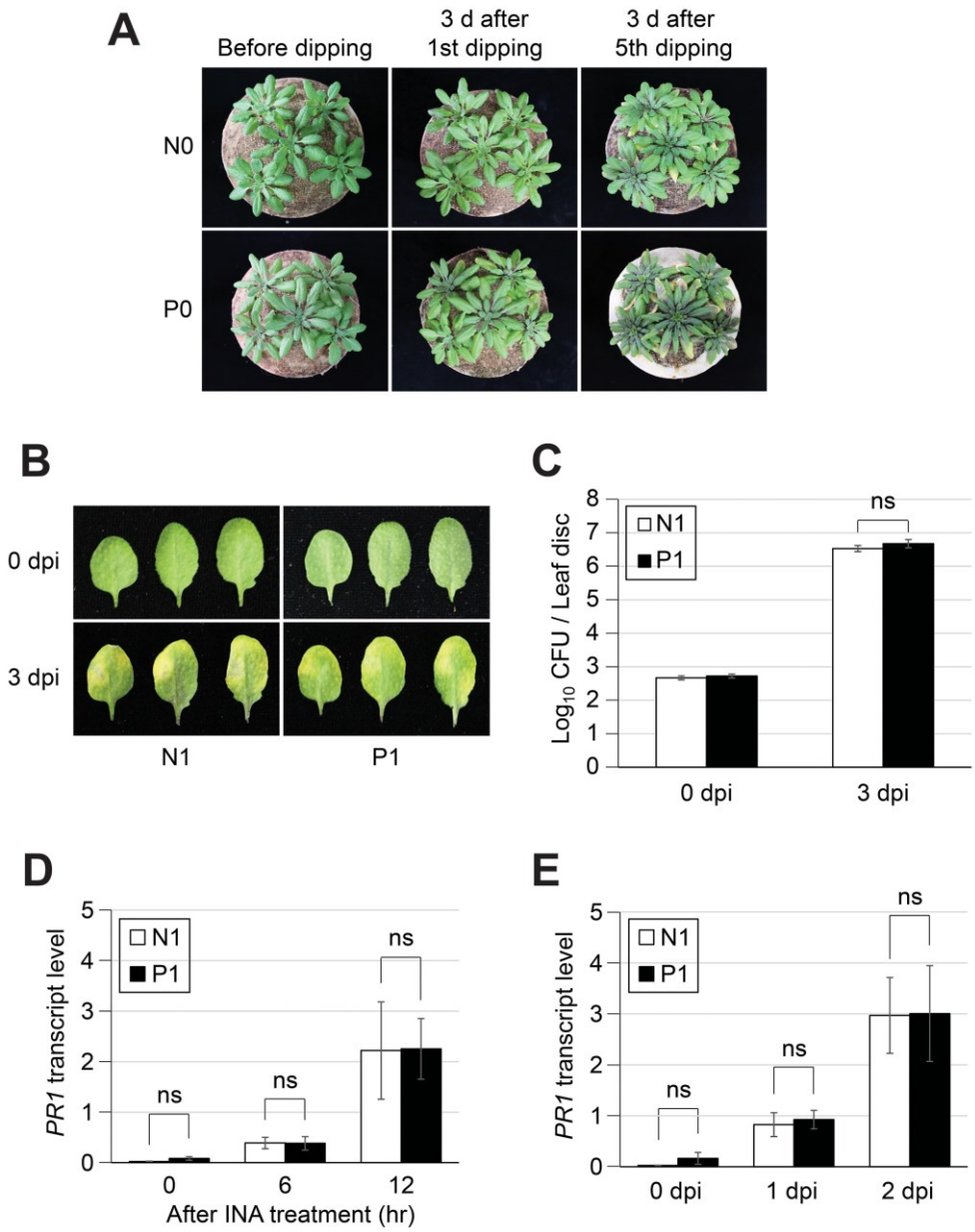
A
Before dipping
3 d after 1st dipping
3 d after 5th dipping
N0
P0
B
0 dpi
3 dpi
N1
P1
C
Log10 CFU / Leaf disc
N1
P1
ns
0 dpi
3 dpi
D
PR1 transcript level
N1
P1
ns
ns
ns
0
6
12
After INA treatment (hr)
E
PR1 transcript level
N1
P1
ns
ns
ns
0 dpi
1 dpi
2 dpi

Figure 6. Assays to test transgenerational defense priming in the descendants of plants infected with *Pst* DC3000 by dipping before flowering.

(**A**) N0 and P0 plants were grown under 12L/12D. Dipping was performed with 10 mM $MgCl_2$ (N0) or *Pst* DC3000 (P0) five times with 3-d intervals. The first dipping was carried out when plants were 3-w-old.

(**B**) Representative leaves of N1 and P1 plants at 0 and 3 dpi.

(**C**) Assays for bacterial cell growth using N1 and P1 plants at 0 and 3 dpi. Values are the means ± SE of three biological replicates. 'ns' means a statistically no significant difference in a Student's t-test.

(**D, E**) RT-qPCR analyses of *PR1* transcript levels in N1 and P1 plants after INA treatment (D) or *Pst* DC3000 infection (E). Values were normalized to *UBQ10*. Means ± SE of three biological replicates are shown.

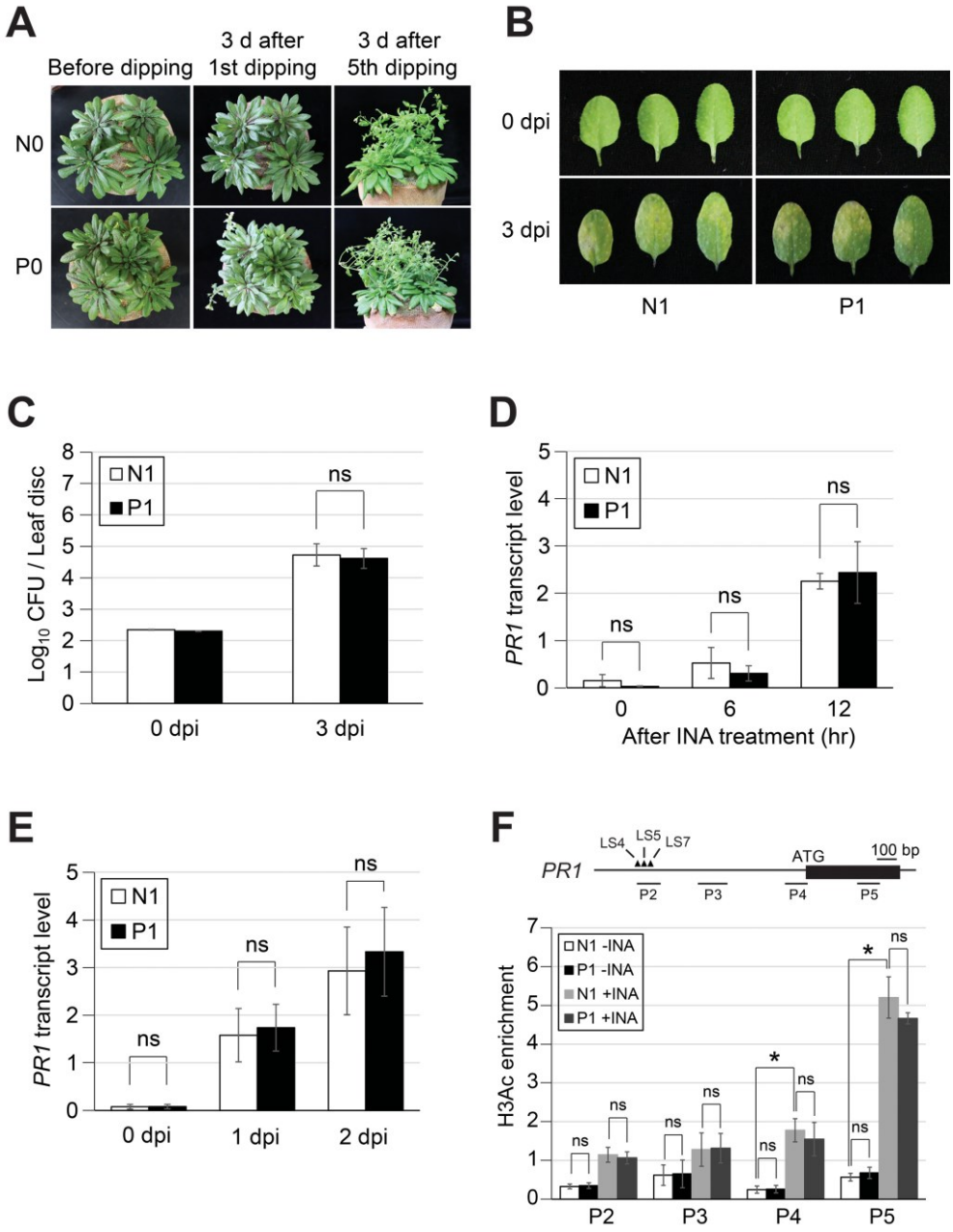
A
Before dipping
3 d after 1st dipping
3 d after 5th dipping
N0
P0
B
0 dpi
3 dpi
N1
P1
C
Log10 CFU / Leaf disc
N1
P1
ns
0 dpi
3 dpi
D
PR1 transcript level
N1
P1
ns
ns
ns
0
6
12
After INA treatment (hr)
E
PR1 transcript level
N1
P1
ns
ns
ns
0 dpi
1 dpi
2 dpi
F
PR1
LS4
LS5
LS7
ATG
100 bp
P2
P3
P4
P5
H3Ac enrichment
N1 -INA
P1 -INA
N1 +INA
P1 +INA
*
ns
P2
P3
P4
P5

Figure 7. Assays to test transgenerational defense priming in the descendants of plants infected with *Pst* DC3000 by dipping after flowering.

(**A**) N0 and P0 plants grown under 12L/12D. Dipping was performed with 10 mM $MgCl_2$ (N0) or *Pst* DC3000 (P0) five times with 3-d intervals. The first dipping was carried out when plants were 5-w-old.

(**B**) Representative leaves of N1 and P1 plants at 0 and 3 dpi.

(**C**) Assays for bacterial cell growth using N1 and P1 plants at 0 and 3 dpi. Values are the means ± SE of three biological replicates. 'ns' means a statistically no significant difference in a Student's t-test.

(**D, E**) RT-qPCR analyses of *PR1* transcript levels in N1 and P1 plants after INA treatment (D) or *Pst* DC3000 infection (E). Values were normalized to *UBQ10*. Means ± SE of three biological replicates are shown.

(**F**) H3Ac levels within *PR1* chromatin in N1 and P1 plants before (−) and after (+) INA treatment. Values were normalized to input and *UBQ10*. Means ± SE of three biological replicates are shown. Asterisks indicate statistically significant differences between −INA and +INA samples ($P < 0.05$ in a Student's t-test).

5. Discussion

Non-DNA sequence-based transgenerational inheritances have been reported in various organisms (Perez and Lehner, 2019). Especially in plants, transgenerational inheritance of disease resistance is an attractive subject because of its great application value. Recently, several studies reported that plant defense systems are transcriptionally primed, enabling faster and stronger immune responses in the progeny generation of parental plants suffered from repeated biotic stresses (Luna et al., 2012; Rasmann et al., 2012; Lopez Sanchez et al., 2016). Although DNA methylation has previously been proposed as a candidate epigenetic mark that might be responsible for the defense priming (Luna et al., 2012; Rasmann et al., 2012; Lopez Sanchez et al., 2016), there has been no direct demonstration of the role of DNA methylation. Therefore, I intended to understand an epigenetic mechanism and mark responsible for the transgenerational defense priming. However, I found, in contrast to the previous reports, no evidence of inheritance of acquired disease resistance in the next-generation plants in this study. In my study, the descendants of parental plants which experienced repeated pathogen attacks regardless of the infection methods (pressure-infiltration or dipping) and developmental statuses (vegetative or reproductive) did not show any evidence of acquired resistance against bacterial pathogens.

One possibility for the conflicting results might be in the differences in experimental conditions such as plant growth conditions, plant developmental states when the pathogen infection occurred, pathogen infection methods, etc. Such differences might affect the extent of host responses to pathogens. For example,

photoperiods, critical environmental cues for plant growth and development, can affect biochemical and physiological features of plant cells which in turn may influence the level of susceptibility to pathogens. Although severely stressed parental phenotypes were commonly observed under two different photoperiodic regimes (8L/16D photoperiod (Slaughter et al., 2012) and 16L/8D photoperiod (Luna et al., 2012), the same phenotypes were not observed under my 12L/12L photoperiod. Thus, photoperiods might not be the sole factor affecting parental susceptibility. Among other environmental factors, humidity is especially considered important for the virulence of pathogens (Xin et al., 2016). Given that surrounding humidity could substantially affect plant-pathogen interaction, the conflicting results from other groups might also have be caused by different humidity conditions given during pathogen inoculation. Under the assumption that the extent of stress given to parental plants is likely one of the factors affecting the transgenerational inheritance, the infection stresses used by the groups reported the transgenerational resistance of defense priming might be strong enough to generate defense priming that is transmittable to the next generation, whereas those used in my experiments might not be strong enough.

I also noticed that the approaches used to assess the disease resistance of progeny generation were different between groups. Luna et al. (Luna et al., 2012) used less bacterial cells to infect the progenies in comparison to my study. In addition, Luna et al. (Luna et al., 2012) and Slaughter et al. (Slaughter et al., 2012) quantified *Pst* DC3000 in the infected leaves of progenies by measuring bioluminescence from luxCDABE-tagged *Pst* strain and the transcript level of a *Pst* gene, respectively, instead of counting the number of bacterial cells as I did.

Thus, the differences in the infection methods and measuring the infection status of progenies might be other reasons for the discrepancies between the groups. At this point, I am not sure which methods would allow more accurate assays on the status of defense priming of the progeny generations.

For the transgenerational inheritance of defense priming, the primed state should be transmitted through the germline to progenies and thus maintained through cell divisions (i.e., mitosis and meiosis). Although DNA methylation has been considered as an epigenetic mark implicated in transgenerational inheritance of acquired resistance, there is still a lack of direct evidence showing that environmental stress-induced changes in DNA methylation are stably inherited to successive generations in the absence of the stress and linked to changes in stress-specific and phenotype-related gene expressions (Luna et al., 2012; Rasmann et al., 2012; Lopez Sanchez et al., 2016). Furthermore, inheritance of the altered cytosine methylation and gene-expression patterns after pathogen attack were not evident, especially at disease-related loci (Stassen et al., 2018).

The magnitude of given pathogen stresses appears to determine how long the acquired resistance and DNA-methylation change will last over subsequent generations (Luna et al., 2012; Slaughter et al., 2012; Stassen et al., 2018). Luna et al. (Luna et al., 2012) reported that the disease resistance was inherited through one pathogen stress-free generation contrary to Slaughter et al. (Slaughter et al., 2012). It is noteworthy that in the report of Luna et al. (Luna et al., 2012), parental plants were given repeated pathogen stresses until they reached the reproductive phase. This raises a question on whether the reported defense priming in the progenies can be considered as true transgenerational inheritance, excluding the effects from

direct germline-cell infection or germline cells received SAR signal. Therefore, to evaluate whether the acquired resistance is inherited across generations, it would be critical to avoid the possibility of germline cells (intergenerational inheritance), zygotes, and/or developing embryos being directly affected by pathogen stress. On the other hand, it is difficult to tell between intergenerational inheritances from transgenerational inheritances in plants considering the characteristics of plant development: Unlike animals that possess differentiated germline cells from early embryogenesis stages, plants keep producing new organs including reproductive organs from the shoot apical meristem (SAM). Therefore, if the SAM is affected by environmental stresses, it might be possible that the information recorded in the SAM passes onto gametes generated later from the SAM. For this reason, and to eliminate the confusion and question on the transgenerational inheritance of defense priming in plants, researchers should study descendants after at least one stress-free generation (if the stress is given only during the vegetative phase) or on progenies produced from the crosses using male gametes from stress-free plants of the stressed-lineage and female gametes from plants that were never exposed to the stress.

Chapter III

Genomic overview of salicylic acid-induced NPR1 targeting and transcriptional cascades in Arabidopsis

---

In this study, Irfan Ullah Khan helped to collect DNA for the 4th biological replicate of NPR1:GFP chromatin immunoprecipitation with sequencing (ChIP-seq) by performing ChIP assays.

1. Abstract

The phytohormone salicylic acid (SA) triggers transcriptional reprogramming that leads to SA-induced immunity in plants. NONEXPRESSER OF PATHOGENESIS-RELATED GENES1 (NPR1) is an SA receptor and master transcriptional regulator in SA-triggered transcriptional reprogramming. Despite the indispensable role of NPR1, genome-wide direct targets of NPR1 specific to SA signaling have not been identified. Here, I report SA-specific genome-wide targets of *Arabidopsis thaliana* NPR1 in plants transgenically expressing native *NPR1*. Analyses of *NPR1*-dependently expressed direct NPR1 targets revealed that NPR1 primarily activates genes encoding transcription factors upon SA signaling, triggering transcriptional cascades required for SA-induced transcriptional reprogramming and immunity. I identified genome-wide targets of a histone acetyltransferase, HISTONE ACETYLTRANSFERASE OF THE CBP FAMILY1 (HAC1), including hundreds of co-targets shared with NPR1, and showed that *NPR1* and *HAC1* regulate SA-induced histone acetylation and expression of a subset of the co-targets. Genomic NPR1 targeting was principally mediated by TGACG-motif binding protein (TGA) transcription factors. Furthermore, a group of NPR1 targets was already bound to NPR1 in the basal state, allowing for a more rapid and robust induction than other NPR1 targets upon SA signaling. Thus, I reveal how NPR1 orchestrates SA-triggered transcriptional reprogramming and the cooperative roles of NPR1, HAC1, and TGAs in SA-triggered immunity.

2. Introduction

Throughout their lifetime, plants are threatened by pathogens. Unlike animals, plants do not differentiate specialized immune cells or organs, but instead transition their cell identity from a growth-optimized to an immunity-equipped state partially through genome-wide transcriptional reprogramming. Salicylic acid (SA) is a key phytohormone that induces disease resistance against biotrophic and hemi-biotrophic pathogens (Pieterse et al., 2009). Upon pathogen attack, plant SA levels increase, which induces genome-wide transcriptional reprogramming to elicit immune responses (Wang et al., 2006; Jin et al., 2018; Hickman et al., 2019).

SA-triggered transcriptional reprogramming is dependent on NONEXPRESSOR OF PATHOGENESIS-RELATED GENES1 (NPR1). Thus, *npr1* mutants fail to develop disease resistance or express pathogenesis-related (*PR*) genes after SA treatment or pathogen challenge (Cao et al., 1994; Delaney et al., 1995; Cao et al., 1997; Shah et al., 1997). Furthermore, NPR1 is an SA receptor (Wu et al., 2012; Ding et al., 2018) and undergoes a conformational change that enables its transcriptional co-activator function upon SA binding (Wu et al., 2012; Kumar et al., 2022). In a microarray-based study, an *npr1* mutation affected the expression of 99% of genes that are induced by benzothiadiazole S-methylester (BTH; a functional SA analog) (Wang et al., 2006), and an RNA sequencing (RNA-seq)-based study showed that the expression of 71% of 2,6-dichloroisonicotinic acid (INA; a synthetic SA analog)-inducible genes is affected by an *npr1* mutation (Jin et al., 2018), all supporting an essential and central role of NPR1 in mediating SA-triggered transcriptional reprogramming.

As NPR1 itself does not contain domains directly involved in DNA binding and transcriptional activation, it might act together with other transcriptional regulators (Kumar et al., 2022). The TGACG-motif binding proteins (TGAs) are basic leucine-zipper (bZIP) transcription factors, and several TGAs physically interact with NPR1 to induce *PR* gene expression (Zhang et al., 1999; Zhou et al., 2000; Després et al., 2003; Shearer et al., 2009). NPR1 forms a complex with CBP/p300-family histone acetyltransferases, HISTONE ACETYLTRANSFERASE OF THE CBP FAMILY1 (HAC1) and HAC5 (HAC1/5), and the complex is then recruited to *PR* genes via TGAs upon SA signaling to induce histone H3 acetylation (H3Ac)-mediated gene activation (Jin et al., 2018). Furthermore, 21% of SA- and *NPR1*-dependently expressed genes are regulated in an *HAC1/5*-dependent manner (Jin et al., 2018). Thus, TGAs and HACs seem to be part of components that confer DNA-binding and co-activator functions, respectively, to NPR1.

Despite the indispensable role of NPR1 in SA-triggered immunity, how NPR1 conveys the SA signal to induce transcriptional reprogramming at a genome scale is unclear. Genome-wide targets of NPR1, identified after co-treating *Arabidopsis thaliana* plants constitutively overexpressing *NPR1* with SA and jasmonic acid (JA), were recently reported (Nomoto et al., 2021). In contrast to SA, which induces resistance against biotrophic and hemi-biotrophic pathogens, JA activates defense against necrotrophic pathogens and insects and acts antagonistically to SA in plant immunity (Pieterse et al., 2009). SA-specific genome-wide direct targets of NPR1 identified under a native *NPR1*-expressing condition are yet to be reported.

In this study, I identified SA-specific genome-wide NPR1 targets using Arabidopsis expressing *NPR1* under its native promoter. Through comparative analyses with RNA-seq data showing SA- and *NPR1*-dependently expressed genes, I demonstrate that NPR1 primarily targets and activates transcription factor-encoding genes in an SA-dependent manner, triggering transcriptional cascades during SA-induced immunity. Furthermore, I report genome-wide co-targets of NPR1 and HAC1 and show that the co-targeting activity of NPR1 and HAC1 is essential for SA-dependent H3Ac and expression of a subset of NPR1 target genes. My study reveals that the TGACG motif is abundant in NPR1-targeting regions and that TGA2 targets regions containing this motif. Finally, I report that a fraction of genes bound to NPR1 in the basal state show more rapid and robust induction upon SA treatment compared to genes targeted by NPR1 only after SA signaling and propose that NPR1 pre-targeting might be a mechanism for defense priming.

3. Materials and methods

3.1. Plasmid construction

For the construction of *pHAC1::HAC1:mCherry*, a *HAC1* genomic DNA harboring ~550 bp upstream promoter region was amplified by PCR with HAC1 promoter-F and HAC1-R (w/o stop) primer pairs (Table 3). The PCR product was inserted into pENTR/SD/D-TOPO plasmid (Invitrogen, K242020) and then transferred into pEarleyGate 301 plasmid by recombination using Gateway LR clonase II (Invitrogen, 11791-020). For the construction of *pTGA2::TGA2:mCherry*, the *TGA2* coding region was amplified by PCR using NdeI-TGA2-ORF-F and TGA2-ORF-R (w/o stop) primers (Table 3) and cloned into pENTR/SD/D-TOPO plasmid. For *TGA2* promoter cloning, a genomic DNA containing ~1.5 kb promoter region of *TGA2* was amplified by PCR with NotI-TGA2 promoter-F and NdeI-TGA2 promoter-R primers (Table 3) and then inserted into NotI and NdeI sites within the plasmid with cloned TGA2-coding region. The resulting *TGA2* construct composed of the promoter and coding region was transferred into pEarleyGate 301 plasmid by recombination. Finally, the HA tag within the *HAC1*- and *TGA2*-containing pEarleyGate 301 plasmids was replaced by mCherry tag derived from pGGC015 plasmid by using AscI and PacI sites.

3.2. Plant materials and growth conditions

Arabidopsis thaliana accession Columbia-0 (Col) was used as a genetic background for all experiments in this study. *pHAC1::HAC1:mCherry* transgenic

plant was generated by the transformation of *hac1-2* with *pHAC1::HAC1:mCherry* plasmid. *pTGA2::TGA2:mCherry* transgenic plant was generated by introducing *pTGA2::TGA2:mCherry* plasmid into the *tga2 tga5 tga6* triple mutants. The *hac1-2* and *tga2 tga5 tga6* mutants and *pNPR1::NPR1:GFP* and *pHAC1::HAC1:HA* transgenic plants were described previously (Jin et al., 2018). Floral dip method via *Agrobacterium tumefaciens* strain GV3101 was used for plant transformation. All plants were grown on Murashige and Skoog basal medium under 8-hour (h) light/16-h dark photoperiod for 4 weeks (w) at 22℃. For 2,6-dichloroisonicotinic acid (INA) treatment, 4-w-old seedlings were sprayed with distilled water (–INA) or 300 μM INA (+INA; Sigma-Aldrich 456543) and then incubated for 12 h before harvesting.

3.3. Chromatin immunoprecipitation (ChIP) assays

4-w-old seedlings were infiltrated with 1% formaldehyde solution under vacuum for cross-linking. The cross-linking was then quenched by adding glycine to final 125 mM and applying vacuum. After grinding the cross-linked seedlings to fine powder, nuclei were extracted by following the protocol of Saleh et al. (Saleh et al., 2008) with minor modifications. Briefly, ground powder was suspended in 25 ml of nuclei isolation buffer (0.25 M sucrose, 15 mM PIPES pH 6.8, 15 mM NaCl, 5 mM $MgCl_2$, 60 mM KCl, 1 mM $CaCl_2$, 9% Triton X-100, 1 mM PMSF, 0.05 μg/ml antipain, 0.5 μg/ml bestatin, 0.5 μg/ml leupeptin, and 4 μg/ml pepstatin) and incubated on ice for 10 minutes (min). Then, the suspension was filtered twice through two-layered miracloth and centrifuged at 8,700 rpm for 20 min at 4℃. For chromatin digestion using micrococcal nuclease (MNase), nuclei pellet was

resuspended in 700 µl of MNase working buffer (50 mM HEPES pH 7.5, 3 mM $CaCl_2$, 1 mM PMSF, 100 µM MG132, and protease inhibitor cocktail) with MNase (NEB, M0247S) at 10,000 gel units/ml. MNase digestion was performed at 25℃ for 15 min followed by at 28℃ for 5 min. 5xMNase stop buffer (50 mM HEPES pH 7.5, 50 mM EDTA, 0.5% SDS, 1 mM PMSF, and protease inhibitor cocktail) was then added, and the solution was incubated on ice for 10 min. To extract chromatin from nuclei, sonication was performed with 15 cycles of 5-second (sec) on/10-sec off pulse at 15% amplitude using Sonic Dismembrator 500 (Fisher Scientific). After centrifugation at 13,000 rpm for 10 min, the supernatant was diluted 5 folds with ChIP dilution buffer (20 mM HEPES pH 7.5, 187.5 mM NaCl, 7% sucrose, 0.625% Triton X-100, 1 mM PMSF, 0.05 µg/ml antipain, 0.5 µg/ml bestatin, 0.5 µg/ml leupeptin, and 4 µg/ml pepstatin). Subsequently, the lysate was precleared by adding 60 µl of protein A agarose beads (Santa Cruz, sc-2001) and incubated with rotation at 4℃ for 1 h. For immunoprecipitation, GFP- or RFP-trap agarose beads (Chromotek, gta-20 or rta-20, respectively) were added to the lysate after the removal of protein A agarose beads by centrifugation. After overnight incubation at 4℃, GFP- or RFP-trap agarose beads within the lysate were then collected by centrifugation and washed as following: 1) Once with low salt wash buffer (20 mM Tris-HCl pH 8.0, 150 mM NaCl, 2 mM EDTA, 0.2% SDS, and 0.5% Triton X-100), 2) once with high salt wash buffer (20 mM Tris-HCl pH 8.0, 500 mM NaCl, 2 mM EDTA, 0.2% SDS, and 0.5% Triton X-100), 3) once with LiCl wash buffer (10 mM Tris-HCl pH 8.0, 0.25 M LiCl, 1 mM EDTA, 0.5% NP-40, and 0.5% sodium deoxycholate), and 4) twice with TE buffer (10 mM Tris-HCl pH 8.0 and 1 mM EDTA). Next, immunoprecipitated DNA-protein complexes were eluted using 300 µl of elution buffer (1% SDS and 100 mM $NaHCO_3$) at 65℃

for 20 min with high-speed agitation. Then, the eluate was incubated at 65℃ for at least 6 h in the presence of 200 mM NaCl for reverse cross-linking. Proteins separated from DNA within the eluate were cleaved by using proteinase K (Roche, 03 115 828 001). Finally, DNA was purified using QIAquick PCR Purification Kit (Qiagen, 28106).

ChIP assays involving sonication for chromatin shearing were performed essentially as described by Saleh et al., (Saleh et al., 2008) with the following minor modifications. Nuclei, which were extracted as above, were resuspended in 1 ml of nuclei lysis buffer (50 mM HEPES pH 7.5, 150 mM NaCl, 1 mM EDTA, 1% SDS, 0.1% sodium deoxycholate, 1% Triton X-100, 1 mM PMSF, 0.05 μg/ml antipain, 0.5 μg/ml bestatin, 0.5 μg/ml leupeptin, and 4 μg/ml pepstatin) and incubated on ice for 10 min. Then the lysate was divided into two equal-volume aliquots, and chromatin within the aliquots was sheared by sonication with 9 cycles of 15-sec on/1-min off pulse at 33% amplitude using Sonic Dismembrator 500 (Fisher Scientific). After centrifugation, combined supernatant from the aliquots was diluted 5 folds with the nuclei lysis buffer described above. The rest of procedures was the same with the one for MNase digestion.

3.4. ChIP quantitative PCR (ChIP-qPCR) assays

The amount of DNA obtained from ChIP was measured by qPCR with primers listed in Table 4. The $2^{-\Delta\Delta C_T}$ method (Livak et al., 2001) was used to calculate the relative amount of amplified DNA in sample. The value of product amplified from each IP sample was normalized to the values generated from the respective input

DNA and *Actin 2* (*ACT2*) to assess enrichment levels.

3.5. ChIP-sequencing (ChIP-seq)

For DNA collected from ChIP involving MNase digestion, sonication was additionally performed with 14 cycles of 30-sec on/30-sec off pulse using Bioruptor Pico (Diagenode) to maximize the production of DNA in the size range proper for sequencing. ChIP DNA libraries were generated by using NEBNext® Ultra™ II DNA Library Prep with Sample Purification Beads (NEB, E7103) and NEBNext® Multiplex Oligos for Illumina® (NEB, E7335) following the supplier's instruction. ChIP-seq with 101-bp paired-end reads was performed on Illumina HiSeq 4000.

3.6. Next-generation sequencing (NGS) data analysis

NGS data analyses were mainly performed on the public server at the Galaxy (https://usegalaxy.org/) with the following details. Reads generated from ChIP-seq were first trimmed by using Trimmomatic (Bolger et al., 2014) with options of "-phred33 ILLUMINACLIP:TruSeq3-PE.fa:2:30:10 LEADING:3 TRAILING:3 SLIDINGWINDOW:4:15 MINLEN:36". Read mapping was then performed on Bowtie (Langmead et al., 2009) with options of "-S --best --strata -X 500 -m 1 --chunkmbs 500" to align the reads to the TAIR10 Arabidopsis genome. Sequence alignment/map (SAM) files generated through read mapping were converted to binary alignment/map (BAM) files by using SAMtools (Li et al., 2009). Subsequently, peak calling was executed using Model-based Analysis of ChIP-Seq

(MACS2) (Zhang et al., 2008) with options of "-f BAMPE -g 1.10e8 –bw 300 –mfold 10,100 -q 0.05". Input data were used as controls for peak calling. Differential peaks between genotypes and/or treatments were identified by using MACS2 bdgdiff with options of $\log_{10}$ likelihood ratio cutoff 0.5 and minimum length 100. By intersecting differential peaks between two biological replicates using BEDTools (Quinlan et al., 2010), overlapping peaks were identified and finally determined as NPR1:GFP- or HAC1:mCherry-peaks. Likewise, common peaks between NPR1:GFP- and HAC1:mCherry-peaks were determined by identifying overlapping peaks in the same way. Next, binding peaks were annotated with the nearest gene by using ChIPseeker (Yu et al., 2015). To visualize sequence reads using the integrative genomics viewer (IGV), bigwig files were generated as following: BAM files were deduplicated using Picard markDuplicate, and then the deduplicated BAM files were converted to bedgraph files using bedtools genomecov. Finally, bedgraph files were converted to bigwig files using bedGraphToBigWig. Enrichment scores were calculated as following: Using BamCompare, all ChIP-seq reads were normalized to reads per kilobase of bin per million mapped reads (RPKM) values with a bin size of 5 bp, and the RPKM values derived from an IP sample were then subtracted by the RPKM values derived from the corresponding input sample to obtain enrichment scores. Next, average enrichment scores between two biological repeats were calculated on BigwigCompare with bigwig files generated from BamCompare with option of bin size 5. Enrichment scores for the selected genomic regions were then calculated by using ComputeMatrix with option of bin size 5. PlotHeatmap was used to visualize enrichment scores within genomic regions enriched with NPR1:GFP or HAC1:mCherry. DNA motif sequences enriched in binding peaks were predicted

by using Multiple Em for Motif Elicitation (MEME; https://meme-suite.org/meme/; Bailey et al., 2009) with options of "-mod zoops –minw 6 –maxw 10 -markov_order 1".

Histone H3 acetylation (H3Ac) ChIP-seq and RNA-seq data used in this study were obtained from a previous study (Jin et al., 2018). Normalization of H3Ac ChIP-seq reads and calculation of H3Ac enrichment scores were performed as described above, and profile plots for H3Ac enrichment were generated by using PlotHeatmap. To visualize sequence reads of RNA-seq as IGV snapshots, bigwig files of RNA-seq were generated from BAM files on BamCoverage with options of "–bs 10 –normalizeUsing RPKM".

To analyze the transcriptomes of 1 mM SA-treated WT Col, I downloaded the raw RNA-seq data (BioProject ID PRJNA224133; Caarls et al., 2017) from the Short Read Archive (https://www.ncbi.nlm.nih.gov/sra/). The data of two biological replicates each including four technical runs were analyzed as following: Fastq files were first trimmed by using Trimmomatic with default parameters. The trimmed reads were then aligned to the TAIR10 Arabidopsis genome by using Bowtie2 with default sets, generating four BAM files from four technical runs of each sample. After merging BAM files, read counting was performed on HTSeq-count (Anders et al., 2015) with options of "-m intersection-strict –a 10". For differential expression analysis between SA- and mock-treatment samples, DESeq2 (Love et al., 2014) with parameters of $\log_2$ fold change (FC) ≥ 1 and p-value < 0.05 was used with the count data of two biological replicates to obtain differentially expressed genes (DEGs) between the two samples.

Pheatmap R package was used to visualize gene expression levels. Gene

ontology (GO) enrichment analysis was performed at the database for annotation, visualization, and integrated discovery (DAVID) (https://david.ncifcrf.gov/; Dennis et al., 2003). GO terms satisfied with FDR < 0.05 were visualized using ggplot2 R package. To construct and visualize a network of gene-sets within GO terms, Enrichment Map (Merico et al., 2010) was used with options of *p*-value < 0.005, Q-value < 0.05, and Jaccard Overlap combined coefficient > 0.25 with combined constant = 0.15 or 0.25. The network was then clustered by using AutoAnnotate (Kucera et al., 2016), and the label of each cluster was manually edited.

Table 3. Primers used for plasmid constructions.

Name	Sequence
HAC1 promoter-F	5’- CACCGATTTGGGAAAACCTGAATTCATTCGCT -3’
HAC1-R (w/o stop)	5’- ACCTGAGCCCCCAGCGACTTCTGCAGCTC -3’
NotI-TGA2 promoter-F	5’-CAAGGCGGCCGCTAATGAGTTAAGAATAGAGAATG-3’
NdeI-TGA2 promoter-R	5’-CTTGCATATGATTACTTTCTCACCACTTTTCTGTAC-3’
NdeI-TGA2-ORF-F	5’-CACCCATATGGCTGTACCAGTCCGAGAAC-3’
TGA2-ORF-R (w/o stop)	5’-CTCTCTGGGTCGAGCAGCCATAAGG-3’
AscI-mCherry-F	5’-GCGGGCGCGCCATGGTGAGCAAGGGCGAG-3’
PacI-mCherry-stop-R	5’-GGATTAATTAATCACTTGTACAGCTCGTCCATGCCGCCGGT-3’

Table 4. Primers used for ChIP-qPCR.

Gene	Name	Sequence
ACT2	F	5’-TGATGCACTTGTGTGTGACAA-3’
	R	5’-AAAGAGGCATCAATTCGATCA-3’
AGC2-1	A-F	5’-GCTTTAACGCTCGAAGGCCG-3’
	A-R	5’-GACAAACACGTGGTGTTCTAGAG-3’
	B-F	5’-GCGGAGCTTGTATTAGCACTTG-3’
	B-R	5’-GCGGCGTTCTTGGAGCTAGATTTG-3’
AT3G28510	A-F	5’-GGTGTGCCACGTTAATTTAGACC-3’
	A-R	5’-GTCGTCTTGTTTAGTATGCTCGG-3’
	B-F	5’-GATCCCAAAGAGCAAGCCTAG-3’
	B-R	5’-CTACATGTGTTCAGGAAACTACATG-3’
AT3G46080	A-F	5’-GGAGGAAAGCACCAAGAACATTCC-3’
	A-R	5’-CCATTTGTGACTTGCTGCGTAAGG-3’
	B-F	5’-GTGAGAAAGCCTCACCAGGCAC-3’
	B-R	5’-CGAATCTAAGTCCAAACAAGCCACTC-3’
GRXS13	A-F	5’-GGACGTGTACTGGGTAGTGGGTAC-3’
	A-R	5’-GTCTTCGTAAGGTTACGTTTTATGG-3’
	B-F	5’-GATCAAGCAACCTAGTTGTGATGG-3’
	B-R	5’-CTCAACCACCACTGGATTCACGCC-3’
IBH1	A-F	5’-GAGAGAAAGGAAAGTGGAGGTG-3’
	A-R	5’-GGAGTGAAACCAAATGAATAAGAAGG-3’
	B-F	5’-CCTCCAATCCCTCTCAAATCTCAG-3’
	B-R	5’-GCAAGAGGGCTCTGCTCCATAG-3’
INVH	A-F	5’-GCAAGCATCGTCTTTCACGG-3’
	A-R	5’-CAAGTGGTCTCCCCACGTTC-3’
	B-F	5’-GCAGAAAAGTACTGACCAGAATCAAC-3’
	B-R	5’-GTGTTGTGGTTCCAGAGTTGG-3’
LSU3	A-F	5’-CGTGTTTCATTGGTGCGACG-3’
	A-R	5’-GAATCGGTGAACGTCGTGGAG-3’
	B-F	5’-GAACGGAGAGTTGGAGAGAGAA-3’
	B-R	5’-GCCTGATCTAAAGACTCGACCT-3’
LURP1	A-F	5’-GCATGTATCTACTATCTCTCCCACCT-3’
	A-R	5’-CTTAGAGCATCTCCAGTGGTTGGT-3’
	B-F	5’-CGGAGGAGGGTGCTCTACTATAC-3’
	B-R	5’-CTTCTCCTCTACGTTGTTAGCC-3’

NHO1	A-F	5’-CTCCACCGGATTGGATGATG-3’
	A-R	5’-CCAATGAAAGAGAGCCACGTG-3’
	B-F	5’-GCATTGTCCGTGAAGCATTGG-3’
	B-R	5’-GCTATCAAGAAAGGGGATGCC-3’
NIMIN-1	A-F	5’-GTGACATCATCTCGTAACCGC-3’
	A-R	5’-AGGGACCAGGGGTAAAAGAGT-3’
	B-F	5’-CCTAGAGACCATGAGCAAGGATG-3’
	B-R	5’-CCGTGCTTCTTGATAGTGTTTG-3’
SARD1	A-F	5’-CCAATCGGGTGGGAAGATCG-3’
	A-R	5’-CTGGCAATATCCAAAGAAGTCCG-3’
	B-F	5’-CTTGCAGGCCAATTTCCAGTG-3’
	B-R	5’-CTTACAACTTTTCTAATAACGGGCTC-3’
SPL8	A-F	5’-CCCACGCCATTACCAATTACAAAA-3’
	A-R	5’-CTCACGCGCTGCTATCTCTAC-3’
	B-F	5’-CACTACCACAGAAGGCACAAAG-3’
	B-R	5’-GTACGGACGAAGAGAAGAGAAGATAG-3’
WRKY38	A-F	5’-GTTCTGACGTCAATCTGCTGAATC-3’
	A-R	5’-GCGATGTAGCTGGCGAGTGG-3’
	B-F	5’-TCACGCATATAAGTCTAGCAGAGC-3’
	B-R	5’-ACGTTCCCAAATGACTTTGC-3’
WRKY62	A-F	5’-TTATTCGCCGTTCCATCTTC-3’
	A-R	5’-TCGTCGCGTAAAATCAACTG-3’
	B-F	5’-CCAAGTCCGTCCTCCATTGTT-3’
	B-R	5’-AGCTCTCAAGCACAGGAGAAGA-3’
WRKY63(ABO3)	A-F	5’-CTCTTCATTTGTCCTCGACTGG-3’
	A-R	5’-GATTTACACACATGTTCAATGTTGAC-3’
	B-F	5’-CATTTTCGAGCTAGGGAACTTTC-3’
	B-R	5’-CAGCCTTGTGATCGATGTTTG-3’
WRKY70	A-F	5’-GGACCCTAAGTTTGGATTTCAGC-3’
	A-R	5’-TGTGTGAGGAAATGAGATGGAAC-3’
	B-F	5’-AGGAGATGGGTTCGAAGGTA-3’
	B-R	5’-TCGTTGAAGGCCATGACTTA-3’
WRKY75	A-F	5’-GCACGGATAAAATGATGACGTTCGAC-3’
	A-R	5’-GCATGCACCGACGTAGAACACAG-3’
	B-F	5’-GGAATTCAGGTGGATCGGTCTG-3’
	B-R	5’-TCCTTGTTTGAAACGCATACCTTTGTT-3’

4. Results

4.1. NPR1 is usually targeted to promoters or promoter-vicinity regions in an SA-dependent manner.

To gain an unbiased, holistic view of the role of NPR1 in SA-induced transcriptional reprogramming required for plant immunity, I investigate genome-wide direct targets of NPR1 in Arabidopsis. For this, I performed chromatin immunoprecipitation followed by sequencing (ChIP-seq) using seedlings expressing green fluorescent protein (GFP)-fused NPR1 under a native *NPR1* promoter (*pNPR1::NPR1:GFP*, hereafter *NPR1:GFP*) and treated or not with the synthetic SA analog, INA. For the first two ChIP-seq biological replicates (hereafter rep1&2), I performed immunoprecipitation (IP) with 1% sodium dodecyl sulfate (SDS), which might improve the signal-to-noise ratio in peak calling and thus only detect robust binding. For IP of the other two biological replicates (hereafter rep3&4), I used 0.02% SDS to also detect weaker binding. In addition, as sonication might dissociate protein complexes, I used two different chromatin fragmentation methods: sonication for rep1&2 and chromatin digestion by micrococcal nuclease (MNase) treatment for rep3&4. Consequently, I generated two different ChIP-seq datasets, each including two biological repeats, to identify genome-wide NPR1 targets with or without INA treatment. Then, for each dataset, I called NPR1 peaks by identifying common peaks among the two biological replicates.

To study the genome-wide distribution of NPR1, I classified genomic regions containing NPR1 peaks. In the case of the rep1&2 dataset, 96% of NPR1

peaks identified without INA treatment were located within the promoter regions and 76% of NPR1 peaks identified with INA treatment were located within promoters or promoter-vicinity regions (Figure 8A). Likewise, 92% or 79% of NPR1 peaks identified without or with INA treatment, respectively, from the rep3&4 dataset were located within promoters or promoter-vicinity regions (Figure 8B). As expected from my experimental design, I identified more NPR1 peaks from the rep3&4 dataset (Figure 8B) than from the rep1&2 dataset (Figure 8A). Comparative analyses using enrichment scores obtained from *NPR1:GFP* and wild-type (WT) Columbia-0 (Col-0) plants showed that the identified peaks are specific to the *NPR1:GFP* plants (Figure 8A and B), confirming the reliability of my peak calling. Thus, NPR1 peaks reside usually within promoters or promoter-vicinity regions of the Arabidopsis genome.

To identify genome-wide NPR1-target genes, I assigned NPR1 peaks obtained from INA treated (+INA) or untreated (−INA) plants to the nearest genes, which I named NPR1+INA or NPR1−INA targets, respectively (Table 5). Comparisons between NPR1+INA and NPR1−INA targets revealed that 93% (328/353 of the rep1&2 dataset) or 97% (988/1,021 of the rep3&4 dataset) of the NPR1+INA targets show INA-dependent NPR1-targeting activity, whereas the remaining 7% (25/353 of the rep1&2 dataset) or 3% (33/1,021 of the rep3&4 dataset) show INA-independent NPR1-targeting activity (Figure 8C). In addition, 88% (311/353) of the NPR1+INA targets identified from the rep1&2 dataset were also identified as NPR1+INA targets from the rep3&4 dataset (Figure 8D), indicating that most robust NPR1+INA targets were reproducibly identified in the two experimental conditions. Together, these results indicate that NPR1 targeting is

largely INA (SA analog) dependent.

As Nomoto et al. (Nomoto et al., 2021) recently reported the genome-wide NPR1 targets in Arabidopsis plants overexpressing *NPR1* and co-treated with SA and JA (Nomoto et al., 2021), I compared their data with the NPR1 targets I identified. Only 25% (626/2,554) of the NPR1 targets reported by Nomoto et al. (Nomoto et al., 2021) were among my NPR1+INA targets (Figure 8D). This large discrepancy is probably due to differences in the experimental conditions: Nomoto et al. (Nomoto et al., 2021) used Arabidopsis plants constitutively overexpressing *NPR1* and treated with SA and JA for ChIP-seq, while I used Arabidopsis expressing *NPR1* from its native promoter and treated only with INA. Therefore, I identified INA-specific genome-wide NPR1 targets in cells natively expressing *NPR1*.

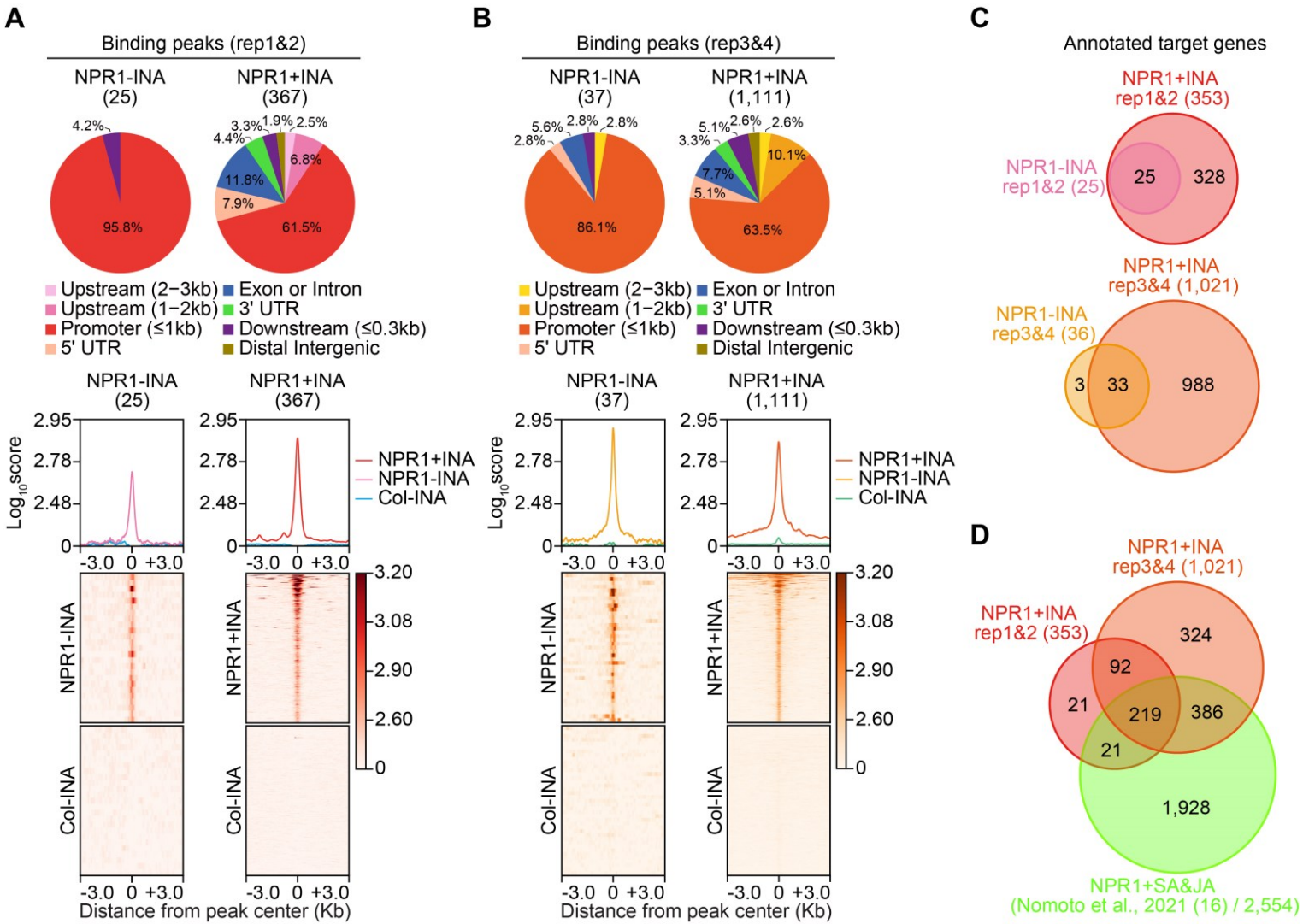
A
Binding peaks (rep1&2)
NPR1-INA (25)
NPR1+INA (367)
4.2%
95.8%
3.3%
1.9%
2.5%
4.4%
6.8%
11.8%
7.9%
61.5%
Upstream (2−3kb)
Upstream (1−2kb)
Promoter (≤1kb)
5' UTR
Exon or Intron
3' UTR
Downstream (≤0.3kb)
Distal Intergenic
NPR1-INA (25)
NPR1+INA (367)
Log10score
2.95
2.78
2.48
0
-3.0 0 +3.0
NPR1+INA
NPR1-INA
Col-INA
NPR1-INA
Col-INA
3.20
3.08
2.90
2.60
0
Distance from peak center (Kb)
B
Binding peaks (rep3&4)
NPR1-INA (37)
NPR1+INA (1,111)
5.6%
2.8%
2.8%
2.8%
86.1%
5.1%
2.6%
2.6%
3.3%
10.1%
7.7%
5.1%
63.5%
Upstream (2−3kb)
Upstream (1−2kb)
Promoter (≤1kb)
5' UTR
Exon or Intron
3' UTR
Downstream (≤0.3kb)
Distal Intergenic
NPR1-INA (37)
NPR1+INA (1,111)
Log10score
NPR1+INA
NPR1-INA
Col-INA
Distance from peak center (Kb)
C
Annotated target genes
NPR1+INA rep1&2 (353)
NPR1-INA rep1&2 (25)
25
328
NPR1+INA rep3&4 (1,021)
NPR1-INA rep3&4 (36)
3
33
988
D
NPR1+INA rep3&4 (1,021)
NPR1+INA rep1&2 (353)
324
92
21
219
386
21
1,928
NPR1+SA&JA (Nomoto et al., 2021 (16) / 2,554)

Figure 8. NPR1 is targeted usually to promoters or promoter-vicinity regions in a salicylic acid (SA)-dependent manner.

(**A**-**B**) Genome-wide distribution and enrichment of NPR1:GFP binding peaks. Pie-charts illustrate the distribution of genomic regions enriched with NPR1:GFP. Profile plots show the average scores of NPR1:GFP enrichment in regions from the 3 kb upstream to the 3 kb downstream of NPR1:GFP-peak centers. Heatmaps visualize enrichment scores corresponding to individual peaks. NPR1:GFP peaks were identified through two biological repeats of chromatin immunoprecipitation followed by sequencings (ChIP-seqs) using *pNPR1::NPR1:GFP* transgenic (NPR1) or WT Col plants and anti-GFP antibody in the absence (NPR1−INA or Col−INA) or presence (NPR1+INA) of 2,6-dichloroisonicotinic acid (INA; synthetic SA analog) treatment. Peak numbers are indicated in parentheses below the names of binding peaks. All enrichment scores presented as profile plots or heatmaps are $\log_{10}$ values of the means of enrichment levels derived from two biological repeats and were compared to the enrichment scores of Col−INA, a negative control. To calculate enrichment scores, ChIP-seq reads were normalized using reads per kilobase of bin per million mapped reads (RPKM) method with a bin size of 5 bp. The RPKM values derived from each IP sample were then subtracted by the RPKM values derived from the input sample to calculate enrichment levels. The extended regions from the peak centers were equally divided into 5 bp bins. (**A**) or (**B**) presents data analyzed from the replicates 1 and 2 (rep1&2) or replicate 3 and 4 (rep3&4), respectively. The two datasets each consisting of two biological repeats were derived from ChIP-seqs performed at different experimental conditions (see Materials and Methods section).

(**C**) Venn diagrams showing the numbers and overlaps between NPR1-target genes identified under –INA or +INA conditions. Total numbers of annotated targets are indicated in parentheses.

(**D**) Venn diagram illustrating overlaps and differences in NPR1-target genes identified by different ChIP-seqs. The NPR1-target genes identified from my two datasets (rep1&2 and rep3&4) were also compared to the NPR1-target genes reported by Nomoto et al. (Nomoto et al., 2021), which was obtained by ChIP-seq after the co-treatment (SA&JA) of SA and jasmonic acid (JA).

Table 5. Representative genomic regions of NPR1 peaks, and the list of NPR1-target genes annotated from the NPR1 peaks.

Group	Chrom	Start	End	Annotation	GeneID	Gene Symbol	Gene Model Type
NPR1-INA rep1&2	Chr1	436810	437014	Promoter (<=1kb)	AT1G02230	NAC004	protein_coding
NPR1-INA rep1&2	Chr1	498639	499081	Promoter (<=1kb)	AT1G02450	NIMIN1	protein_coding
NPR1-INA rep1&2	Chr1	6927519	6927746	Promoter (<=1kb)	AT1G19960		protein_coding
NPR1-INA rep1&2	Chr1	10014018	10014256	Promoter (<=1kb)	AT1G28480	GRX480	protein_coding
NPR1-INA rep1&2	Chr1	30295788	30295940	Downstream (<1kb)	AT1G80590	WRKY66	protein_coding
NPR1-INA rep1&2	Chr2	9338043	9338604	Promoter (<=1kb)	AT2G21905		pseudogene
NPR1-INA rep1&2	Chr2	17002500	17002802	Promoter (<=1kb)	AT2G40750	WRKY54	protein_coding
NPR1-INA rep1&2	Chr3	7846753	7846989	Promoter (<=1kb)	AT3G22231	PCC1	protein_coding
NPR1-INA rep1&2	Chr3	7855732	7856160	Promoter (<=1kb)	AT3G22235	ATHCYSTM8	protein_coding
NPR1-INA rep1&2	Chr3	9470977	9471202	Promoter (<=1kb)	AT3G25882	NIMIN-2	protein_coding
NPR1-INA rep1&2	Chr3	11190741	11191153	Promoter (<=1kb)	AT3G29240	DUF179-3	protein_coding
NPR1-INA rep1&2	Chr3	20910594	20910866	Promoter (<=1kb)	AT3G56400	WRKY70	protein_coding
NPR1-INA rep1&2	Chr4	10698696	10698905	Promoter (<=1kb)	AT4G19660		protein_coding
NPR1-INA rep1&2	Chr4	15379173	15379450	Promoter (<=1kb)	AT4G08565		long_noncoding_rna
NPR1-INA rep1&2	Chr4	16740689	16740830	Promoter (<=1kb)	AT4G35180	LHT7	protein_coding
NPR1-INA rep1&2	Chr5	352451	352911	Promoter (<=1kb)	AT5G01900	WRKY62	protein_coding
NPR1-INA rep1&2	Chr5	816635	816922	Promoter (<=1kb)	AT5G03350	SAI-LLP1	protein_coding
NPR1-INA rep1&2	Chr5	2860892	2861083	Promoter (<=1kb)	AT5G08790	ATAF2	protein_coding
NPR1-INA rep1&2	Chr5	7497765	7498207	Promoter (<=1kb)	AT5G22570	WRKY38	protein_coding
NPR1-INA rep1&2	Chr5	8377763	8378078	Promoter (<=1kb)	AT5G24530	DMR6	protein_coding
NPR1-INA rep1&2	Chr5	18228169	18228516	Promoter (<=1kb)	AT5G45110	NPR3	protein_coding
NPR1-INA rep1&2	Chr5	18276479	18276915	Promoter (<=1kb)	AT5G45180		protein_coding
NPR1-INA rep1&2	Chr5	25528190	25528465	Promoter (<=1kb)	AT5G63790		protein_coding
NPR1-INA rep1&2	Chr5	25907995	25908182	Promoter (<=1kb)	AT5G64810	WRKY51	protein_coding
NPR1-INA rep1&2	Chr5	26721226	26721497	Promoter (<=1kb)	AT5G66910	NRG1.2	protein_coding

Group	Chrom	Start	End	Annotation	GeneID	Gene Symbol	Gene Model Type
NPR1+INA rep1&2	Chr1	498425	499226	Promoter (<=1kb)	AT1G02450	NIMIN1	protein_coding
NPR1+INA rep1&2	Chr1	957895	958227	5' UTR	AT1G03800	ERF10	protein_coding
NPR1+INA rep1&2	Chr1	24831255	24831754	Promoter (1-2kb)	AT1G66560	WRKY64	protein_coding
NPR1+INA rep1&2	Chr1	26043144	26043386	Promoter (<=1kb)	AT1G69270	RPK1	protein_coding
NPR1+INA rep1&2	Chr1	27638269	27638705	Downstream (<1kb)	AT1G73500	MKK9	protein_coding
NPR1+INA rep1&2	Chr1	30380399	30380893	Promoter (2-3kb)	AT1G80840	WRKY40	protein_coding
NPR1+INA rep1&2	Chr2	6210525	6211193	Promoter (<=1kb)	AT2G00570		novel_transcribed_region
NPR1+INA rep1&2	Chr2	6242944	6243160	Promoter (<=1kb)	AT2G14610	PR1	protein_coding
NPR1+INA rep1&2	Chr2	9340513	9340706	Promoter (<=1kb)	AT2G21910	CYP96A5	protein_coding
NPR1+INA rep1&2	Chr2	12112760	12112867	Promoter (1-2kb)	AT2G28350	ARF10	protein_coding
NPR1+INA rep1&2	Chr2	16705923	16706136	Promoter (1-2kb)	AT2G09105		long_noncoding_rna
NPR1+INA rep1&2	Chr2	17002344	17002936	Promoter (<=1kb)	AT2G40750	WRKY54	protein_coding
NPR1+INA rep1&2	Chr3	1063830	1064239	Promoter (<=1kb)	AT3G04070	NAC047	protein_coding
NPR1+INA rep1&2	Chr3	5518279	5519021	Promoter (<=1kb)	AT3G16280	ERF036	protein_coding
NPR1+INA rep1&2	Chr3	6801719	6802023	3' UTR	AT3G19580	ZF2	protein_coding
NPR1+INA rep1&2	Chr3	9470684	9471326	Promoter (<=1kb)	AT3G25882	NIMIN-2	protein_coding
NPR1+INA rep1&2	Chr3	17178039	17178509	Downstream (<1kb)	AT3G07505		long_noncoding_rna
NPR1+INA rep1&2	Chr3	20910389	20911199	Promoter (<=1kb)	AT3G56400	WRKY70	protein_coding
NPR1+INA rep1&2	Chr4	7305847	7306374	Exon (AT4G12290.	AT4G12290	CUAO	protein_coding
NPR1+INA rep1&2	Chr4	10591140	10591283	Promoter (<=1kb)	AT4G06885		long_noncoding_rna
NPR1+INA rep1&2	Chr4	12395921	12396322	Promoter (1-2kb)	AT4G23810	WRKY53	protein_coding
NPR1+INA rep1&2	Chr4	15381413	15381628	Promoter (1-2kb)	AT4G31800	WRKY18	protein_coding
NPR1+INA rep1&2	Chr4	16344777	16345172	Promoter (<=1kb)	AT4G34131	UGT73B3	protein_coding
NPR1+INA rep1&2	Chr4	16801245	16801634	Promoter (<=1kb)	AT4G35310	CPK5	protein_coding
NPR1+INA rep1&2	Chr5	816217	817089	Promoter (<=1kb)	AT5G03350	SAI-LLP1	protein_coding
NPR1+INA rep1&2	Chr5	4151550	4151725	Promoter (<=1kb)	AT5G13080	WRKY75	protein_coding
NPR1+INA rep1&2	Chr5	4431138	4431276	Promoter (<=1kb)	AT5G13730	SIG4	protein_coding
NPR1+INA rep1&2	Chr5	18227971	18228901	Promoter (<=1kb)	AT5G45110	NPR3	protein_coding
NPR1+INA rep1&2	Chr5	24766482	24766862	3' UTR	AT5G61600	ERF104	protein_coding
NPR1+INA rep1&2	Chr5	25805968	25806479	Promoter (<=1kb)	AT5G64550		protein_coding

Group	Chrom	Start	End	Annotation	GeneID	Gene Symbol	Gene Model Type
NPR1-INA rep3&4	Chr1	436877	437114	Promoter (<=1kb)	AT1G02230	NAC004	protein_coding
NPR1-INA rep3&4	Chr1	498612	499140	Promoter (<=1kb)	AT1G02450	NIMIN1	protein_coding
NPR1-INA rep3&4	Chr1	3131407	3131520	Promoter (<=1kb)	AT1G09660	ATKH1	protein_coding
NPR1-INA rep3&4	Chr1	10014105	10014223	5' UTR	AT1G28480	GRX480	protein_coding
NPR1-INA rep3&4	Chr1	23855071	23855343	Exon (AT1G08667.	AT1G08667		antisense_long_noncoding_rna
NPR1-INA rep3&4	Chr1	24831304	24831482	Promoter (2-3kb)	AT1G66560	WRKY64	protein_coding
NPR1-INA rep3&4	Chr1	27749347	27749559	Promoter (<=1kb)	AT1G73805	SARD1	protein_coding
NPR1-INA rep3&4	Chr1	30295770	30295986	Downstream (<1kb)	AT1G80590	WRKY66	protein_coding
NPR1-INA rep3&4	Chr2	801384	801511	Promoter (<=1kb)	AT2G02810	UTR1	protein_coding
NPR1-INA rep3&4	Chr2	9337938	9338642	Promoter (<=1kb)	AT2G21905		pseudogene
NPR1-INA rep3&4	Chr2	17002490	17002849	Promoter (<=1kb)	AT2G40750	WRKY54	protein_coding
NPR1-INA rep3&4	Chr2	18150888	18151528	Promoter (<=1kb)	AT2G43820	UGT74F2	protein_coding
NPR1-INA rep3&4	Chr3	2749252	2749436	Promoter (<=1kb)	AT3G09010		protein_coding
NPR1-INA rep3&4	Chr3	7846698	7847019	Promoter (<=1kb)	AT3G22231	PCC1	protein_coding
NPR1-INA rep3&4	Chr3	7855736	7856193	Promoter (<=1kb)	AT3G22235	ATHCYSTM8	protein_coding
NPR1-INA rep3&4	Chr3	9470898	9471183	Promoter (<=1kb)	AT3G25882	NIMIN-2	protein_coding
NPR1-INA rep3&4	Chr3	11190774	11191134	Promoter (<=1kb)	AT3G29240	DUF179-3	protein_coding
NPR1-INA rep3&4	Chr3	20910483	20910997	Promoter (<=1kb)	AT3G56400	WRKY70	protein_coding
NPR1-INA rep3&4	Chr4	10698677	10698924	Promoter (<=1kb)	AT4G19660		protein_coding
NPR1-INA rep3&4	Chr4	15379206	15379372	Promoter (<=1kb)	AT4G08565		long_noncoding_rna
NPR1-INA rep3&4	Chr4	16740638	16740866	Promoter (<=1kb)	AT4G35180	LHT7	protein_coding
NPR1-INA rep3&4	Chr5	352353	352897	Promoter (<=1kb)	AT5G01900	WRKY62	protein_coding
NPR1-INA rep3&4	Chr5	816825	816895	Promoter (<=1kb)	AT5G03350	SAI-LLP1	protein_coding
NPR1-INA rep3&4	Chr5	2860825	2861040	Promoter (<=1kb)	AT5G08790	ATAF2	protein_coding
NPR1-INA rep3&4	Chr5	7497673	7498299	Promoter (<=1kb)	AT5G22570	WRKY38	protein_coding
NPR1-INA rep3&4	Chr5	8377571	8378161	Promoter (<=1kb)	AT5G24530	DMR6	protein_coding
NPR1-INA rep3&4	Chr5	8381339	8381560	Intron (AT5G24530	AT5G24530	DMR6	protein_coding
NPR1-INA rep3&4	Chr5	18228136	18228478	Promoter (<=1kb)	AT5G45110	NPR3	protein_coding
NPR1-INA rep3&4	Chr5	25908034	25908204	Promoter (<=1kb)	AT5G64810	WRKY51	protein_coding
NPR1-INA rep3&4	Chr5	26721262	26721416	Promoter (<=1kb)	AT5G66910	NRG1.2	protein_coding

Group	Chrom	Start	End	Annotation	GeneID	Gene Symbol	Gene Model Type
NPR1+INA rep3&4	Chr1	1729049	1730212	Promoter (<=1kb)	AT1G04427		long_noncoding_rna
NPR1+INA rep3&4	Chr1	1882587	1882770	Promoter (<=1kb)	AT1G06160	ORA59	protein_coding
NPR1+INA rep3&4	Chr1	3804116	3804285	Promoter (<=1kb)	AT1G11310	MLO2	protein_coding
NPR1+INA rep3&4	Chr1	5338430	5338592	Promoter (<=1kb)	AT1G15520	ABCG40	protein_coding
NPR1+INA rep3&4	Chr1	19697261	19697411	3' UTR	AT1G52890	NAC019	protein_coding
NPR1+INA rep3&4	Chr1	24766944	24767314	Distal Intergenic	AT1G66390	MYB90	protein_coding
NPR1+INA rep3&4	Chr2	2289659	2289787	Promoter (<=1kb)	AT2G05940	RIPK	protein_coding
NPR1+INA rep3&4	Chr2	10119669	10119749	Downstream (<1kb)	AT2G23770	LYK4	protein_coding
NPR1+INA rep3&4	Chr2	12822811	12822981	Exon (AT2G30040.	AT2G30040	MAPKKK14	protein_coding
NPR1+INA rep3&4	Chr2	17003868	17003979	Promoter (1-2kb)	AT2G40750	WRKY54	protein_coding
NPR1+INA rep3&4	Chr2	18493808	18494594	Promoter (<=1kb)	AT2G44840	ERF13	protein_coding
NPR1+INA rep3&4	Chr2	19486748	19486999	Promoter (<=1kb)	AT2G47490	NDT1	protein_coding
NPR1+INA rep3&4	Chr3	7115729	7115832	Promoter (<=1kb)	AT3G20410	CPK9	protein_coding
NPR1+INA rep3&4	Chr3	7676220	7676277	Exon (AT3G21781.	AT3G21780	UGT71B6	protein_coding
NPR1+INA rep3&4	Chr3	10910541	10910663	Promoter (<=1kb)	AT3G28910	MYB30	protein_coding
NPR1+INA rep3&4	Chr3	19121147	19121245	Promoter (<=1kb)	AT3G51550	FER	protein_coding
NPR1+INA rep3&4	Chr3	21007541	21009447	Promoter (<=1kb)	AT3G56710	SIB1	protein_coding
NPR1+INA rep3&4	Chr3	22929551	22929905	Exon (AT3G61910.	AT3G61910	NAC066	protein_coding
NPR1+INA rep3&4	Chr4	6891888	6891982	Promoter (<=1kb)	AT4G11330	MPK5	protein_coding
NPR1+INA rep3&4	Chr4	8294142	8294240	Promoter (<=1kb)	AT4G14400	ACD6	protein_coding
NPR1+INA rep3&4	Chr4	14076918	14077185	Promoter (<=1kb)	AT4G28490	HAE	protein_coding
NPR1+INA rep3&4	Chr4	15943393	15943503	Promoter (1-2kb)	AT4G33040	ROXY21	protein_coding
NPR1+INA rep3&4	Chr4	16739481	16739617	Exon (AT4G35180.	AT4G35180	LHT7	protein_coding
NPR1+INA rep3&4	Chr4	17762389	17762496	Promoter (2-3kb)	AT4G37780	MYB87	protein_coding
NPR1+INA rep3&4	Chr5	351793	353805	Promoter (<=1kb)	AT5G01900	WRKY62	protein_coding
NPR1+INA rep3&4	Chr5	2354689	2354926	Promoter (<=1kb)	AT5G00355		novel_transcribed_region
NPR1+INA rep3&4	Chr5	3140619	3140786	Promoter (<=1kb)	AT5G10030	TGA4	protein_coding
NPR1+INA rep3&4	Chr5	7377575	7377747	Promoter (<=1kb)	AT5G22290	NAC089	protein_coding
NPR1+INA rep3&4	Chr5	8377429	8379249	Promoter (<=1kb)	AT5G24530	DMR6	protein_coding
NPR1+INA rep3&4	Chr5	19398613	19399261	Exon (AT5G47910.	AT5G47910	RBOHD	protein_coding

4.2. SA-dependent NPR1 targeting primarily induces the transcriptional activation of genes encoding transcription factors

To determine the influence of NPR1 targeting on transcription at the genome level, I combined the ChIP-seq data from this study with the RNA-seq data from a previous study (Jin et al., 2018). Hundreds of NPR1+INA target genes were *NPR1*-dependently upregulated upon INA treatment (Figure 9A). In the case of the rep1&2 dataset, 33% (116/353) of the NPR1+INA targets were downregulated and 7% (23/353) were upregulated by the *npr1-1* mutation in the presence of INA. In addition, 89% (103/116) of the NPR1+INA targets downregulated by *npr1-1* were induced by INA treatment in the WT. I obtained similar results from the rep3&4 dataset: 27% (278/1,021) and 6% (63/1,021) of the NPR1+INA targets were downregulated and upregulated, respectively, by *npr1-1* in the presence of INA, and 83% (230/278) of the downregulated genes were induced by INA in the WT. I then analyzed the expression patterns of *NPR1*-dependently expressed NPR1+INA targets. Most of these genes were upregulated in an *NPR1*-dependent manner under the +INA condition (Figure 9B): 84% (116/139 of the rep1&2 dataset) or 82% (278/341 of the rep3&4 dataset) of the *NPR1*-dependently expressed NPR1+INA targets were transcriptionally activated in the presence of INA. Thus, SA-induced NPR1 targeting generally results in the transcriptional activation rather than repression of the direct targets.

Next, I functionally classified the genes that are targeted and directly regulated by NPR1 to establish the primary role of NPR1 in SA-triggered immunity at the genome level. As NPR1 targets are generally upregulated after INA treatment (Figure 9B) and NPR1 positively regulates SA-triggered immunity,

I focused on the NPR1+INA target genes showing *NPR1*-dependent upregulation by INA treatment. Gene Ontology (GO) enrichment analysis revealed that NPR1 directly activates genes involved in various phytohormone-mediated signaling pathways, responses to biotic or abiotic stresses, and transcription (Figure 9C and 10A). I then clustered the GO terms based on overlapping gene sets and found that genes encoding DNA-binding factors were most abundant (Figure 9D and 10B). These results indicate that NPR1 primarily activates transcription factor-encoding genes upon SA signaling, and these factors might in turn activate diverse downstream defense genes. Consistent with this idea, when I clustered GO terms for genes that are *NPR1*-dependently upregulated but not identified as direct NPR1 targets, genes related to a variety of defense-related functions except for DNA binding were classified (Figure 10C and D). Genes involved in chloroplast activity, tissue development, and cell division were abundant among the genes indirectly downregulated by NPR1 (Figure 10E and F). The transcription factor genes directly targeted and upregulated by NPR1 were from diverse families (Figure 9E). WRKY family members accounted for about one-third of these transcription factors. In sum, these results indicate that the primary role of NPR1 in SA-induced transcriptional reprogramming is to directly activate the expression of transcription factor-encoding genes and thus trigger transcriptional cascades required for plant immunity.

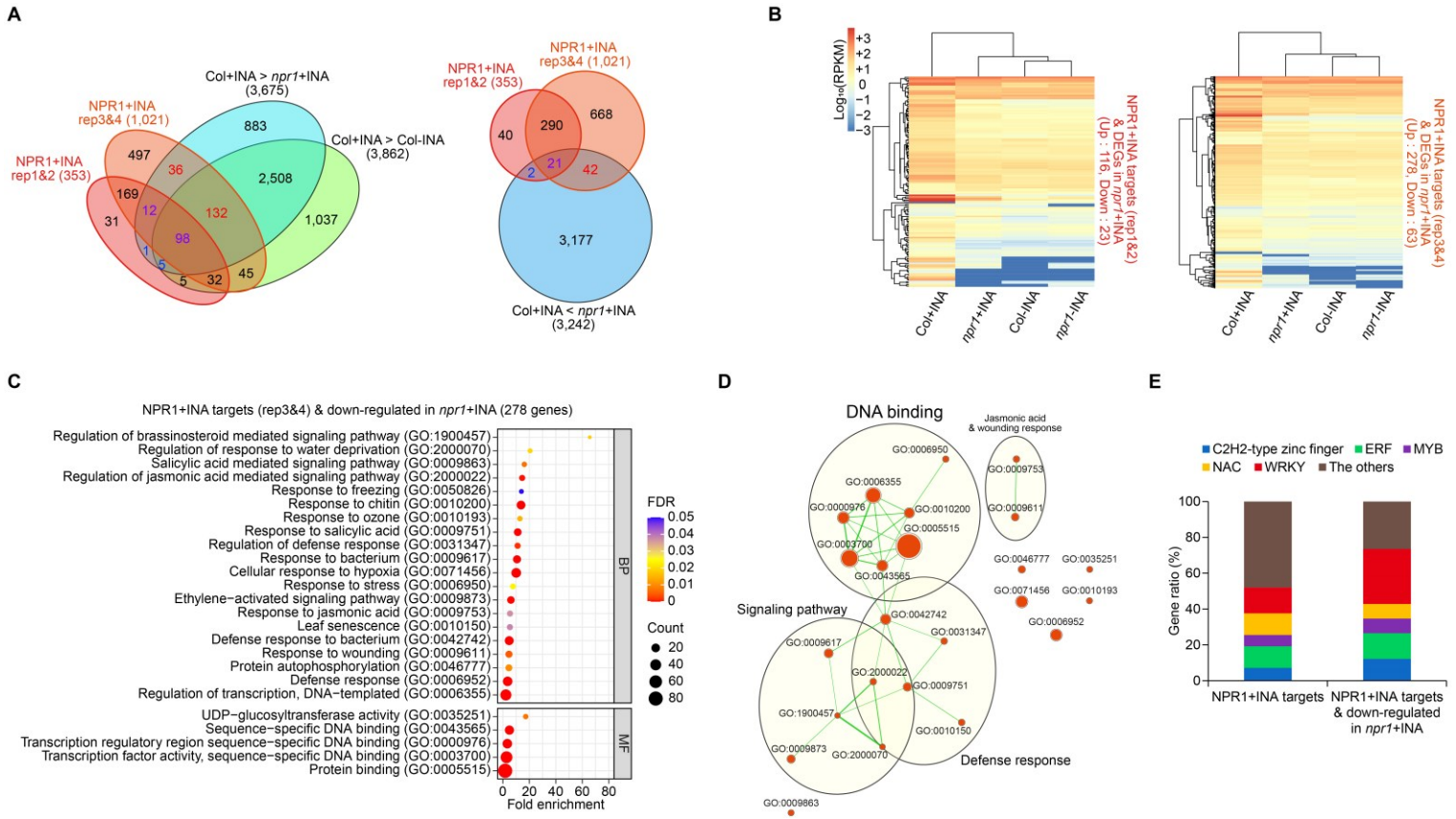
A
Col+INA > npr1+INA
(3,675)
NPR1+INA
rep3&4 (1,021)
Col+INA > Col-INA
(3,862)
NPR1+INA
rep1&2 (353)
883
497
36
2,508
169
12
132
1,037
31
98
1
5
5
32
45
NPR1+INA
rep1&2 (353)
NPR1+INA
rep3&4 (1,021)
40
290
668
21
2
42
3,177
Col+INA < npr1+INA
(3,242)
B
Log10(RPKM)
+3
+2
+1
0
−1
−2
−3
NPR1+INA targets (rep1&2)
& DEGs in npr1+INA
(Up : 116, Down : 23)
NPR1+INA targets (rep3&4)
& DEGs in npr1+INA
(Up : 278, Down : 63)
Col+INA
npr1+INA
Col-INA
npr1-INA
C
NPR1+INA targets (rep3&4) & down-regulated in npr1+INA (278 genes)
Regulation of brassinosteroid mediated signaling pathway (GO:1900457)
Regulation of response to water deprivation (GO:2000070)
Salicylic acid mediated signaling pathway (GO:0009863)
Regulation of jasmonic acid mediated signaling pathway (GO:2000022)
Response to freezing (GO:0050826)
Response to chitin (GO:0010200)
Response to ozone (GO:0010193)
Response to salicylic acid (GO:0009751)
Regulation of defense response (GO:0031347)
Response to bacterium (GO:0009617)
Cellular response to hypoxia (GO:0071456)
Response to stress (GO:0006950)
Ethylene−activated signaling pathway (GO:0009873)
Response to jasmonic acid (GO:0009753)
Leaf senescence (GO:0010150)
Defense response to bacterium (GO:0042742)
Response to wounding (GO:0009611)
Protein autophosphorylation (GO:0046777)
Defense response (GO:0006952)
Regulation of transcription, DNA−templated (GO:0006355)
UDP−glucosyltransferase activity (GO:0035251)
Sequence−specific DNA binding (GO:0043565)
Transcription regulatory region sequence−specific DNA binding (GO:0000976)
Transcription factor activity, sequence−specific DNA binding (GO:0003700)
Protein binding (GO:0005515)
BP
MF
0 20 40 60 80
Fold enrichment
FDR
0.05
0.04
0.03
0.02
0.01
0
Count
20
40
60
80
D
DNA binding
Jasmonic acid
& wounding response
GO:0006950
GO:0006355
GO:0009753
GO:0000976
GO:0010200
GO:0009611
GO:0005515
GO:0003700
GO:0043565
GO:0046777
GO:0035251
GO:0071456
GO:0010193
GO:0006952
Signaling pathway
GO:0042742
GO:0031347
GO:0009617
GO:2000022
GO:0009751
GO:1900457
GO:0010150
GO:0009873
GO:2000070
Defense response
GO:0009863
E
C2H2-type zinc finger
ERF
MYB
NAC
WRKY
The others
Gene ratio (%)
100
80
60
40
20
0
NPR1+INA targets
NPR1+INA targets
& down-regulated
in npr1+INA

Figure 9. Direct NPR1 targets include hundreds of genes NPR1-dependently activated during SA-triggered immunity and are enriched mostly with DNA-binding factor encoding genes.

(**A**) Venn diagrams illustrating the numbers of genes that are targeted and regulated by NPR1 after INA treatment (+INA). Genes showing *NPR1*-dependent or INA-induced expression (absolute $\log_2$ fold change value $\geq$ 1, FDR $\leq$ 0.2) were identified from the reported RNA-seq data (Jin et al., 2018). Total numbers of NPR1-target genes or differentially expressed genes (DEGs) are indicated in parentheses. Blue or red numbers mean the numbers of genes showing *NPR1*-dependent expression among the NPR1 targets identified from the rep1&2 or rep3&4 dataset, respectively, whereas the numbers of genes co-identified from both datasets are marked in purple.

(**B**) Heatmaps showing the expression levels of genes that are directly regulated by NPR1 upon INA treatment. Expression levels are presented as $\log_{10}$ values of reads per kilobase of transcript per million mapped reads (RPKMs). Hierarchical cluster analysis between genotype and/or treatment was performed based on similarity of gene expression.

(**C**) Gene ontology (GO) terms enriched among the genes that are targeted and directly activated by NPR1 upon INA treatment. Two GO categories are indicated in the grey boxes (BP; biological process, MF; molecular function). The enriched GO terms were selected with cutoff of FDR < 0.05. NPR1 targets within the rep3&4 dataset of ChIP-seq were analyzed.

(**D**) Enrichment map visualizing the networks and clusters of gene sets obtained

from the GO analysis in (C). Each node represents an enriched GO term. Node size or edge width is proportional to the number of genes within the node or shared between two connected nodes, respectively. The gene sets were selected with Q-value < 0.05, and the edge cutoff meaning a similarity between a pair of gene sets was 0.25 with 0.25 of Jaccard and overlap combined constant. Representative biological or molecular functions of clustered gene sets are highlighted. The font size of cluster label is proportional to the cluster size.

(**E**) Stacked bar chart indicating the proportion of each transcription-factor family among the total transcription factors of which genes are directly targeted by NPR1 upon INA treatment. Right-side bar indicates NPR1-target transcription factors that are also activated in an *NPR1*-dependent manner. Analyzed transcription factors were selected from the GO analysis in (C).

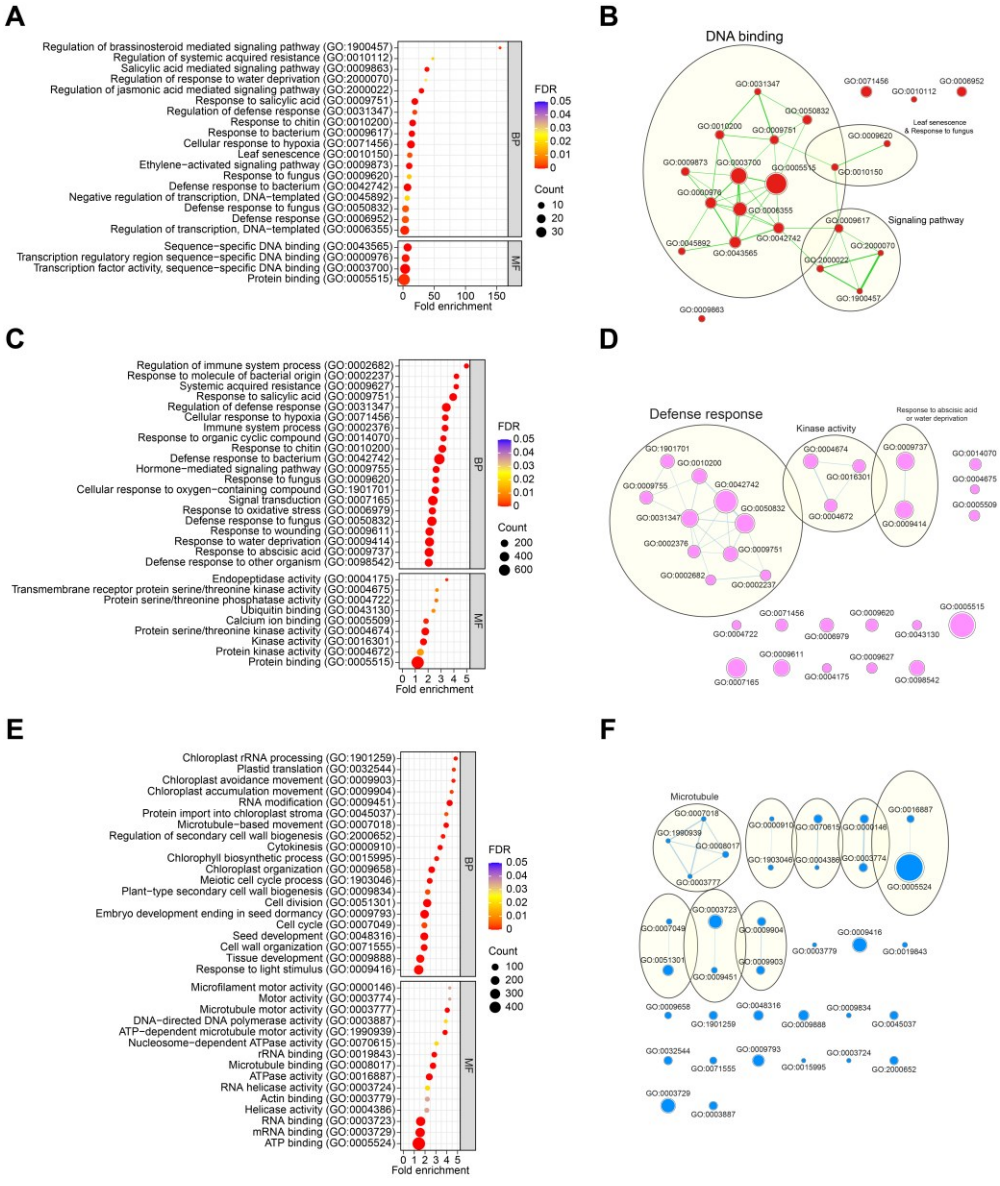
A
Regulation of brassinosteroid mediated signaling pathway (GO:1900457)
Regulation of systemic acquired resistance (GO:0010112)
Salicylic acid mediated signaling pathway (GO:0009863)
Regulation of response to water deprivation (GO:2000070)
Regulation of jasmonic acid mediated signaling pathway (GO:2000022)
Response to salicylic acid (GO:0009751)
Regulation of defense response (GO:0031347)
Response to chitin (GO:0010200)
Response to bacterium (GO:0009617)
Cellular response to hypoxia (GO:0071456)
Leaf senescence (GO:0010150)
Ethylene−activated signaling pathway (GO:0009873)
Response to fungus (GO:0009620)
Defense response to bacterium (GO:0042742)
Negative regulation of transcription, DNA−templated (GO:0045892)
Defense response to fungus (GO:0050832)
Defense response (GO:0006952)
Regulation of transcription, DNA−templated (GO:0006355)
Sequence−specific DNA binding (GO:0043565)
Transcription regulatory region sequence−specific DNA binding (GO:0000976)
Transcription factor activity, sequence−specific DNA binding (GO:0003700)
Protein binding (GO:0005515)
BP
MF
FDR
0.05
0.04
0.03
0.02
0.01
0
Count
10
20
30
0 50 100 150
Fold enrichment
B
DNA binding
Leaf senescence & Response to fungus
Signaling pathway
GO:0031347
GO:0071456
GO:0006952
GO:0010112
GO:0050832
GO:0010200
GO:0009751
GO:0009620
GO:0009873
GO:0003700
GO:0005515
GO:0010150
GO:0009879
GO:0006355
GO:0009617
GO:0045892
GO:0042742
GO:0043565
GO:2000070
GO:2000022
GO:1900457
GO:0009863
C
Regulation of immune system process (GO:0002682)
Response to molecule of bacterial origin (GO:0002237)
Systemic acquired resistance (GO:0009627)
Response to salicylic acid (GO:0009751)
Regulation of defense response (GO:0031347)
Cellular response to hypoxia (GO:0071456)
Immune system process (GO:0002376)
Response to organic cyclic compound (GO:0014070)
Response to chitin (GO:0010200)
Defense response to bacterium (GO:0042742)
Hormone−mediated signaling pathway (GO:0009755)
Response to fungus (GO:0009620)
Cellular response to oxygen−containing compound (GO:1901701)
Signal transduction (GO:0007165)
Response to oxidative stress (GO:0006979)
Defense response to fungus (GO:0050832)
Response to wounding (GO:0009611)
Response to water deprivation (GO:0009414)
Response to abscisic acid (GO:0009737)
Defense response to other organism (GO:0098542)
Endopeptidase activity (GO:0004175)
Transmembrane receptor protein serine/threonine kinase activity (GO:0004675)
Protein serine/threonine phosphatase activity (GO:0004722)
Ubiquitin binding (GO:0043130)
Calcium ion binding (GO:0005509)
Protein serine/threonine kinase activity (GO:0004674)
Kinase activity (GO:0016301)
Protein kinase activity (GO:0004672)
Protein binding (GO:0005515)
BP
MF
FDR
0.05
0.04
0.03
0.02
0.01
0
Count
200
400
600
0 1 2 3 4 5
Fold enrichment
D
Defense response
Kinase activity
Response to abscisic acid or water deprivation
GO:1901701
GO:0010200
GO:0009755
GO:0042742
GO:0031347
GO:0050832
GO:0002376
GO:0009751
GO:0002682
GO:0002237
GO:0004674
GO:0016301
GO:0004672
GO:0009737
GO:0009414
GO:0014070
GO:0004675
GO:0005509
GO:0071456
GO:0009620
GO:0005515
GO:0004722
GO:0006979
GO:0043130
GO:0009611
GO:0009627
GO:0007165
GO:0004175
GO:0098542
E
Chloroplast rRNA processing (GO:1901259)
Plastid translation (GO:0032544)
Chloroplast avoidance movement (GO:0009903)
Chloroplast accumulation movement (GO:0009904)
RNA modification (GO:0009451)
Protein import into chloroplast stroma (GO:0045037)
Microtubule−based movement (GO:0007018)
Regulation of secondary cell wall biogenesis (GO:2000652)
Cytokinesis (GO:0000910)
Chlorophyll biosynthetic process (GO:0015995)
Chloroplast organization (GO:0009658)
Meiotic cell cycle process (GO:1903046)
Plant−type secondary cell wall biogenesis (GO:0009834)
Cell division (GO:0051301)
Embryo development ending in seed dormancy (GO:0009793)
Cell cycle (GO:0007049)
Seed development (GO:0048316)
Cell wall organization (GO:0071555)
Tissue development (GO:0009888)
Response to light stimulus (GO:0009416)
Microfilament motor activity (GO:0000146)
Motor activity (GO:0003774)
Microtubule motor activity (GO:0003777)
DNA−directed DNA polymerase activity (GO:0003887)
ATP−dependent microtubule motor activity (GO:1990939)
Nucleosome−dependent ATPase activity (GO:0070615)
rRNA binding (GO:0019843)
Microtubule binding (GO:0008017)
ATPase activity (GO:0016887)
RNA helicase activity (GO:0003724)
Actin binding (GO:0003779)
Helicase activity (GO:0004386)
RNA binding (GO:0003723)
mRNA binding (GO:0003729)
ATP binding (GO:0005524)
BP
MF
FDR
0.05
0.04
0.03
0.02
0.01
0
Count
100
200
300
400
0 1 2 3 4 5
Fold enrichment
F
Microtubule
GO:0007018
GO:1990939
GO:0008017
GO:0003777
GO:0000910
GO:1903046
GO:0070615
GO:0004386
GO:0000146
GO:0003774
GO:0016887
GO:0005524
GO:0007049
GO:0051301
GO:0003723
GO:0009451
GO:0009904
GO:0009903
GO:0009416
GO:0003779
GO:0019843
GO:0009658
GO:1901259
GO:0048316
GO:0009888
GO:0009834
GO:0045037
GO:0032544
GO:0071555
GO:0009793
GO:0015995
GO:0003724
GO:2000652
GO:0003729
GO:0003887

Figure 10. Ontology of *NPR1*-regulated genes that are either directly targeted by NPR1 or not upon INA treatment.

(**A**, **C**, **E**) GO terms enriched among genes showing *NPR1*-dependent regulation and either directly targeted by NPR1 or not upon INA treatment. The enriched GO terms were selected with cutoff of FDR < 0.05. See Figure 9C legend for more details. (**A**) presents GO terms enriched among genes that are directly targeted and activated by NPR1 upon INA treatment. NPR1 targets within the rep1&2 dataset of ChIP-seq were analyzed. (**C** and **E**) present GO terms enriched among genes that are NPR1-dependently activated (**C**) or repressed (**E**) but not directly targeted by NPR1 upon INA treatment. NPR1 targets within the rep3&4 dataset of ChIP-seq were excluded from the total genes showing *NPR1*-dependent activation (for C) or repression (for E) in the presence of INA. Top 20 results in ascending order of FDR were chosen and displayed for biological process (BP).

(**B**, **D**, **F**) Enrichment map visualizing the networks and clusters of gene sets obtained from the GO analysis in (A), (C), and (E), respectively. The gene sets were selected with Q-value < 0.05, and the edge cutoff meaning a similarity between a pair of gene sets was 0.25 with 0.15 of Jaccard and overlap combined constant. See Figure 9D legend for more explanations.

4.3. NPR1 directly activates genes in diverse SA-dependent immunity pathways

Although not functionally classified by my GO analyses, I also found genes involved in the SA-dependent immunity pathway among the genes directly upregulated by NPR1 (Figure 11). Among them, *RESPIRATORY BURST OXIDASE HOMOLOG D* (*RBOHD*) encodes an NADPH oxidase that generates reactive oxygen species (ROS) upon pathogen attack (Torres et al., 2002; Li et al., 2014), and *ATP-BINDING CASSETTE G40* (*ABCG40*) encodes a transporter responsible for abscisic acid (ABA) import-mediated stomatal closure to restrict pathogen entry (Kang et al., 2010). I also found genes encoding calmodulin domain-containing protein kinases, and one of these kinases, CALMODULIN-DOMAIN PROTEIN KINASE5 (CPK5), interacts with and phosphorylates LYSM-CONTAINING RECEPTOR-LIKE KINASE5 (LYK5), a major chitin receptor, to activate downstream immunity signaling pathways (Huang et al., 2020). CPK5 also directly phosphorylates WRKY33 and increases its DNA-binding ability, contributing to camalexin (an antimicrobial substance) biosynthesis (Zhou et al., 2020).

I also identified genes that encode regulators of effector-triggered immunity (ETI) among the direct NPR1 activation targets. Among them, I found *RPM1-INDUCED PROTEIN KINASE* (*RIPK*), a receptor-like cytoplasmic kinase gene, which encodes a protein kinase that enables RESISTANCE TO P. SYRINGAE PV MACULICOLA1 (RPM1) to recognize the bacterial effectors AvrB and AvrRpm1 and triggers RPM1-dependent immunity (Innes, 2011). In addition, *UDP-GLUCOSYL TRANSFERASE 73B3* (*UGT73B3*) and *UGT73B5* are directly activated by NPR1, and their protein products detoxify secondary

metabolites accumulated after infection by bacteria harboring AvrRpm1 and consequently modulate redox-sensitive signaling pathways (Simon et al., 2014). I also found *SA-INDUCED LEGUME LECTIN-LIKE PROTEIN1* (*SAI-LLP1*), which encodes a protein that positively regulates ETI induced by AvrRpm1 (Armijo et al., 2013). These examples indicate that NPR1 not only triggers transcriptional cascades but also directly regulates diverse genes involved in SA-induced immunity.

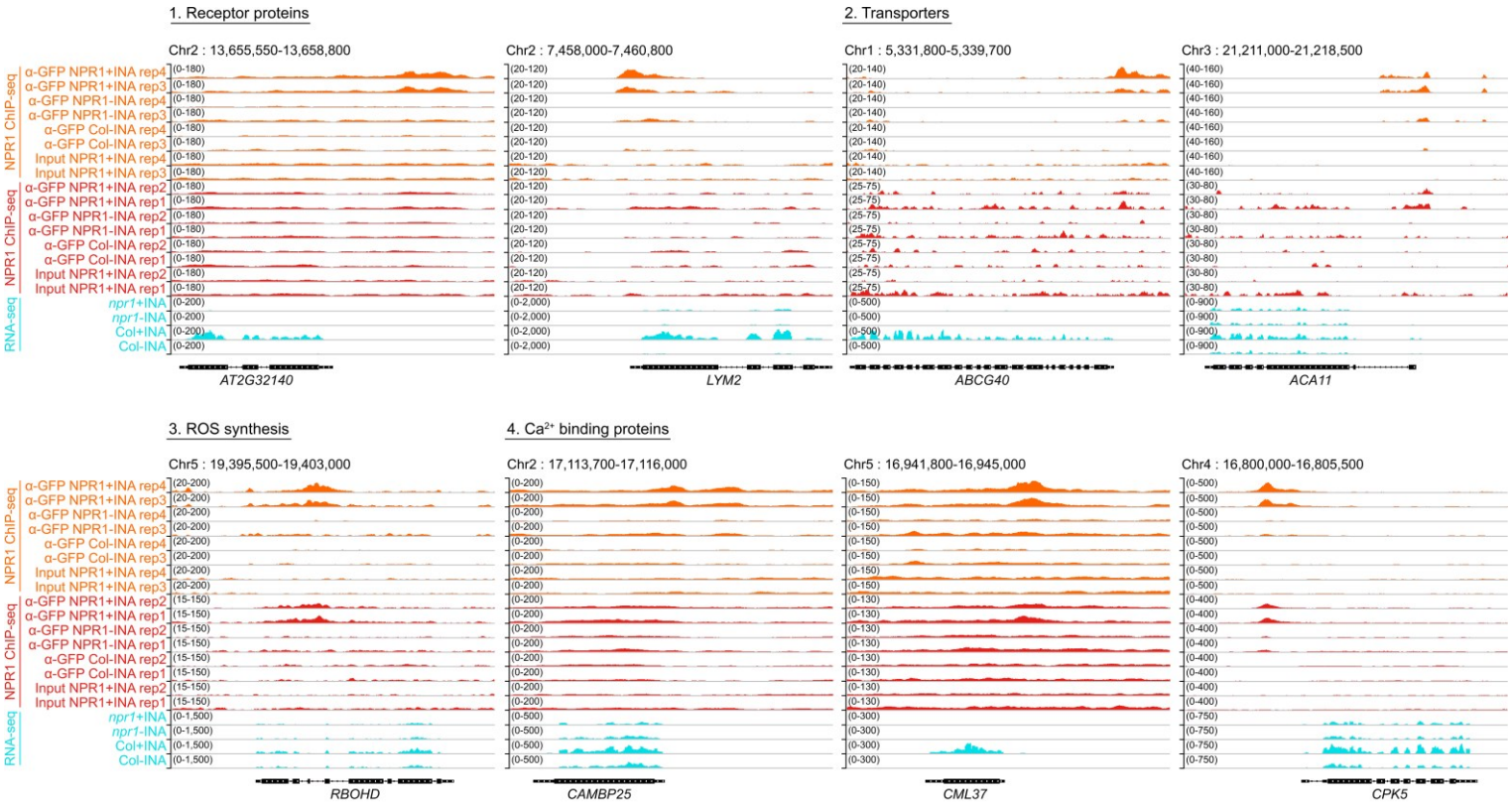
1. Receptor proteins
2. Transporters
3. ROS synthesis
4. Ca2+ binding proteins
Chr2 : 13,655,550-13,658,800
Chr2 : 7,458,000-7,460,800
Chr1 : 5,331,800-5,339,700
Chr3 : 21,211,000-21,218,500
Chr5 : 19,395,500-19,403,000
Chr2 : 17,113,700-17,116,000
Chr5 : 16,941,800-16,945,000
Chr4 : 16,800,000-16,805,500
NPR1 ChIP-seq
NPR1 ChIP-seq
RNA-seq
α-GFP NPR1+INA rep4
α-GFP NPR1+INA rep3
α-GFP NPR1-INA rep4
α-GFP NPR1-INA rep3
α-GFP Col-INA rep4
α-GFP Col-INA rep3
Input NPR1+INA rep4
Input NPR1+INA rep3
α-GFP NPR1+INA rep2
α-GFP NPR1+INA rep1
α-GFP NPR1-INA rep2
α-GFP NPR1-INA rep1
α-GFP Col-INA rep2
α-GFP Col-INA rep1
Input NPR1+INA rep2
Input NPR1+INA rep1
npr1+INA
npr1-INA
Col+INA
Col-INA
AT2G32140
LYM2
ABCG40
ACA11
RBOHD
CAMBP25
CML37
CPK5

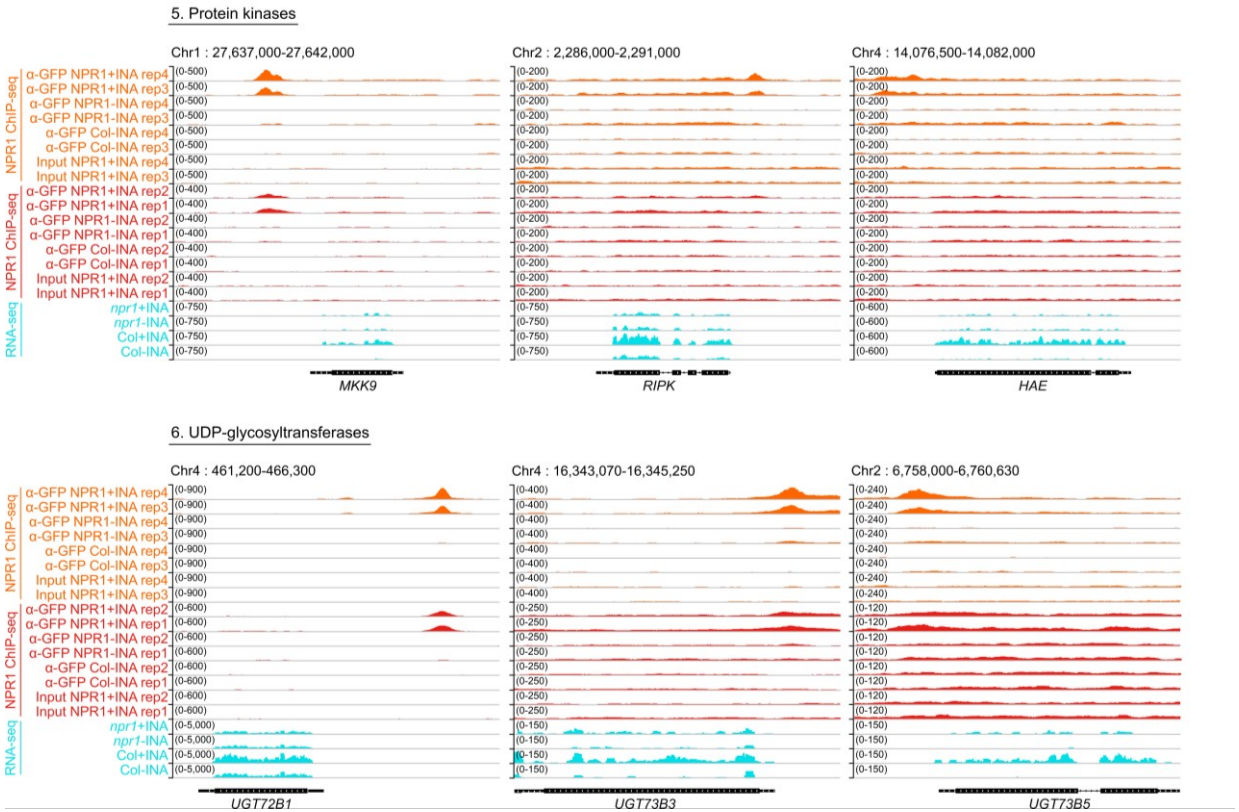
5. Protein kinases
Chr1 : 27,637,000-27,642,000
Chr2 : 2,286,000-2,291,000
Chr4 : 14,076,500-14,082,000
NPR1 ChIP-seq
RNA-seq
α-GFP NPR1+INA rep4
α-GFP NPR1+INA rep3
α-GFP NPR1-INA rep4
α-GFP NPR1-INA rep3
α-GFP Col-INA rep4
α-GFP Col-INA rep3
Input NPR1+INA rep4
Input NPR1+INA rep3
α-GFP NPR1+INA rep2
α-GFP NPR1+INA rep1
α-GFP NPR1-INA rep2
α-GFP NPR1-INA rep1
α-GFP Col-INA rep2
α-GFP Col-INA rep1
Input NPR1+INA rep2
Input NPR1+INA rep1
npr1+INA
npr1-INA
Col+INA
Col-INA
MKK9
RIPK
HAE
6. UDP-glycosyltransferases
Chr4 : 461,200-466,300
Chr4 : 16,343,070-16,345,250
Chr2 : 6,758,000-6,760,630
UGT72B1
UGT73B3
UGT73B5

Figure 11. IGV snapshots of the functionally classified direct NPR1-targets showing *NPR1*-dependent expression in the presence of INA.

Integrative Genomics Viewer (IGV) snapshots of NPR1 ChIP-seq and RNA-seq data for representative functionally classified genes that are targeted and activated by NPR1 upon INA treatment. Data scales are indicated in parentheses on the right side of y-axes. Chromosome (Chr) numbers and genomic regions are shown at the top of images.

4.4. SA-dependent NPR1 targeting is principally mediated by TGACG (TGA) motif-binding transcription factors

As NPR1 does not have a DNA-binding domain, NPR1 targeting must be mediated by transcription factors. To search for candidate transcription factors capable of recruiting NPR1 onto chromatin, I analyzed transcription factor-binding motifs using DNA sequences found in NPR1+INA peaks (Figure 12A). Motif analysis with the rep1&2 dataset identified only the TGACG motif with a greater frequency than the number of NPR1-binding peaks (406 vs. 367), highlighting the dominance of the TGACG motif within the NPR1 peaks. Motif analysis using the rep3&4 dataset revealed the TGACG motif as the most abundant DNA sequence and that CACGTG (G-box) and WGGWCCMM sequences (putative TCP-binding motif; Martin-Trillo and Cubas, 2010) were also enriched within the NPR1 peaks. As the IP condition used for the rep1&2 dataset (with 1% SDS) was harsher than that used for the rep3&4 dataset (with 0.02% SDS), these results indicate that NPR1-targeting factors have higher affinity for chromatin harboring the TGACG motif than chromatin harboring the other transcription factor-binding motifs.

Because the TGACG motif is targeted by bZIP family TGA transcription factors and several TGA transcription factors interact with NPR1 (Zhang et al., 1999; Zhou et al., 2000; Després et al., 2003; Shearer et al., 2009; Jin et al., 2018), I examined if the well-known TGA transcription factor TGA2 targeted to several NPR1 peaks containing the TGACG motif by ChIP-quantitative PCR (ChIP-qPCR) assays (Figure 12B and C). mCherry-fused TGA2 (TGA2:mCherry) targeted to the TGACG motif-containing NPR1 peaks in an INA-independent manner but not to regions distant from the peaks. Surprisingly, TGA2:mCherry also targeted to NPR1

peaks containing the G-box but not the TGACG motif (Figure 13). Taken together, these results indicate that TGA transcription factors are likely the most important mediator of NPR1 targeting at the genome level.

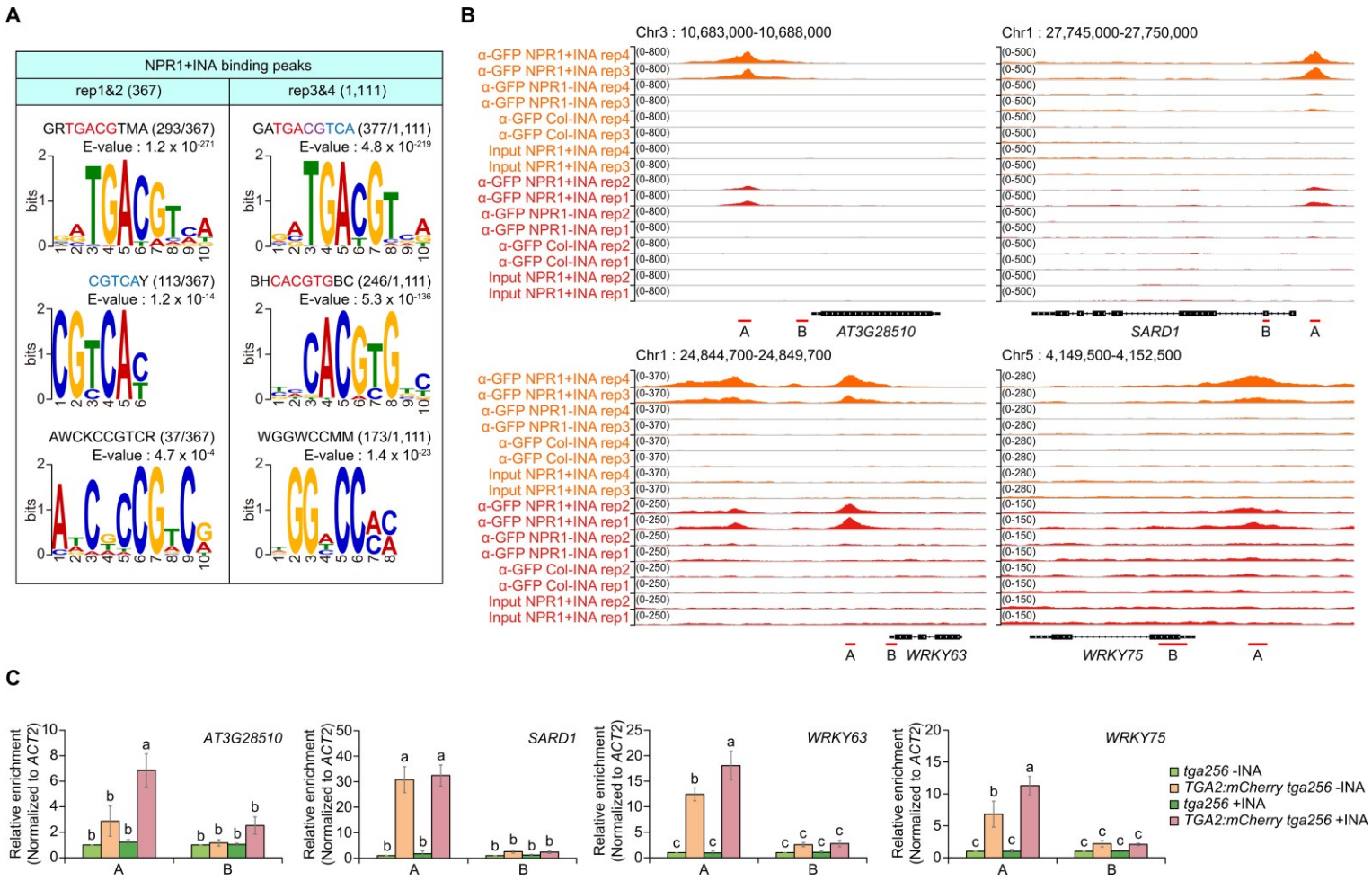
A
NPR1+INA binding peaks
rep1&2 (367)
rep3&4 (1,111)
GRTGACGTMA (293/367)
E-value : 1.2 x 10-271
GATGACGTCA (377/1,111)
E-value : 4.8 x 10-219
CGTCAY (113/367)
E-value : 1.2 x 10-14
BHCACGTGBC (246/1,111)
E-value : 5.3 x 10-136
AWCKCCGTCR (37/367)
E-value : 4.7 x 10-4
WGGWCCMM (173/1,111)
E-value : 1.4 x 10-23
bits
B
Chr3 : 10,683,000-10,688,000
Chr1 : 27,745,000-27,750,000
Chr1 : 24,844,700-24,849,700
Chr5 : 4,149,500-4,152,500
α-GFP NPR1+INA rep4
α-GFP NPR1+INA rep3
α-GFP NPR1-INA rep4
α-GFP NPR1-INA rep3
α-GFP Col-INA rep4
α-GFP Col-INA rep3
Input NPR1+INA rep4
Input NPR1+INA rep3
α-GFP NPR1+INA rep2
α-GFP NPR1+INA rep1
α-GFP NPR1-INA rep2
α-GFP NPR1-INA rep1
α-GFP Col-INA rep2
α-GFP Col-INA rep1
Input NPR1+INA rep2
Input NPR1+INA rep1
A
B
AT3G28510
SARD1
WRKY63
WRKY75
C
Relative enrichment (Normalized to ACT2)
AT3G28510
SARD1
WRKY63
WRKY75
tga256 -INA
TGA2:mCherry tga256 -INA
tga256 +INA
TGA2:mCherry tga256 +INA

Figure 12. **DNA motif with TGACG sequence is enriched in NPR1-binding regions, and TGA2 is targeted to the motif-containing regions.**

(**A**) DNA sequences enriched in INA-dependent NPR1-targeting regions. The top 3 results are displayed in descending order of E-value. The defined motif sequences are shown above E-values. Well-known motif sequences are in red for forward orientation or in blue for reverse orientation. Purple indicates overlaps between sequences colored in red and blue. Numbers of each motif occurrence are indicated in parentheses in comparison to the total numbers of input sequences. Motif analysis was performed using the MEME with option of zero or one occurrence per sequence and 1st order Markov background model. DNA sequences within regions from the 250 bp upstream to the 250 bp downstream of NPR1-binding peak centers were used for analysis.

(**B**) Integrative Genomics Viewer (IGV) snapshots of NPR1 ChIP-seq data for representative NPR1-target loci containing the TGACG motif. Red lines below gene models marked with A or B indicate NPR1-binding peaks with the TGACG motif or regions distant from the peaks, respectively. Data scales are indicated in parentheses on the right side of y-axes. Chromosome (Chr) numbers and genomic regions are shown at the top of images.

(**C**) TGA2-targeting activity to the NPR1-targeting regions containing the TGACG motif (regions A) or distant regions (regions B) with (+INA) or without (–INA) INA treatment. A and B regions indicated in (B) were amplified in ChIP-quantitative PCR (ChIP-qPCR) assays. To calculate relative enrichments, the values of *tga256*–INA were set to 1 after normalization by input and *actin2* (*ACT2*). Means ± SE of three biological replicates are shown. Two-way ANOVA

analysis with Tukey's Honest Significant Differences (HSD) test was performed. Different letters above each bar mean statistically significant differences (p-value < 0.05).

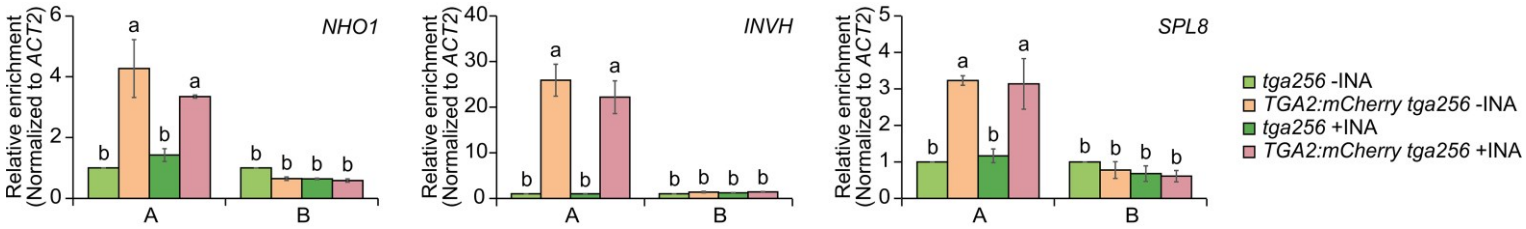

Figure 13. TGA2-targeting activity to the NPR1-targeting regions containing CACGTG sequences (G-box motif) but not TGACG sequences (TGA-binding motif).

TGA2:mCherry enrichment was determined without (–INA) or with (+INA) INA treatment by ChIP-qPCR. Tested regions (A and B) are described in Figure 12B. See Figure 12C legend for more details.

4.5. SA-dependent co-targeting of NPR1 and HAC1 to several hundred loci induces transcriptional activation of a subset of NPR1 target genes

A previous study demonstrated that NPR1 recruits HAC1 to the *PATHOGENESIS-RELATED GENE1* (*PR1*) promoter by forming a transcriptional co-activator complex upon INA treatment (Jin et al., 2018). As a CBP/p300-family histone acetyltransferase, HAC1 may facilitate gene activation by loosening chromatin through H3Ac. HAC1 and its homolog HAC5 affect the expression of 21% of genes that show INA- and *NPR1*-dependent expression (Jin et al., 2018). These results suggest that NPR1 and HAC1 might co-target other genomic loci besides *PR1* during INA-induced transcriptional reprogramming.

To investigate the genomic distribution and targeting activity of HAC1, I performed HAC1 ChIP-seq in the absence (–INA) or presence (+INA) of INA using seedlings expressing *mCherry*-fused *HAC1* under a native *HAC1* promoter (*HAC1:mCherry*). I performed two biological replicates of HAC1:mCherry ChIP-seq for –INA and +INA samples using the same method as used for the rep3&4 of NPR1:GFP ChIP-seq. After peak calling, I designated common peaks between the two biological replicates as HAC1-binding peaks. Comparative analyses using enrichment scores obtained from *HAC1:mCherry* and WT (Col-0) plants showed that the HAC1 peaks identified were specific to *HAC1:mCherry* (Figure 14A), demonstrating that my peak calling was accurate. I found that nearly 80% of the HAC1 peaks located at promoters or promoter-vicinity regions (Figure 14B), consistent with the idea that HAC1 mainly affects transcription. I then annotated the HAC1 peaks obtained from –INA or +INA *HAC1:mCherry* samples to the nearest genes to identify HAC1–INA or HAC1+INA target genes, respectively

(Figure 14C and Table 6). When I compared the two target groups, 87% (7,529/8,641) of the HAC1+INA targets overlapped with the HAC1−INA targets, while only 13% (1,112/8,641) of the HAC1+INA targets occurred exclusively in the +INA condition (Figure 14C). Thus, these results indicate that HAC1 peaks reside usually within promoters or promoter-vicinity regions, and, unlike NPR1 with largely SA-dependent targeting (Figure 8C), HAC1 targeting at the whole-genome level is mainly SA independent.

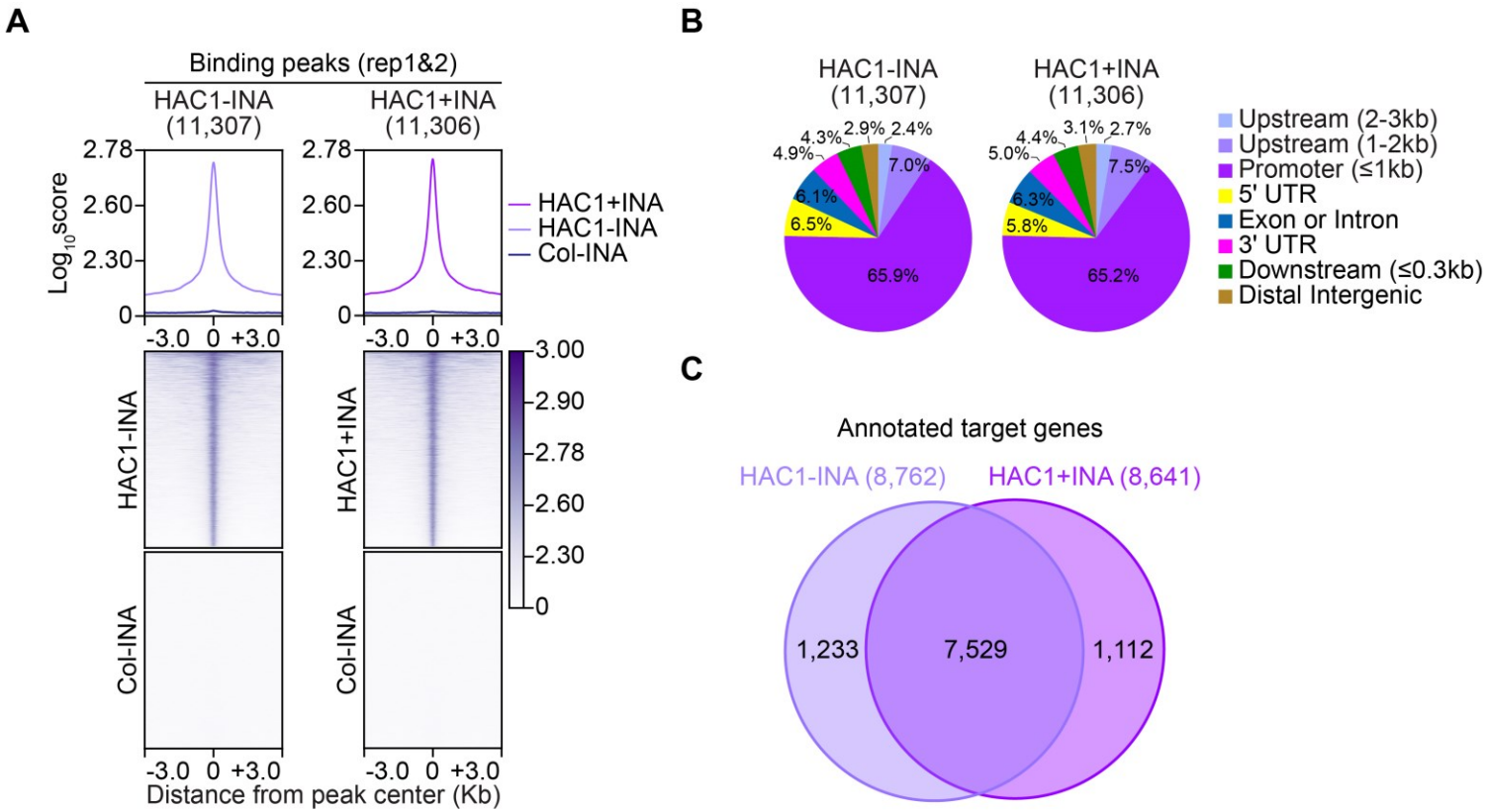
A
Binding peaks (rep1&2)
HAC1-INA (11,307)
HAC1+INA (11,306)
Log10score
2.78
2.60
2.30
0
HAC1+INA
HAC1-INA
Col-INA
-3.0 0 +3.0
3.00
2.90
2.78
2.60
2.30
0
Distance from peak center (Kb)
B
HAC1-INA (11,307)
HAC1+INA (11,306)
7.0%
6.1%
6.5%
65.9%
4.9%
4.3%
2.9%
2.4%
7.5%
6.3%
5.8%
65.2%
5.0%
4.4%
3.1%
2.7%
Upstream (2-3kb)
Upstream (1-2kb)
Promoter (≤1kb)
5' UTR
Exon or Intron
3' UTR
Downstream (≤0.3kb)
Distal Intergenic
C
Annotated target genes
HAC1-INA (8,762)
HAC1+INA (8,641)
1,233
7,529
1,112

Figure 14. HAC1 is usually targeted to promoters or promoter-vicinity regions in an SA-independent manner.

(**A**) Enrichment scores of HAC1:mCherry in the absence (–INA) or presence (+INA) of INA. Profile plots show average scores of HAC1:mCherry enrichment in regions from the 3 kb upstream to the 3 kb downstream of HAC1:mCherry-peak centers. Heatmaps visualize enrichment scores corresponding to individual peaks. HAC1:mCherry peaks were identified through two biological repeats of ChIP-seqs using the same conditions as the rep3&4 of NPR1:GFP ChIP-seqs. See Figure 8A-B legend for more details.

(**B**) Pie-charts illustrating the distribution of genomic regions enriched with HAC1:mCherry in the absence or presence of INA.

(**C**) Venn diagram showing the numbers and overlaps between HAC1-target genes identified under –INA or +INA conditions. Total numbers of annotated targets are indicated in parentheses.

Table 6. Representative genomic regions of HAC1 peaks, and the list of HAC1-target genes annotated from the HAC1 peaks.

Group	Chrom	Start	End	Annotation	GeneID	Gene Symbol	Gene Model Type
HAC1-INA rep1&2	Chr1	420090	420344	5' UTR	AT1G02205	CER1	protein_coding
HAC1-INA rep1&2	Chr1	574443	576446	Promoter (<=1kb)	AT1G02660	PLIP2	protein_coding
HAC1-INA rep1&2	Chr1	673138	673331	Promoter (<=1kb)	AT1G02970	WEE1	protein_coding
HAC1-INA rep1&2	Chr1	1103259	1103412	Promoter (1-2kb)	AT1G04180	YUC9	protein_coding
HAC1-INA rep1&2	Chr1	1215598	1216289	Promoter (<=1kb)	AT1G04263	U5-6	small_nuclear_rna
HAC1-INA rep1&2	Chr1	1469199	1469424	Promoter (<=1kb)	AT1G05100	MAPKKK18	protein_coding
HAC1-INA rep1&2	Chr1	1820099	1820636	Promoter (<=1kb)	AT1G06002		antisense_long_noncoding_rna
HAC1-INA rep1&2	Chr1	2083120	2083304	Promoter (<=1kb)	AT1G06780	GAUT6	protein_coding
HAC1-INA rep1&2	Chr1	2304541	2305495	Promoter (<=1kb)	AT1G07500	SMR5	protein_coding
HAC1-INA rep1&2	Chr1	3658536	3659005	Promoter (<=1kb)	AT1G10940	SNRK2.4	protein_coding
HAC1-INA rep1&2	Chr2	16346586	16346939	Promoter (<=1kb)	AT2G39180	CCR2	protein_coding
HAC1-INA rep1&2	Chr2	16908534	16908748	Promoter (<=1kb)	AT2G40475	ASG8	protein_coding
HAC1-INA rep1&2	Chr2	17506312	17506628	Promoter (<=1kb)	AT2G41940	ZFP8	protein_coding
HAC1-INA rep1&2	Chr2	18363296	18363960	Promoter (<=1kb)	AT2G44490	PEN2	protein_coding
HAC1-INA rep1&2	Chr2	18580268	18580604	Promoter (2-3kb)	AT2G45050	GATA2	protein_coding
HAC1-INA rep1&2	Chr2	18640932	18641475	Promoter (<=1kb)	AT2G45210	SAUR36	protein_coding
HAC1-INA rep1&2	Chr2	18908367	18910455	Promoter (<=1kb)	AT2G45960	PIP1B	protein_coding
HAC1-INA rep1&2	Chr2	18922420	18923194	Promoter (<=1kb)	AT2G46020	BRM	protein_coding
HAC1-INA rep1&2	Chr2	19486495	19487750	Promoter (<=1kb)	AT2G47490	NDT1	protein_coding
HAC1-INA rep1&2	Chr2	19643454	19644117	Promoter (<=1kb)	AT2G48020	ZIF2	protein_coding
HAC1-INA rep1&2	Chr3	10754857	10755129	5' UTR	AT3G28690	PBL36	protein_coding
HAC1-INA rep1&2	Chr3	12449985	12452128	Promoter (<=1kb)	AT3G30775	ERD5	protein_coding
HAC1-INA rep1&2	Chr3	16735819	16736093	Promoter (<=1kb)	AT3G45600	TET3	protein_coding
HAC1-INA rep1&2	Chr3	17185201	17185352	3' UTR	AT3G46640	PCL1	protein_coding
HAC1-INA rep1&2	Chr3	17449361	17449426	Promoter (1-2kb)	AT3G47360	HSD3	protein_coding

Group	Chrom	Start	End	Annotation	GeneID	Gene Symbol	Gene Model Type
HAC1-INA rep1&2	Chr3	17581051	17581188	Promoter (<=1kb)	AT3G47690	EB1A	protein_coding
HAC1-INA rep1&2	Chr3	18003569	18004032	Promoter (<=1kb)	AT3G48560	CSR1	protein_coding
HAC1-INA rep1&2	Chr3	18392806	18393306	Promoter (<=1kb)	AT3G49620	DIN11	protein_coding
HAC1-INA rep1&2	Chr3	18563167	18563468	Downstream (1-2kb	AT3G50070	CYCD3;3	protein_coding
HAC1-INA rep1&2	Chr3	18915213	18915401	Promoter (<=1kb)	AT3G50890	HB28	protein_coding
HAC1-INA rep1&2	Chr3	20005531	20006162	Promoter (<=1kb)	AT3G54020	AtIPCS1	protein_coding
HAC1-INA rep1&2	Chr4	1365387	1365571	Promoter (<=1kb)	AT4G03080	BSL1	protein_coding
HAC1-INA rep1&2	Chr4	6734342	6734447	5' UTR	AT4G11010	NDPK3	protein_coding
HAC1-INA rep1&2	Chr4	7862438	7862703	Promoter (1-2kb)	AT4G13520	SMAP1	protein_coding
HAC1-INA rep1&2	Chr4	8711437	8712348	Promoter (<=1kb)	AT4G06300		long_noncoding_rna
HAC1-INA rep1&2	Chr4	9347672	9347979	Promoter (1-2kb)	AT4G16600	PGSIP8	protein_coding
HAC1-INA rep1&2	Chr4	9932873	9932997	Downstream (<1kb)	AT4G17880	MYC4	protein_coding
HAC1-INA rep1&2	Chr4	10773703	10773949	Promoter (<=1kb)	AT4G19840	PP2-A1	protein_coding
HAC1-INA rep1&2	Chr4	11658979	11659225	Promoter (<=1kb)	AT4G21990	APR3	protein_coding
HAC1-INA rep1&2	Chr4	12407998	12408503	Promoter (<=1kb)	AT4G23850	LACS4	protein_coding
HAC1-INA rep1&2	Chr4	13673463	13677776	Promoter (<=1kb)	AT4G27310	BBX28	protein_coding
HAC1-INA rep1&2	Chr4	15066672	15067230	Promoter (<=1kb)	AT4G30960	SIP3	protein_coding
HAC1-INA rep1&2	Chr4	16479266	16479589	Promoter (<=1kb)	AT4G34460	AGB1	protein_coding
HAC1-INA rep1&2	Chr5	72656	72788	Exon (AT5G01190.	AT5G01190	LAC10	protein_coding
HAC1-INA rep1&2	Chr5	888055	888249	Promoter (<=1kb)	AT5G03530	RABC2A	protein_coding
HAC1-INA rep1&2	Chr5	1887573	1887807	Promoter (<=1kb)	AT5G06230	TBL9	protein_coding
HAC1-INA rep1&2	Chr5	3444305	3444784	Downstream (<1kb)	AT5G10930	CIPK5	protein_coding
HAC1-INA rep1&2	Chr5	4722103	4722815	Promoter (<=1kb)	AT5G14640	SK13	protein_coding
HAC1-INA rep1&2	Chr5	5666583	5666828	Promoter (<=1kb)	AT5G17240	SDG40	protein_coding
HAC1-INA rep1&2	Chr5	7227678	7229499	Exon (AT5G21482.	AT5G21482	CKX7	protein_coding
HAC1-INA rep1&2	Chr5	8587371	8587486	Promoter (1-2kb)	AT5G24930	COL4	protein_coding
HAC1-INA rep1&2	Chr5	9966124	9966987	Promoter (<=1kb)	AT5G04595		long_noncoding_rna
HAC1-INA rep1&2	Chr5	10038973	10039288	Promoter (<=1kb)	AT5G28040	VFP4	protein_coding
HAC1-INA rep1&2	Chr5	15514945	15515151	Promoter (<=1kb)	AT5G00550		novel_transcribed_region
HAC1-INA rep1&2	Chr5	16410531	16410919	Promoter (<=1kb)	AT5G40945		pre_trna

Group	Chrom	Start	End	Annotation	GeneID	Gene Symbol	Gene Model Type
HAC1+INA rep1&2	Chr1	1240321	1240480	Promoter (<=1kb)	AT1G04550	IAA12	protein_coding
HAC1+INA rep1&2	Chr1	2338658	2338853	5' UTR	AT1G07600	MT1A	protein_coding
HAC1+INA rep1&2	Chr1	3484157	3485108	Promoter (<=1kb)	AT1G10560	PUB18	protein_coding
HAC1+INA rep1&2	Chr1	4290619	4291522	Promoter (<=1kb)	AT1G12610	DDF1	protein_coding
HAC1+INA rep1&2	Chr1	4906395	4906736	Promoter (1-2kb)	AT1G14350	FLP	protein_coding
HAC1+INA rep1&2	Chr1	5525051	5525716	Promoter (<=1kb)	AT1G16130	WAKL2	protein_coding
HAC1+INA rep1&2	Chr1	6884642	6884795	Promoter (1-2kb)	AT1G19850	MP	protein_coding
HAC1+INA rep1&2	Chr1	7388518	7389081	Promoter (<=1kb)	AT1G21100	IGMT1	protein_coding
HAC1+INA rep1&2	Chr1	7881293	7881408	Promoter (<=1kb)	AT1G22300	GRF10	protein_coding
HAC1+INA rep1&2	Chr1	8169102	8169658	Promoter (<=1kb)	AT1G23052		other_rna
HAC1+INA rep1&2	Chr1	9257446	9258976	Distal Intergenic	AT1G06023		long_noncoding_rna
HAC1+INA rep1&2	Chr1	10690674	10691058	Promoter (<=1kb)	AT1G30330	ARF6	protein_coding
HAC1+INA rep1&2	Chr2	7493680	7493882	Downstream (<1kb)	AT2G17230	EXL5	protein_coding
HAC1+INA rep1&2	Chr2	8708454	8708623	Promoter (1-2kb)	AT2G20180	PIL5	protein_coding
HAC1+INA rep1&2	Chr2	10063122	10064078	Promoter (<=1kb)	AT2G23670	YCF37	protein_coding
HAC1+INA rep1&2	Chr2	11196867	11197370	Promoter (<=1kb)	AT2G26300	GP ALPHA 1	protein_coding
HAC1+INA rep1&2	Chr2	12173501	12173780	Promoter (<=1kb)	AT2G28470	BGAL8	protein_coding
HAC1+INA rep1&2	Chr2	12857622	12857785	Promoter (<=1kb)	AT2G30110	UBA1	protein_coding
HAC1+INA rep1&2	Chr2	14146495	14146862	Promoter (<=1kb)	AT2G33380	RD20	protein_coding
HAC1+INA rep1&2	Chr2	15481271	15481701	Promoter (<=1kb)	AT2G36880	MAT3	protein_coding
HAC1+INA rep1&2	Chr2	17242657	17242990	Promoter (2-3kb)	AT2G41370	BOP2	protein_coding
HAC1+INA rep1&2	Chr2	18749430	18749781	Promoter (<=1kb)	AT2G45490	AUR3	protein_coding
HAC1+INA rep1&2	Chr2	19406648	19406966	5' UTR	AT2G47260	WRKY23	protein_coding
HAC1+INA rep1&2	Chr2	19643433	19644260	Promoter (<=1kb)	AT2G48020	ZIF2	protein_coding
HAC1+INA rep1&2	Chr3	1352815	1352994	Promoter (1-2kb)	AT3G04910	WNK1	protein_coding
HAC1+INA rep1&2	Chr3	2034443	2034609	Downstream (<1kb)	AT3G06540	REP	protein_coding
HAC1+INA rep1&2	Chr3	3386046	3387166	Promoter (<=1kb)	AT3G10815	BTL03	protein_coding
HAC1+INA rep1&2	Chr3	4493777	4494128	Promoter (<=1kb)	AT3G13710	PRA1.F4	protein_coding
HAC1+INA rep1&2	Chr3	5058674	5059145	Promoter (2-3kb)	AT3G15030	TCP4	protein_coding
HAC1+INA rep1&2	Chr3	5861053	5861688	Promoter (<=1kb)	AT3G17185	TAS3	other_rna

Group	Chrom	Start	End	Annotation	GeneID	Gene Symbol	Gene Model Type
HAC1+INA rep1&2	Chr3	6671909	6672138	Promoter (<=1kb)	AT3G19260	LOH2	protein_coding
HAC1+INA rep1&2	Chr3	8019602	8019779	Promoter (<=1kb)	AT3G22670	MISF2	protein_coding
HAC1+INA rep1&2	Chr3	8762309	8762415	Exon (AT3G24220.	AT3G24220	NCED6	protein_coding
HAC1+INA rep1&2	Chr3	11648161	11648510	Promoter (<=1kb)	AT3G29770	MES11	protein_coding
HAC1+INA rep1&2	Chr3	17907893	17908108	3' UTR	AT3G48350	CEP3	protein_coding
HAC1+INA rep1&2	Chr3	20116404	20116525	Intron (AT3G54320	AT3G54320	WRI1	protein_coding
HAC1+INA rep1&2	Chr4	1931681	1932008	Promoter (<=1kb)	AT4G04020	FIB	protein_coding
HAC1+INA rep1&2	Chr4	8305273	8305374	Exon (AT4G14430.	AT4G14430	IBR10	protein_coding
HAC1+INA rep1&2	Chr4	9646318	9646411	Promoter (<=1kb)	AT4G17170	RABB1C	protein_coding
HAC1+INA rep1&2	Chr4	10288369	10288726	Downstream (<1kb)	AT4G18700	CIPK12	protein_coding
HAC1+INA rep1&2	Chr4	10964236	10964430	Distal Intergenic	AT4G20310	S2P	protein_coding
HAC1+INA rep1&2	Chr4	11658940	11659236	Promoter (<=1kb)	AT4G21990	APR3	protein_coding
HAC1+INA rep1&2	Chr4	12166922	12167557	Promoter (<=1kb)	AT4G23250	emb1290	protein_coding
HAC1+INA rep1&2	Chr4	13014994	13016909	Promoter (<=1kb)	AT4G25470	CBF2	protein_coding
HAC1+INA rep1&2	Chr4	14495709	14496065	Promoter (<=1kb)	AT4G29520	SES1	protein_coding
HAC1+INA rep1&2	Chr4	15231228	15231588	Distal Intergenic	AT4G31380	FLP1	protein_coding
HAC1+INA rep1&2	Chr4	16582735	16583343	Promoter (<=1kb)	AT4G34760	SAUR50	protein_coding
HAC1+INA rep1&2	Chr4	18556865	18557219	Promoter (<=1kb)	AT4G40030	H3.3	protein_coding
HAC1+INA rep1&2	Chr5	3065740	3065937	Promoter (<=1kb)	AT5G09850	MED26C	protein_coding
HAC1+INA rep1&2	Chr5	4470957	4471169	Promoter (<=1kb)	AT5G13840	FZR3	protein_coding
HAC1+INA rep1&2	Chr5	6378178	6378308	5' UTR	AT5G19080	LUL3	protein_coding
HAC1+INA rep1&2	Chr5	7379022	7379470	Promoter (<=1kb)	AT5G22300	NIT4	protein_coding
HAC1+INA rep1&2	Chr5	15877190	15877876	Promoter (<=1kb)	AT5G39660	CDF2	protein_coding
HAC1+INA rep1&2	Chr5	19347795	19347986	Promoter (<=1kb)	AT5G47780	GAUT4	protein_coding
HAC1+INA rep1&2	Chr5	21957769	21958341	Promoter (<=1kb)	AT5G54110	MAMI	protein_coding
HAC1+INA rep1&2	Chr5	24101485	24103874	Promoter (<=1kb)	AT5G59820	RHL41	protein_coding
HAC1+INA rep1&2	Chr5	25286011	25286142	Promoter (<=1kb)	AT5G63020	SUT1	protein_coding
HAC1+INA rep1&2	Chr5	26644166	26644399	5' UTR	AT5G66730	IDD1	protein_coding
HAC1+INA rep1&2	Chr5	26809118	26810363	Promoter (<=1kb)	AT5G67190	DEAR2	protein_coding
HAC1+INA rep1&2	Chr5	26890207	26890260	Promoter (<=1kb)	AT5G09895		long_noncoding_rna

Next, to understand the roles of NPR1 and HAC1 during SA-induced transcriptional reprogramming, I identified genome-wide common peaks of NPR1 and HAC1 under the +INA condition (Table 7 and Figure 15A). Enrichment scores of both NPR1:GFP and HAC1:mCherry were the highest at the center of the common peaks (Figure 15A), indicating that I appropriately determined the common peaks. The common peaks accounted for 71% (262/367 of the rep1&2 dataset) or 84% (937/1,111 of the rep3&4 dataset) of the NPR1 peaks identified under the +INA condition (Figures 8A-B and 15A). Therefore, NPR1 generally targets together with HAC1 to several hundred promoter regions during SA-induced transcriptional reprogramming. These results are consistent with a previous study (Jin et al., 2018), which revealed the genome-wide roles of HAC1/5 and NPR1 in SA-induced immunity and the requirement of HAC1/5 and NPR1 in the formation of the SA-induced high-molecular-weight HAC-NPR1-TGA complex.

I then examined if NPR1 and HAC1 co-targeting activates the transcription of the common target genes. To analyze the transcriptomic changes caused by *npr1* or *hac1 hac5* mutations, I used RNA-seq data generated in a previous study (Jin et al., 2018), which also showed a functional redundancy between *HAC1* and *HAC5* with *HAC1* dominance. Integrating ChIP-seq and RNA-seq data revealed that 18 or 61 of the common target genes are co-dependent on *NPR1* and *HAC1/5* for their INA-induced transcriptional activation depending on the rep1&2 or rep3&4 dataset of NPR1+INA ChIP-seq used, respectively (Figure 15B). INA-induced upregulation of these genes was more severely disturbed by the *npr1* mutation than by the *hac1/5* mutations (Figure 15C). In addition, I observed

increased INA-induced H3Ac around the NPR1 and HAC1 co-targeting sites in the WT but not in the *npr1* and *hac1/5* mutants (Figure 16A and B). In summary, NPR1 and HAC1 co-target hundreds of genomic loci during SA-induced transcriptional reprogramming and cooperatively activate a subset of the common target genes through NPR1- and HAC1/5-dependent H3Ac.

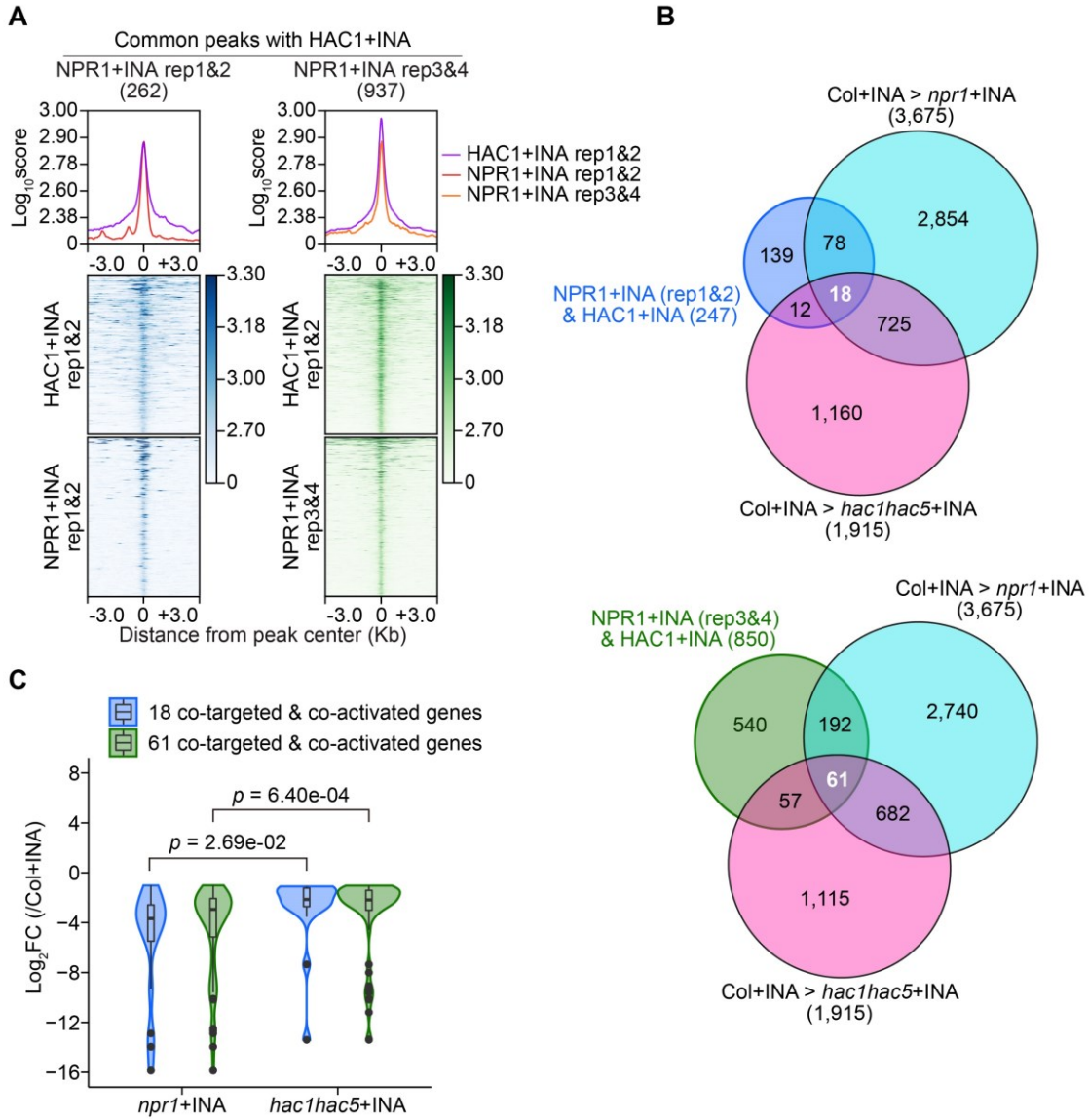
A
Common peaks with HAC1+INA
NPR1+INA rep1&2
(262)
NPR1+INA rep3&4
(937)
Log10score
HAC1+INA rep1&2
NPR1+INA rep1&2
NPR1+INA rep3&4
HAC1+INA rep1&2
NPR1+INA rep1&2
NPR1+INA rep3&4
Distance from peak center (Kb)
B
Col+INA > npr1+INA
(3,675)
2,854
139
78
NPR1+INA (rep1&2)
& HAC1+INA (247)
12
18
725
1,160
Col+INA > hac1hac5+INA
(1,915)
NPR1+INA (rep3&4)
& HAC1+INA (850)
540
192
61
57
682
1,115
C
18 co-targeted & co-activated genes
61 co-targeted & co-activated genes
p = 6.40e-04
p = 2.69e-02
Log2FC (/Col+INA)
npr1+INA
hac1hac5+INA

Figure 15. Hundreds of genes are co-targeted by NPR1 and HAC1, and this co-targeting activity is required for the transcriptional activation of a subset of the genes upon SA signaling.

(**A**) Enrichment scores of the common peaks of NPR1 and HAC1 in the presence of INA. Profile plots show the average scores of enrichments in the surrounding regions harboring the common peaks of NPR1 and HAC1. Heatmaps visualize enrichment scores of NPR1 and HAC1 in individual genomic regions. The rep1&2 or rep3&4 dataset of NPR1:GFP ChIP-seq was used to obtain common peaks with the rep1&2 dataset of HAC1:mCherry ChIP-seq, respectively. Numbers of common peaks are indicated in parentheses above the profile plots. All enrichment scores are presented as $\log_{10}$ values of means of enrichment levels derived from two biological repeats. To calculate enrichment scores, ChIP-seq reads were normalized using RPKM method with a bin size of 5 bp. The RPKM values derived from each IP sample were then subtracted by the RPKM values derived from the corresponding input sample to calculate enrichment levels. Regions from the 3 kb upstream to the 3 kb downstream of the common-peak centers were analyzed. The extended regions from the peak centers were equally divided into 5 bp bins.

(**B**) Venn diagrams illustrating the numbers of NPR1 and HAC1 co-targets showing *NPR1*- and *HAC1 HAC5*-dependent expression in the presence of INA. The co-targets were identified by annotation of the common peaks presented in (D). Genes downregulated in *npr1-1* or *hac1-2 hac-5-2* mutants compared to WT Col in the presence of INA were identified from the reported RNA-seq data (Jin et al., 2018) (absolute $\log_2$ fold change value ≥ 1, FDR ≤ 0.2). The numbers colored white

indicate the numbers of genes that are directly co-targeted and co-activated by NPR1 and HAC1 in the presence of INA.

(**C**) Violin plot with included box plot showing the effects of *npr1* or *hac1 hac5* mutations on the expression of co-targets. The genes that are directly co-targeted and co-activated by NPR1 and HAC1 as identified in (E) were used for analysis. From RNA-seq data, RPKMs in *npr1-1* or *hac1-2 hac5-2* mutants were divided by RPKMs in WT (Col). Log_2 values of the calculated fold change (FC) are presented. *P*-values shown were calculated using Wilcoxon signed rank test.

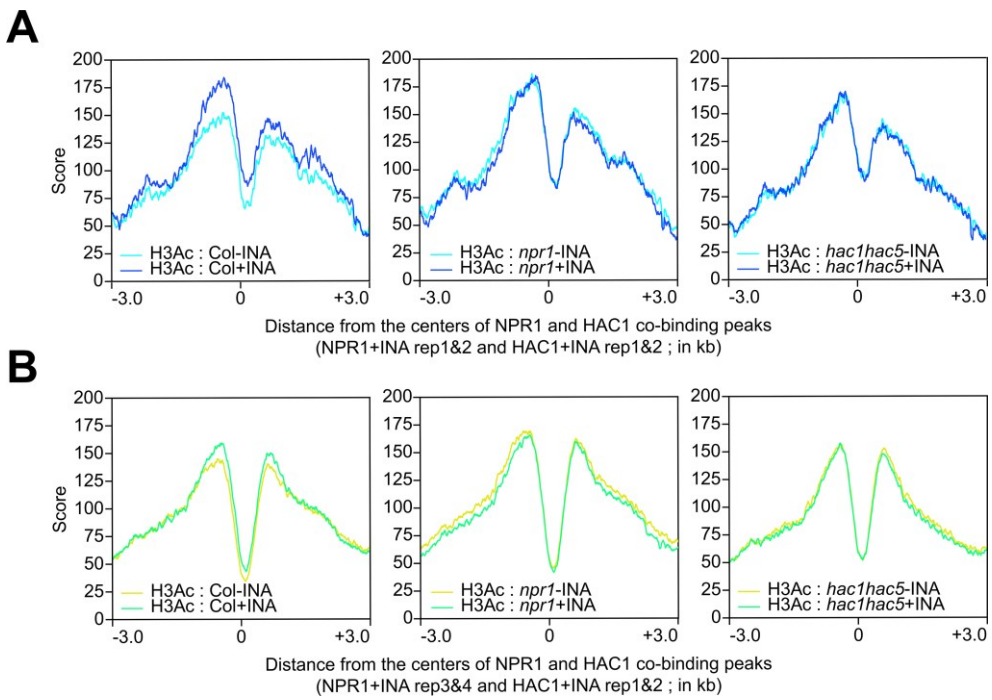

Figure 16. Effects of *npr1* and *hac1 hac5* mutations on INA-induced histone H3 acetylation (H3Ac) in genomic regions co-targeted by NPR1 and HAC1 in the presence of INA.

(**A**-**B**) Profile plots showing H3Ac levels before and after INA treatment in WT (Col), *npr1-1*, and *hac1-2 hac5-2*. The H3Ac profiles were analyzed using the H3Ac ChIP-seq data previously reported (Jin et al., 2018). Divided into 5 bins, genomic regions were scanned from the 3 kb upstream to the 3 kb downstream of the centers of ChIP-seq peaks that show co-targeting activities of NPR1 and HAC1 in the presence of INA (see Figure 15A). Co-targeting sites identified from the rep1&2 (**A**) or the rep3&4 (**B**) of NPR1:GFP ChIP-seq dataset were analyzed.

Table 7. Representative genome-wide common peaks of NPR1 and HAC1 identified under +INA condition, and the list of common target genes.

Group	Chrom	Start	End	GeneID	Gene Symbol	Gene Model Type
NPR1+INA (rep1&2) & HAC1+INA (rep1&2)	Chr1	1659381	1659545	AT1G05570	CALS1	protein_coding
NPR1+INA (rep1&2) & HAC1+INA (rep1&2)	Chr1	4139986	4140221	AT1G12210	RFL1	protein_coding
NPR1+INA (rep1&2) & HAC1+INA (rep1&2)	Chr1	9950025	9950174	AT1G28360	ERF12	protein_coding
NPR1+INA (rep1&2) & HAC1+INA (rep1&2)	Chr1	10860351	10860632	AT1G30640	NDR7	protein_coding
NPR1+INA (rep1&2) & HAC1+INA (rep1&2)	Chr1	24831255	24831507	AT1G66560	WRKY64	protein_coding
NPR1+INA (rep1&2) & HAC1+INA (rep1&2)	Chr1	26591582	26591872	AT1G70530	CRK3	protein_coding
NPR1+INA (rep1&2) & HAC1+INA (rep1&2)	Chr1	27638269	27638705	AT1G73500	MKK9	protein_coding
NPR1+INA (rep1&2) & HAC1+INA (rep1&2)	Chr1	27749297	27749682	AT1G73805	SARD1	protein_coding
NPR1+INA (rep1&2) & HAC1+INA (rep1&2)	Chr1	30380399	30380860	AT1G80840	WRKY40	protein_coding
NPR1+INA (rep1&2) & HAC1+INA (rep1&2)	Chr2	801339	801549	AT2G02810	UTR1	protein_coding
NPR1+INA (rep1&2) & HAC1+INA (rep1&2)	Chr2	6243016	6243084	AT2G14610	PR1	protein_coding
NPR1+INA (rep1&2) & HAC1+INA (rep1&2)	Chr2	9340513	9340706	AT2G21910	CYP96A5	protein_coding
NPR1+INA (rep1&2) & HAC1+INA (rep1&2)	Chr2	12822781	12822975	AT2G30040	MAPKKK14	protein_coding
NPR1+INA (rep1&2) & HAC1+INA (rep1&2)	Chr2	14217103	14217359	AT2G33570	GALS1	protein_coding
NPR1+INA (rep1&2) & HAC1+INA (rep1&2)	Chr2	17002344	17002936	AT2G40750	WRKY54	protein_coding
NPR1+INA (rep1&2) & HAC1+INA (rep1&2)	Chr2	18822993	18823127	AT2G45680	TCP9	protein_coding
NPR1+INA (rep1&2) & HAC1+INA (rep1&2)	Chr2	19045270	19045695	AT2G46400	WRKY46	protein_coding
NPR1+INA (rep1&2) & HAC1+INA (rep1&2)	Chr2	19486818	19486953	AT2G47490	NDT1	protein_coding
NPR1+INA (rep1&2) & HAC1+INA (rep1&2)	Chr3	3555644	3555891	AT3G11340	UGT76B1	protein_coding
NPR1+INA (rep1&2) & HAC1+INA (rep1&2)	Chr3	5861167	5861529	AT3G17185	TAS3	other_rna
NPR1+INA (rep1&2) & HAC1+INA (rep1&2)	Chr3	7675956	7676256	AT3G21780	UGT71B6	protein_coding
NPR1+INA (rep1&2) & HAC1+INA (rep1&2)	Chr3	7846641	7847023	AT3G22231	PCC1	protein_coding
NPR1+INA (rep1&2) & HAC1+INA (rep1&2)	Chr3	9195086	9195306	AT3G25250	AGC2-1	protein_coding

Group	Chrom	Start	End	GeneID	Gene Symbol	Gene Model Type
NPR1+INA (rep1&2) & HAC1+INA (rep1&2)	Chr3	9470684	9471193	AT3G25882	NIMIN-2	protein_coding
NPR1+INA (rep1&2) & HAC1+INA (rep1&2)	Chr3	9577004	9577284	AT3G26170	CYP71B19	protein_coding
NPR1+INA (rep1&2) & HAC1+INA (rep1&2)	Chr3	10790637	10790836	AT3G28740	CYP81D11	protein_coding
NPR1+INA (rep1&2) & HAC1+INA (rep1&2)	Chr3	20911424	20911576	AT3G56400	WRKY70	protein_coding
NPR1+INA (rep1&2) & HAC1+INA (rep1&2)	Chr3	21007626	21008040	AT3G56710	SIB1	protein_coding
NPR1+INA (rep1&2) & HAC1+INA (rep1&2)	Chr4	7011351	7011560	AT4G11600	GPX6	protein_coding
NPR1+INA (rep1&2) & HAC1+INA (rep1&2)	Chr4	7189926	7190144	AT4G11990	TPXL2	protein_coding
NPR1+INA (rep1&2) & HAC1+INA (rep1&2)	Chr4	10437689	10437898	AT4G19040	EDR2	protein_coding
NPR1+INA (rep1&2) & HAC1+INA (rep1&2)	Chr4	11967990	11968037	AT4G22770	AHL2	protein_coding
NPR1+INA (rep1&2) & HAC1+INA (rep1&2)	Chr4	12395921	12396322	AT4G23810	WRKY53	protein_coding
NPR1+INA (rep1&2) & HAC1+INA (rep1&2)	Chr4	12573329	12573470	AT4G24240	WRKY7	protein_coding
NPR1+INA (rep1&2) & HAC1+INA (rep1&2)	Chr4	15381413	15381628	AT4G31800	WRKY18	protein_coding
NPR1+INA (rep1&2) & HAC1+INA (rep1&2)	Chr4	16344777	16345172	AT4G34131	UGT73B3	protein_coding
NPR1+INA (rep1&2) & HAC1+INA (rep1&2)	Chr4	16371508	16371596	AT4G34180	CYCLASE1	protein_coding
NPR1+INA (rep1&2) & HAC1+INA (rep1&2)	Chr4	16740228	16741111	AT4G35180	LHT7	protein_coding
NPR1+INA (rep1&2) & HAC1+INA (rep1&2)	Chr4	16801294	16801634	AT4G35310	CPK5	protein_coding
NPR1+INA (rep1&2) & HAC1+INA (rep1&2)	Chr5	352115	353005	AT5G01900	WRKY62	protein_coding
NPR1+INA (rep1&2) & HAC1+INA (rep1&2)	Chr5	2860291	2861417	AT5G08790	ATAF2	protein_coding
NPR1+INA (rep1&2) & HAC1+INA (rep1&2)	Chr5	7497696	7498381	AT5G22570	WRKY38	protein_coding
NPR1+INA (rep1&2) & HAC1+INA (rep1&2)	Chr5	8381261	8381645	AT5G24530	DMR6	protein_coding
NPR1+INA (rep1&2) & HAC1+INA (rep1&2)	Chr5	16943548	16943699	AT5G42380	CML37	protein_coding
NPR1+INA (rep1&2) & HAC1+INA (rep1&2)	Chr5	18227971	18228901	AT5G45110	NPR3	protein_coding
NPR1+INA (rep1&2) & HAC1+INA (rep1&2)	Chr5	23693031	23693166	AT5G58620	TZF9	protein_coding
NPR1+INA (rep1&2) & HAC1+INA (rep1&2)	Chr5	24482348	24482583	AT5G08975		long_noncoding_rna
NPR1+INA (rep1&2) & HAC1+INA (rep1&2)	Chr5	24766482	24766862	AT5G61600	ERF104	protein_coding
NPR1+INA (rep1&2) & HAC1+INA (rep1&2)	Chr5	25518324	25518544	AT5G63770	DGK2	protein_coding
NPR1+INA (rep1&2) & HAC1+INA (rep1&2)	Chr5	25907870	25908353	AT5G64810	WRKY51	protein_coding

Group	Chrom	Start	End	GeneID	Gene Symbol	Gene Model Type
NPR1+INA (rep3&4) & HAC1+INA (rep1&2)	Chr1	984001	984224	AT1G03870	FLA9	protein_coding
NPR1+INA (rep3&4) & HAC1+INA (rep1&2)	Chr1	2437192	2437300	AT1G07890	APX1	protein_coding
NPR1+INA (rep3&4) & HAC1+INA (rep1&2)	Chr1	3242060	3242264	AT1G09950	RAS1	protein_coding
NPR1+INA (rep3&4) & HAC1+INA (rep1&2)	Chr1	3809739	3810258	AT1G11330	RDA2	protein_coding
NPR1+INA (rep3&4) & HAC1+INA (rep1&2)	Chr1	5532076	5532248	AT1G16150	WAKL4	protein_coding
NPR1+INA (rep3&4) & HAC1+INA (rep1&2)	Chr1	8975722	8975922	AT1G25550	HHO3	protein_coding
NPR1+INA (rep3&4) & HAC1+INA (rep1&2)	Chr1	11620276	11620376	AT1G32230	RCD1	protein_coding
NPR1+INA (rep3&4) & HAC1+INA (rep1&2)	Chr1	18927690	18927836	AT1G51070	bHLH115	protein_coding
NPR1+INA (rep3&4) & HAC1+INA (rep1&2)	Chr1	26587604	26587795	AT1G70520	CRK2	protein_coding
NPR1+INA (rep3&4) & HAC1+INA (rep1&2)	Chr1	29099649	29099879	AT1G77450	NAC032	protein_coding
NPR1+INA (rep3&4) & HAC1+INA (rep1&2)	Chr1	30302179	30302865	AT1G80600	WIN1	protein_coding
NPR1+INA (rep3&4) & HAC1+INA (rep1&2)	Chr2	1137338	1137453	AT2G03730	ACR5	protein_coding
NPR1+INA (rep3&4) & HAC1+INA (rep1&2)	Chr2	6243016	6243084	AT2G14610	PR1	protein_coding
NPR1+INA (rep3&4) & HAC1+INA (rep1&2)	Chr2	7458987	7459093	AT2G17120	LYP1	protein_coding
NPR1+INA (rep3&4) & HAC1+INA (rep1&2)	Chr2	8534216	8534344	AT2G19800	MIOX2	protein_coding
NPR1+INA (rep3&4) & HAC1+INA (rep1&2)	Chr2	9369328	9369528	AT2G22010	RKP	protein_coding
NPR1+INA (rep3&4) & HAC1+INA (rep1&2)	Chr2	10119669	10119749	AT2G23770	LYK4	protein_coding
NPR1+INA (rep3&4) & HAC1+INA (rep1&2)	Chr2	13106234	13106334	AT2G30766	FEP1	protein_coding
NPR1+INA (rep3&4) & HAC1+INA (rep1&2)	Chr2	17114792	17114927	AT2G41010	CAMBP25	protein_coding
NPR1+INA (rep3&4) & HAC1+INA (rep1&2)	Chr2	17890999	17891130	AT2G43020	PAO2	protein_coding
NPR1+INA (rep3&4) & HAC1+INA (rep1&2)	Chr2	18822948	18823125	AT2G45680	TCP9	protein_coding
NPR1+INA (rep3&4) & HAC1+INA (rep1&2)	Chr2	19027810	19027906	AT2G46340	SPA1	protein_coding
NPR1+INA (rep3&4) & HAC1+INA (rep1&2)	Chr3	1290613	1291266	AT3G04730	IAA16	protein_coding
NPR1+INA (rep3&4) & HAC1+INA (rep1&2)	Chr3	3585907	3586159	AT3G11410	PP2CA	protein_coding
NPR1+INA (rep3&4) & HAC1+INA (rep1&2)	Chr3	4012376	4012493	AT3G12630	SAP5	protein_coding
NPR1+INA (rep3&4) & HAC1+INA (rep1&2)	Chr3	5747417	5747548	AT3G16850	PGF5	protein_coding
NPR1+INA (rep3&4) & HAC1+INA (rep1&2)	Chr3	8086205	8086296	AT3G22840	ELIP1	protein_coding

Group	Chrom	Start	End	GeneID	Gene Symbol	Gene Model Type
NPR1+INA (rep3&4) & HAC1+INA (rep1&2)	Chr3	9472436	9472747	AT3G25882	NIMIN-2	protein_coding
NPR1+INA (rep3&4) & HAC1+INA (rep1&2)	Chr3	9867486	9867725	AT3G26810	AFB2	protein_coding
NPR1+INA (rep3&4) & HAC1+INA (rep1&2)	Chr3	15985620	15985725	AT3G44310	NIT1	protein_coding
NPR1+INA (rep3&4) & HAC1+INA (rep1&2)	Chr3	17976710	17976845	AT3G48520	CYP94B3	protein_coding
NPR1+INA (rep3&4) & HAC1+INA (rep1&2)	Chr3	21008828	21009447	AT3G56710	SIB1	protein_coding
NPR1+INA (rep3&4) & HAC1+INA (rep1&2)	Chr4	7011323	7011610	AT4G11600	GPX6	protein_coding
NPR1+INA (rep3&4) & HAC1+INA (rep1&2)	Chr4	7305829	7306252	AT4G12290	CUAO	protein_coding
NPR1+INA (rep3&4) & HAC1+INA (rep1&2)	Chr4	10398333	10398376	AT4G18980	AtS40-3	protein_coding
NPR1+INA (rep3&4) & HAC1+INA (rep1&2)	Chr4	12488984	12489174	AT4G24040	TRE1	protein_coding
NPR1+INA (rep3&4) & HAC1+INA (rep1&2)	Chr4	12536775	12537001	AT4G24150	GRF8	protein_coding
NPR1+INA (rep3&4) & HAC1+INA (rep1&2)	Chr4	13196294	13196380	AT4G26000	PEP	protein_coding
NPR1+INA (rep3&4) & HAC1+INA (rep1&2)	Chr4	15381239	15382370	AT4G31800	WRKY18	protein_coding
NPR1+INA (rep3&4) & HAC1+INA (rep1&2)	Chr4	16295081	16295418	AT4G34000	ABF3	protein_coding
NPR1+INA (rep3&4) & HAC1+INA (rep1&2)	Chr4	17249781	17249893	AT4G36550	PUB5	protein_coding
NPR1+INA (rep3&4) & HAC1+INA (rep1&2)	Chr4	18206558	18206742	AT4G39070	BZS1	protein_coding
NPR1+INA (rep3&4) & HAC1+INA (rep1&2)	Chr4	18472401	18472520	AT4G39800	MIPS1	protein_coding
NPR1+INA (rep3&4) & HAC1+INA (rep1&2)	Chr5	4053687	4053888	AT5G12840	NF-YA1	protein_coding
NPR1+INA (rep3&4) & HAC1+INA (rep1&2)	Chr5	4432338	4432390	AT5G13740	ZIF1	protein_coding
NPR1+INA (rep3&4) & HAC1+INA (rep1&2)	Chr5	5996745	5996986	AT5G18140	DJC69	protein_coding
NPR1+INA (rep3&4) & HAC1+INA (rep1&2)	Chr5	8215900	8216375	AT5G24210	PRLIP1	protein_coding
NPR1+INA (rep3&4) & HAC1+INA (rep1&2)	Chr5	16576595	16576810	AT5G41410	BEL1	protein_coding
NPR1+INA (rep3&4) & HAC1+INA (rep1&2)	Chr5	18558846	18558972	AT5G45745		pre_trna
NPR1+INA (rep3&4) & HAC1+INA (rep1&2)	Chr5	22123547	22123733	AT5G54500	FQR1	protein_coding
NPR1+INA (rep3&4) & HAC1+INA (rep1&2)	Chr5	24279708	24279930	AT5G60360	ALP	protein_coding
NPR1+INA (rep3&4) & HAC1+INA (rep1&2)	Chr5	25431534	25431679	AT5G63530	FP3	protein_coding
NPR1+INA (rep3&4) & HAC1+INA (rep1&2)	Chr5	26083168	26083313	AT5G65270	RABA4a	protein_coding
NPR1+INA (rep3&4) & HAC1+INA (rep1&2)	Chr5	26846293	26846458	AT5G67280	RLK	protein_coding

4.6. Colocalization of NPR1 and HAC1 onto chromatin is mainly mediated by TGA transcription factors

The TGACG motif and the G-box were enriched in the NPR1 peaks, and TGA2 indeed bound to several of the TGACG motif- or G-box-containing regions (Figure 12 and 13). I then performed DNA-sequence analysis of the co-targeting sites of NPR1 and HAC1. Again, the TGACG motif and the G-box were most abundant at the co-targeting sites (Figure 17A). I tested if TGA2 is also enriched at these co-targeting sites (Figure 17B and 18A) by ChIP-qPCR using *TGA2:mCherry* transgenic plants, and TGA2:mCherry was enriched at the co-targeting sites independently of INA treatment, but not in regions distant from the co-targeting sites (Figure 17C and 18B). These results are consistent with a previous study that showed INA-independent targeting of TGA2 and INA-dependent formation of the HAC-NPR1-TGA complex at the *PR1* promoter (Jin et al., 2018) and suggest that the HAC-NPR1-TGA complex might be targeted to hundreds of TGACG motif- or G-box-containing loci, mostly in an INA-dependent manner.

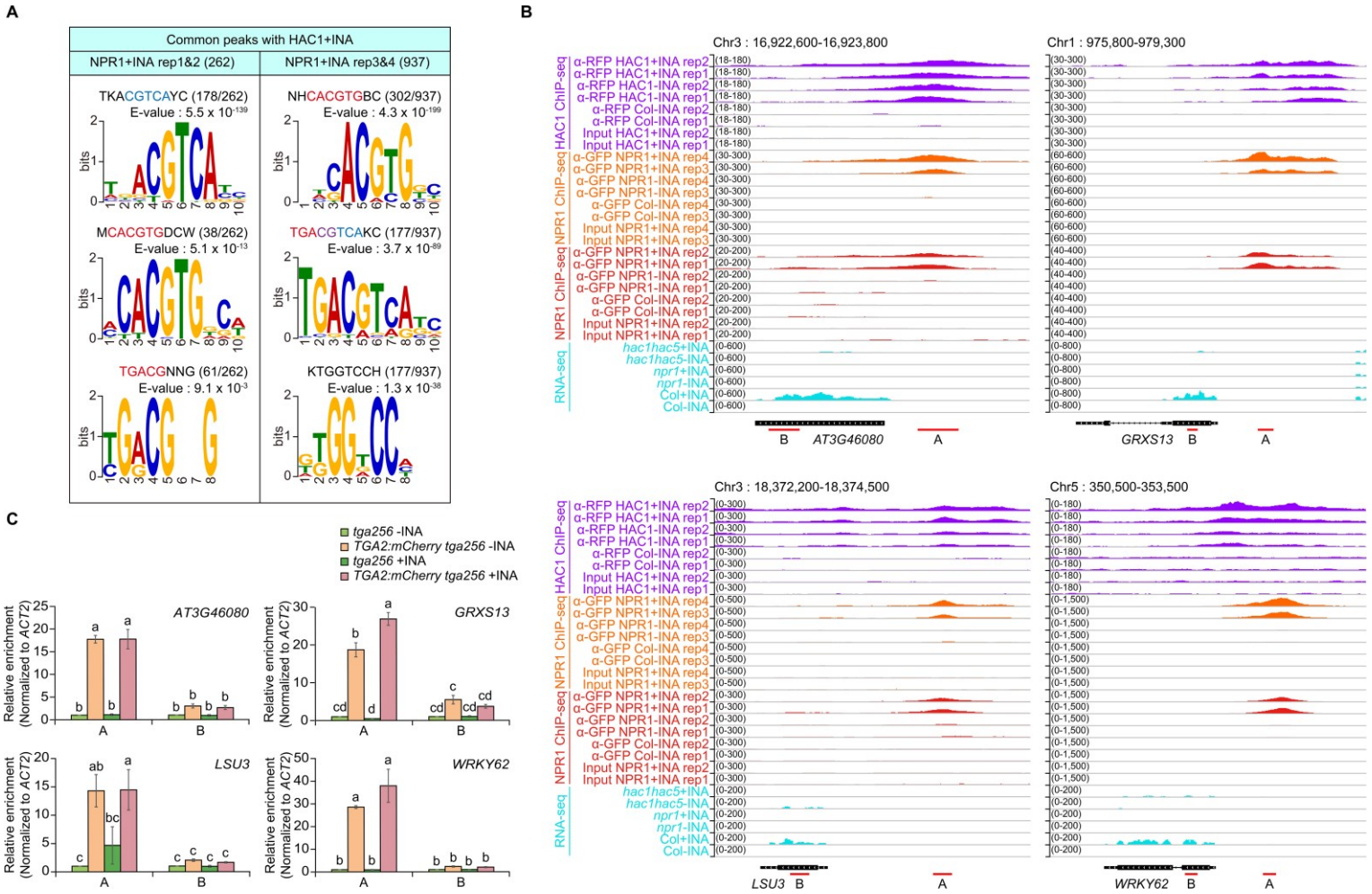
A
Common peaks with HAC1+INA
NPR1+INA rep1&2 (262)
NPR1+INA rep3&4 (937)
TKACGTCAYC (178/262)
E-value : 5.5 x 10-139
NHCACGTGBC (302/937)
E-value : 4.3 x 10-199
MCACGTGDCW (38/262)
E-value : 5.1 x 10-13
TGACGTCAKC (177/937)
E-value : 3.7 x 10-89
TGACGNNG (61/262)
E-value : 9.1 x 10-3
KTGGTCCH (177/937)
E-value : 1.3 x 10-38
bits
B
Chr3 : 16,922,600-16,923,800
Chr1 : 975,800-979,300
Chr3 : 18,372,200-18,374,500
Chr5 : 350,500-353,500
HAC1 ChIP-seq
NPR1 ChIP-seq
RNA-seq
α-RFP HAC1+INA rep2
α-RFP HAC1+INA rep1
α-RFP HAC1-INA rep2
α-RFP HAC1-INA rep1
α-RFP Col-INA rep2
α-RFP Col-INA rep1
Input HAC1+INA rep2
Input HAC1+INA rep1
α-GFP NPR1+INA rep4
α-GFP NPR1+INA rep3
α-GFP NPR1-INA rep4
α-GFP NPR1-INA rep3
α-GFP Col-INA rep4
α-GFP Col-INA rep3
Input NPR1+INA rep4
Input NPR1+INA rep3
α-GFP NPR1+INA rep2
α-GFP NPR1+INA rep1
α-GFP NPR1-INA rep2
α-GFP NPR1-INA rep1
α-GFP Col-INA rep2
α-GFP Col-INA rep1
Input NPR1+INA rep2
Input NPR1+INA rep1
hac1hac5+INA
hac1hac5-INA
npr1+INA
npr1-INA
Col+INA
Col-INA
AT3G46080
GRXS13
LSU3
WRKY62
C
tga256 -INA
TGA2:mCherry tga256 -INA
tga256 +INA
TGA2:mCherry tga256 +INA
Relative enrichment (Normalized to ACT2)
AT3G46080
GRXS13
LSU3
WRKY62
A
B

Figure 17. DNA motif with TGACG sequence is enriched in regions co-targeted by NPR1 and HAC1, and TGA2 is targeted to the motif-containing regions.

(**A**) DNA sequences enriched in the common target regions of NPR1 and HAC1 identified in the presence of INA. The top 3 results are displayed in descending order of E-value. See Figure 12A legend for more details.

(**B**) IGV snapshots of HAC1 ChIP-seq, NPR1 ChIP-seq, and RNA-seq data for the representative co-targets of NPR1 and HAC1. The representative co-targets are the genes that are activated by both *NPR1*- and *HAC1 HAC5*-dependent manners and contain TGACG motifs within the common peaks of NPR1 and HAC1. Red lines below gene models marked with A or B indicate the common peaks of NPR1 and HAC1 or regions distant from the common peaks, respectively. See Figure 12B legend for more details.

(**C**) TGA2-targeting activity to the common peaks containing the TGACG motif (regions A) or distant regions (regions B) presented in (B) in the presence (+INA) or absence (−INA) of INA. A and B regions indicated in (B) were amplified in ChIP-qPCR assays. See Figure 12C legend for more experimental details.

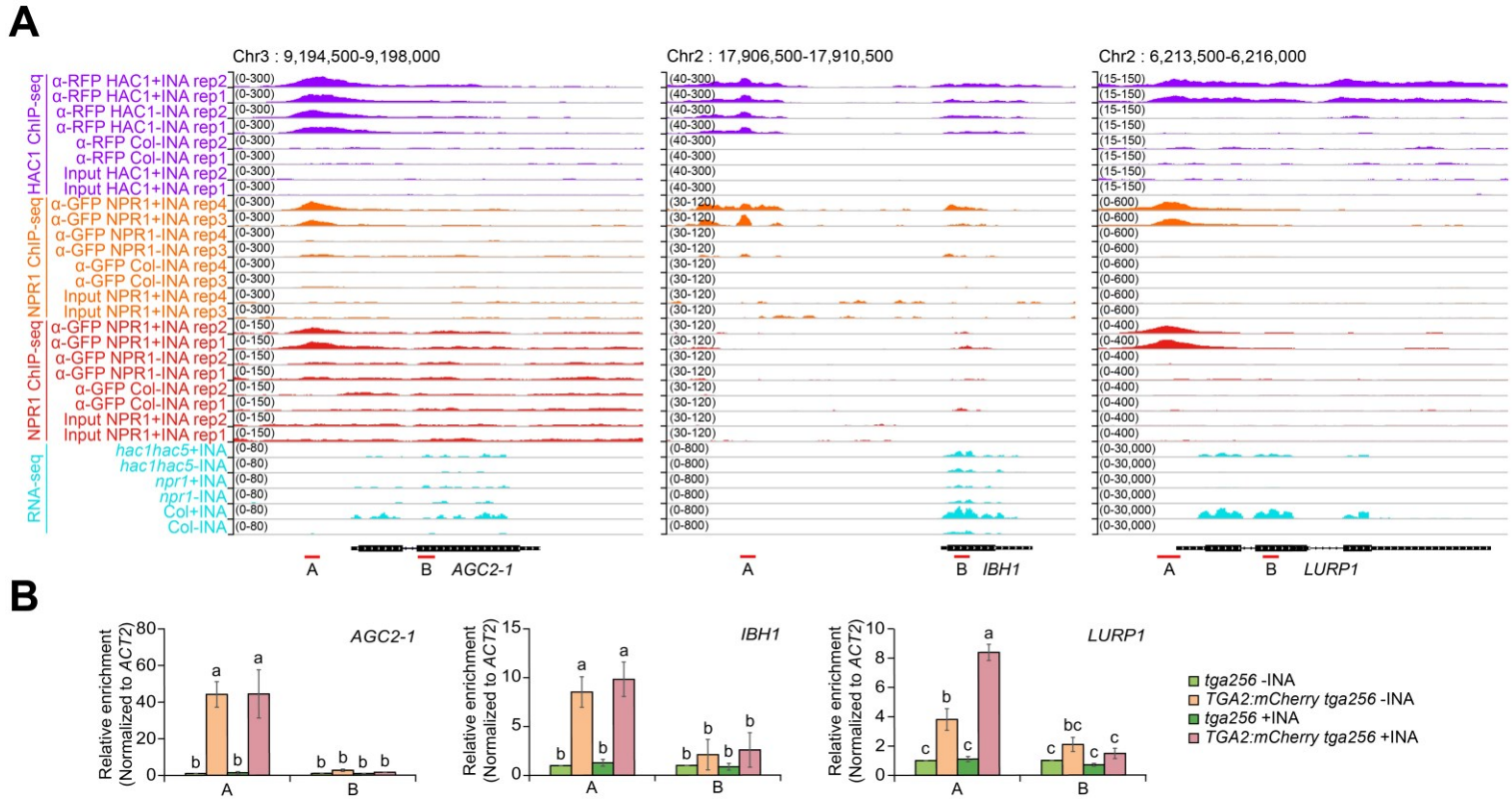
A
Chr3 : 9,194,500-9,198,000
Chr2 : 17,906,500-17,910,500
Chr2 : 6,213,500-6,216,000
HAC1 ChIP-seq
NPR1 ChIP-seq
NPR1 ChIP-seq
RNA-seq
α-RFP HAC1+INA rep2
α-RFP HAC1+INA rep1
α-RFP HAC1-INA rep2
α-RFP HAC1-INA rep1
α-RFP Col-INA rep2
α-RFP Col-INA rep1
Input HAC1+INA rep2
Input HAC1+INA rep1
α-GFP NPR1+INA rep4
α-GFP NPR1+INA rep3
α-GFP NPR1-INA rep4
α-GFP NPR1-INA rep3
α-GFP Col-INA rep4
α-GFP Col-INA rep3
Input NPR1+INA rep4
Input NPR1+INA rep3
α-GFP NPR1+INA rep2
α-GFP NPR1+INA rep1
α-GFP NPR1-INA rep2
α-GFP NPR1-INA rep1
α-GFP Col-INA rep2
α-GFP Col-INA rep1
Input NPR1+INA rep2
Input NPR1+INA rep1
hac1hac5+INA
hac1hac5-INA
npr1+INA
npr1-INA
Col+INA
Col-INA
A
B
AGC2-1
IBH1
LURP1
B
Relative enrichment (Normalized to ACT2)
AGC2-1
IBH1
LURP1
tga256 -INA
TGA2:mCherry tga256 -INA
tga256 +INA
TGA2:mCherry tga256 +INA

Figure 18. TGA2 targeting to regions co-targeted by NPR1 and HAC1.

(**A**) IGV snapshots of HAC1 ChIP-seq, NPR1 ChIP-seq, and RNA-seq data for three representative co-targets of NPR1 and HAC1. The representative co-targets are the genes that are co-activated by both *NPR1*- and *HAC1 HAC5*-dependent manners and contain TGACG motifs within the common peaks of NPR1 and HAC1. See Figure 17B and 12B legends for more details.

(**B**) TGA2-targeting activity to the common peaks containing the TGACG motif (regions A) or distant regions (regions B) presented in (A) in the presence (+INA) or absence (–INA) of INA. See Figure 17C and 12C legend for more details.

4.7. Pre-targeting of NPR1 results in more rapid and robust induction by SA

I identified dozens of genes that are targeted by NPR1 without INA treatment and classified these genes as NPR1−INA targets (Figure 8). Most of these NPR1−INA targets did not show *NPR1*-dependent expression in the absence of INA (Figure 21A). Therefore, I investigated whether NPR1-targeting activity or expression of the NPR1−INA targets might be changed by INA treatment. Upon INA treatment, NPR1 enrichment levels increased not only at the NPR1−INA targets of the rep1&2 dataset but also at the targets of the rep3&4 dataset, which include all the rep1&2 NPR1−INA targets (Figure 19A and B). Heatmaps for the NPR1−INA targets showed that these genes are induced by INA in the WT, and I observed substantial expression differences between WT and *npr1* plants in the presence rather than in the absence of INA (Figure 19C and 21B). Thus, NPR1 targeting activity at the NPR1−INA targets is reinforced by SA signaling, and further enriched NPR1 may lead to SA- and *NPR1*-dependent expression.

To better understand the biological importance of NPR1 pre-targeting, I investigated the RNA-expression dynamics of the NPR1−INA targets identified from the rep3&4 dataset using published RNA-seq data (Caarls et al., 2017). I found that 75% (27/36) of the NPR1−INA targets were induced at 2 h after SA treatment, and this induction was maintained until 12 h after SA treatment (Figure 19D). In contrast, only 15% (157/1,021) of the NPR1+INA targets identified from the rep3&4 dataset were induced at 2 h after SA treatment (Figure 19D). I obtained similar results when I investigated NPR1 targets identified from the rep1&2 dataset: 88% (22/25) or 29% (101/353) of the NPR1−INA or NPR1+INA targets, respectively, were induced at 2 h after SA treatment (Figure 21C and D). When I

compared initial induction times after SA treatment between the NPR1−INA and NPR1+INA targets among SA-induced genes, the NPR1−INA targets tended to be induced more rapidly than the NPR1+INA targets (Figure 19E). Furthermore, the induction fold of the NPR1−INA targets was higher than that of the NPR1 targets identified only in the +INA condition (Figure 19E). These results indicate that NPR1 pre-targeting in the basal state results in more rapid and robust induction of the target genes during SA-triggered immunity.

I then asked which transcription factors mediate NPR1 targeting in the absence of INA. Motif analyses using NPR1−INA target-site sequences revealed the TGACG motif as the sole transcription factor-binding site (Figure 20A and 21E). I then selected three of the NPR1−INA targets, *NIM1-INTERACTING1* (*NIMIN-1*), *WRKY38*, and *WRKY70*, to test TGA2 enrichment in their NPR1-targeting regions containing the TGACG motif, as these genes exhibited increased NPR1 targeting by INA treatment and INA- as well as *NPR1*-dependent expression (Figure 20B). Within the NPR1-targeting regions of these genes, TGA2:mCherry showed an INA-independent targeting activity (Figure 20C). Therefore, NPR1 targeting in the basal state is also mediated by TGA transcription factors.

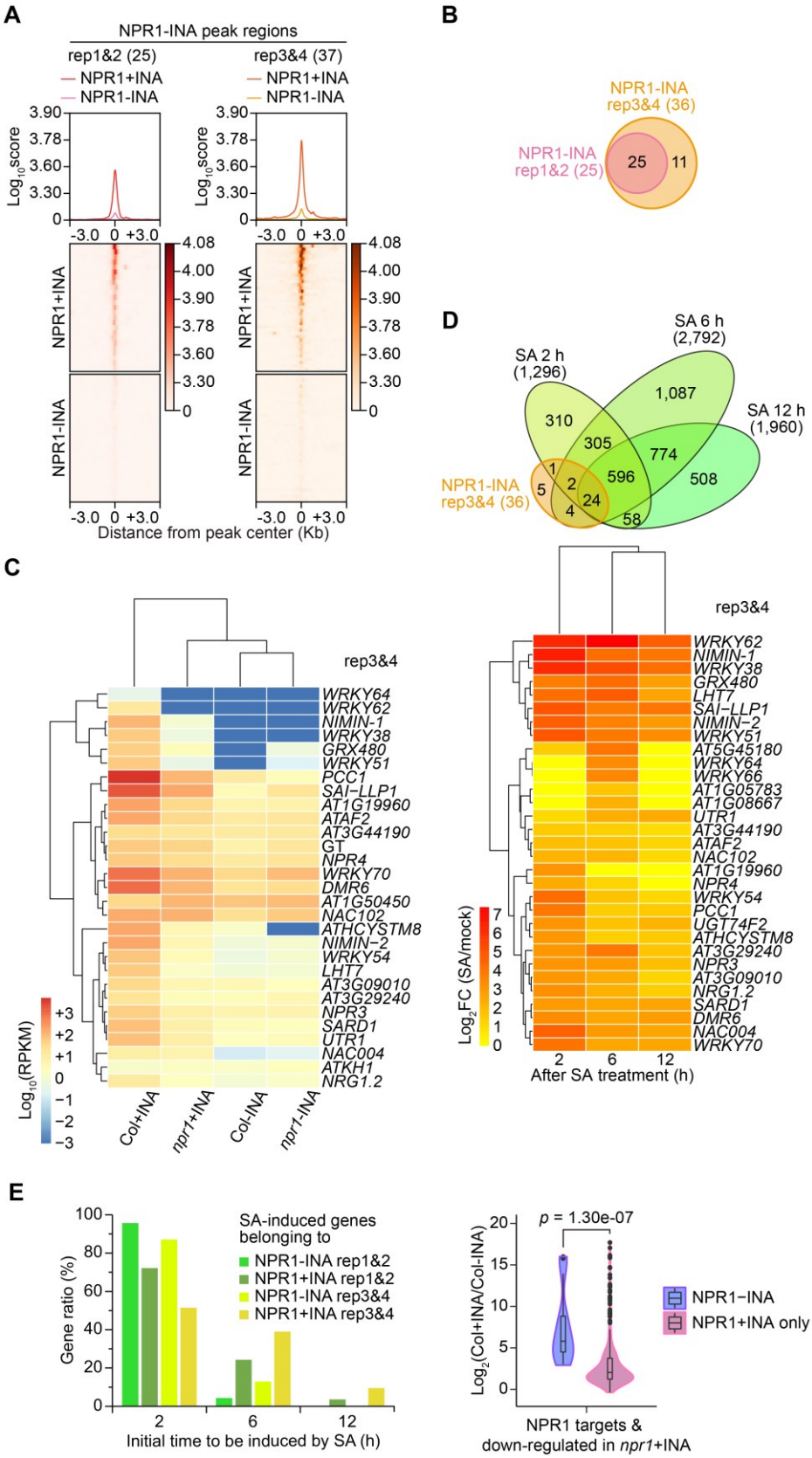
A
NPR1-INA peak regions
rep1&2 (25)
rep3&4 (37)
NPR1+INA
NPR1-INA
Log10 score
3.90
3.78
3.60
3.30
0
-3.0 0 +3.0
4.08
4.00
3.90
3.78
3.60
3.30
0
Distance from peak center (Kb)
B
NPR1-INA rep3&4 (36)
NPR1-INA rep1&2 (25)
25
11
C
rep3&4
WRKY64
WRKY62
NIMIN-1
WRKY38
GRX480
WRKY51
PCC1
SAI-LLP1
AT1G19960
ATAF2
AT3G44190
GT
NPR4
WRKY70
DMR6
AT1G50450
NAC102
ATHCYSTM8
NIMIN-2
WRKY54
LHT7
AT3G09010
AT3G29240
NPR3
SARD1
UTR1
NAC004
ATKH1
NRG1.2
Log10(RPKM)
+3
+2
+1
0
−1
−2
−3
Col+INA
npr1+INA
Col-INA
npr1-INA
D
SA 2 h (1,296)
SA 6 h (2,792)
SA 12 h (1,960)
NPR1-INA rep3&4 (36)
310
1,087
305
774
1
2
596
508
5
24
4
58
rep3&4
WRKY62
NIMIN-1
WRKY38
GRX480
LHT7
SAI-LLP1
NIMIN-2
WRKY51
AT5G45180
WRKY64
WRKY66
AT1G05783
AT1G08667
UTR1
AT3G44190
ATAF2
NAC102
AT1G19960
NPR4
WRKY54
PCC1
UGT74F2
ATHCYSTM8
AT3G29240
NPR3
AT3G09010
NRG1.2
SARD1
DMR6
NAC004
WRKY70
Log2FC (SA/mock)
7
6
5
4
3
2
1
0
2
6
12
After SA treatment (h)
E
Gene ratio (%)
100
80
60
40
20
0
SA-induced genes belonging to
NPR1-INA rep1&2
NPR1+INA rep1&2
NPR1-INA rep3&4
NPR1+INA rep3&4
2
6
12
Initial time to be induced by SA (h)
p = 1.30e-07
Log2(Col+INA/Col-INA)
20
15
10
5
0
NPR1−INA
NPR1+INA only
NPR1 targets & down-regulated in npr1+INA

Figure 19. Genes targeted by NPR1 before SA signal show a tendency for more rapid and robust induction by SA.

(**A**) Enrichment scores of NPR1:GFP in the absence (–INA) or presence (+INA) of INA within the regions enriched with NPR1:GFP in the absence of INA. Profile plots show the average scores of NPR1:GFP enrichment in regions from the 3 kb upstream to the 3 kb downstream of NPR1:GFP-peak centers. Heatmaps visualize enrichment scores corresponding to individual peaks. NPR1 targets identified from the rep1&2 or rep3&4 dataset were used for the analysis. See Figure 8A-B legend for more details.

(**B**) Venn diagram showing the overlap between INA-independent NPR1-target genes identified from the two different ChIP-seq datasets consisting of two biological repeats each. Total numbers of annotated targets are indicated in parentheses.

(**C**) Heatmap illustrating the expression levels of genes that were identified as INA-independent NPR1 targets from the rep3&4 dataset. Expression levels are presented as $\log_{10}$ values of RPKMs in WT (Col) and *npr1-1* mutant in the absence (–INA) or presence (+INA) of INA. Hierarchical clustering between genotype and/or treatment was performed based on similarity of gene expressions.

(**D**) Expression of the INA-independent NPR1-target genes identified from the rep3&4 dataset after 2, 6, and 12 hours (h) of SA treatment. RNA-seq data (Caarls et al., 2017) obtained from BioProject database (ID: PRJNA224133) were used for analysis. The venn diagram illustrates the numbers of NPR1-target genes that are induced by 1 mM SA treatment at each time point. DEGs between SA and mock

treatments were analyzed using two biological repeats including 4 technical runs each ($\log_2$FC ≥ 1, *p*-value < 0.05). The heatmap shows the expression level of each gene as $\log_2$ value of fold change (FC) between SA and mock treated WT.

(**E**) The initial induction time after SA treatment and the induction fold changes by INA of the NPR1-target genes. Bar graph (left) illustrating the percentage of NPR1-target genes showing initial induction by SA. SA-induced genes presented in (D) were classified into 4 groups depending on their NPR1-targeting information provided by the rep1&2 and rep3&4 datasets. The genes in each group were further classified according to their initial induction time by SA, and the numbers of the classified genes were divided by the numbers of total genes of each group for gene-ratio calculation. Violin plot with included box plot (right) showing fold changes in NPR1-target expression before (–INA) and after (+INA) INA treatment in WT (Col) samples. From RNA-seq data (Jin et al., 2018), RPKMs in Col+INA were divided by RPKMs in Col–INA, and the $\log_2$ values of the calculated fold changes are presented. Among genes showing *NPR1*-dependent expression upon INA treatment, INA-independent NPR1-target genes (NPR1–INA) and only INA-dependent NPR1-target genes (NPR1+INA only) were extracted and used for this analysis. The only INA-dependent NPR1-target genes were obtained by excluding the INA-independent NPR1-target genes from the NPR1-target genes identified under INA treatment condition. *P*-value shown was calculated using two-tailed Mann-Whitney U-test.

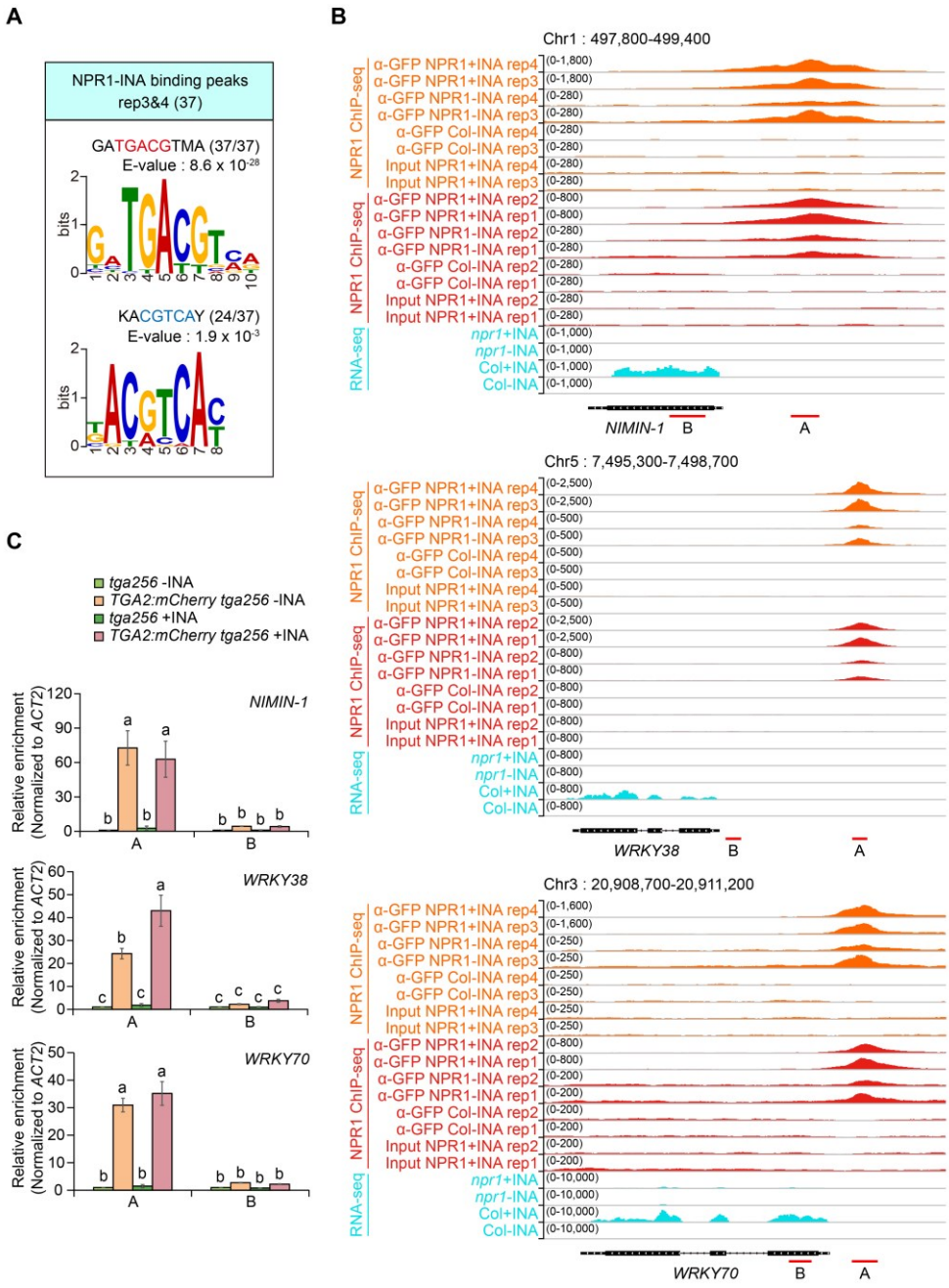
A
NPR1-INA binding peaks
rep3&4 (37)
GATGACGTMA (37/37)
E-value : 8.6 x 10-28
KACGTCAY (24/37)
E-value : 1.9 x 10-3
bits
B
Chr1 : 497,800-499,400
Chr5 : 7,495,300-7,498,700
Chr3 : 20,908,700-20,911,200
NPR1 ChIP-seq
RNA-seq
α-GFP NPR1+INA rep4
α-GFP NPR1+INA rep3
α-GFP NPR1-INA rep4
α-GFP NPR1-INA rep3
α-GFP Col-INA rep4
α-GFP Col-INA rep3
Input NPR1+INA rep4
Input NPR1+INA rep3
α-GFP NPR1+INA rep2
α-GFP NPR1+INA rep1
α-GFP NPR1-INA rep2
α-GFP NPR1-INA rep1
α-GFP Col-INA rep2
α-GFP Col-INA rep1
Input NPR1+INA rep2
Input NPR1+INA rep1
npr1+INA
npr1-INA
Col+INA
Col-INA
NIMIN-1
WRKY38
WRKY70
A
B
C
tga256 -INA
TGA2:mCherry tga256 -INA
tga256 +INA
TGA2:mCherry tga256 +INA
Relative enrichment
(Normalized to ACT2)
NIMIN-1
WRKY38
WRKY70

Figure 20. DNA motif with TGACG sequence is enriched in regions pre-targeted by NPR1, and TGA2 is targeted to the motif-containing regions.

(**A**) DNA sequences enriched in INA-independent NPR1-targeting regions identified from the rep3&4 dataset. The results are displayed in descending order of E-value. The defined motif sequences are shown above E-values. Well-known motif sequences are in red for forward orientation or in blue for reverse orientation. Numbers of each motif occurrence are indicated in parentheses in comparison to the total numbers of input sequences. See Figure 12A legend for more details.

(**B**) IGV snapshots of NPR1 ChIP-seq and RNA-seq data for representative genes displaying INA-independent NPR1 targeting. Red lines below gene models marked with A or B indicate NPR1-binding peaks or regions distant from the peaks, respectively. See Figure 12B legend for more details.

(**C**) TGA2-targeting activity to INA-independent NPR1 targets. A and B regions indicated in (G) were amplified in ChIP-qPCR assays. See Figure 12C legend for more details.

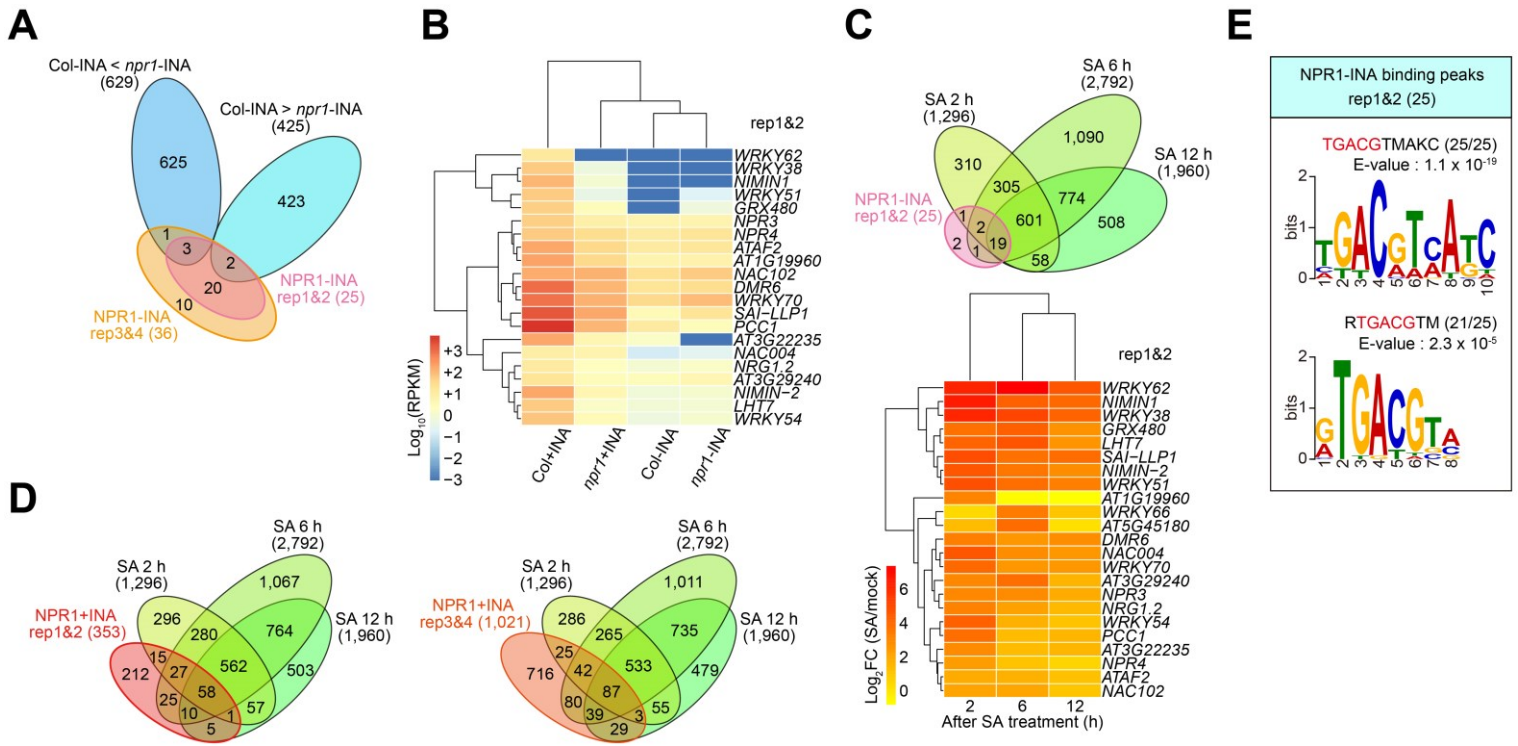
A
Col-INA < npr1-INA
(629)
Col-INA > npr1-INA
(425)
625
423
1
3
2
20
10
NPR1-INA
rep1&2 (25)
NPR1-INA
rep3&4 (36)
B
rep1&2
WRKY62
WRKY38
NIMIN1
WRKY51
GRX480
NPR3
NPR4
ATAF2
AT1G19960
NAC102
DMR6
WRKY70
SAI−LLP1
PCC1
AT3G22235
NAC004
NRG1.2
AT3G29240
NIMIN−2
LHT7
WRKY54
Log10(RPKM)
+3
+2
+1
0
−1
−2
−3
Col+INA
npr1+INA
Col-INA
npr1-INA
C
SA 2 h
(1,296)
SA 6 h
(2,792)
SA 12 h
(1,960)
NPR1-INA
rep1&2 (25)
310
1,090
305
774
1
2
601
508
2
1
19
58
rep1&2
WRKY62
NIMIN1
WRKY38
GRX480
LHT7
SAI−LLP1
NIMIN−2
WRKY51
AT1G19960
WRKY66
AT5G45180
DMR6
NAC004
WRKY70
AT3G29240
NPR3
NRG1.2
WRKY54
PCC1
AT3G22235
NPR4
ATAF2
NAC102
Log2FC (SA/mock)
6
4
2
0
2
6
12
After SA treatment (h)
D
SA 2 h
(1,296)
SA 6 h
(2,792)
SA 12 h
(1,960)
NPR1+INA
rep1&2 (353)
296
1,067
280
764
15
562
212
27
503
58
25
10
57
1
5
SA 2 h
(1,296)
SA 6 h
(2,792)
SA 12 h
(1,960)
NPR1+INA
rep3&4 (1,021)
286
1,011
265
735
25
533
716
42
479
87
80
39
55
3
29
E
NPR1-INA binding peaks
rep1&2 (25)
TGACGTMAKC (25/25)
E-value : 1.1 x 10-19
bits
RTGACGTM (21/25)
E-value : 2.3 x 10-5
bits

Figure 21. INA-independent NPR1 targets show a tendency for rapid induction by SA.

(**A**) Venn diagram illustrating the overlaps between INA-independent NPR1 targets and genes showing *NPR1*-dependent expression in the absence of INA.

(**B**) Heatmaps illustrating the expression levels of INA-independent NPR1 targets identified from the rep1&2 dataset. See Figure 19C for more details.

(**C**) Expression of the INA-independent NPR1-target genes identified from the rep1&2 dataset after 2, 6, and 12 h of SA treatment. See Figure 19D legend for more details.

(**D**) Venn diagrams illustrating the numbers of genes showing INA-dependent NPR1 targeting and SA-induced expression over time. NPR1 targets identified from the rep1&2 or the rep3&4 dataset were analyzed separately.

(**E**) DNA sequences enriched in INA-independent NPR1-targeting regions identified from the rep1&2 dataset. The results are displayed in descending order of E-value. The defined motif sequences are shown above E-values. Well-known motif sequences are in red. Numbers of each motif occurrence are indicated in parentheses in comparison to the total numbers of input sequences. See Figure 20A legend for more details.

5. Discussion

My genome-wide study revealed that NPR1 targets to the genome mostly in an SA-dependent manner and primarily activates genes encoding DNA-binding factors through its direct targeting. The proportion of direct NPR1 targets accounted for only 3% (116/3,675 based on the rep1&2 dataset) or 8% (278/3,675 based on the rep3&4 dataset) of the *NPR1*-dependently expressed genes. Among these *NPR1*-dependently expressed NPR1 targets, genes encoding DNA-binding factors were most abundant. On the other hand, most *NPR1*-dependently expressed defense-related genes were not directly targeted by NPR1. These results suggest that NPR1 elicits transcriptional cascades upon SA perception during genome-wide transcriptional reprogramming that confers host plant immunity. Among various families of transcription factor genes directly targeted and regulated by NPR1, the *WRKY* family was the most abundant. The importance and dominance of WRKYs in SA-triggered transcriptional reprogramming has been studied (Hickman et al., 2019). In addition to *WRKYs*, I identified genes encoding a variety of other types of transcription factors. Thus, diverse families of transcription factors may mediate the SA-induced transcriptional cascades initiated by NPR1 targeting.

Besides triggering transcriptional cascades, NPR1 directly activates various biological processes upon SA perception. For example, my identification of receptor-, NADPH oxidase-, ABA transporter-, protein kinase-, and diverse ETI regulator-encoding genes as direct NPR1 activation targets demonstrates a broad, direct role of NPR1 in SA-triggered immunity. Hence, the master regulatory role of NPR1 seems to be executed through directly activating key regulatory components

of SA-dependent immunity as well as triggering transcriptional cascades.

Balancing the amplitude of immune response is critical for optimal plant fitness. The finding that NPR1 also targets and activates negative regulators of SA-triggered immunity upon SA signaling suggests a role of NPR1 in fine-tuning or balancing SA-triggered immunity. WRKYs positively or negatively regulate SA-triggered immunity (Chen et al., 2019; Fu and Dong, 2013; Wani et al., 2021). My study showed that WRKYs that negatively regulate SA-triggered immunity, such as WRKY18, WRKY38, WRKY40, and WRKY62, are encoded by a group of genes that are directly targeted by NPR1 and activated in SA- and *NPR1*-dependent manners. Another member of this group was NIMIN-1, which inhibits NPR1 during SA-induced *PR1* induction by forming a complex with NPR1 (Weigel et al., 2005). NPR1 homologs, such as NPR3 and NPR4, that were also found in this group, are SA receptors that cause NPR1 degradation (Fu et al., 2012) and act as transcriptional repressors, unlike NPR1 (Ding et al., 2018). Thus, NPR1 not only activated positive regulators but also negative regulators of SA-triggered immunity. Without the opposing function of these negative regulators, NPR1 activity might generate excessive or prolonged immune responses that could be deleterious to plant fitness and create vulnerability to other stresses. Therefore, I suggest that NPR1 fine-tunes the immune response by balancing positive and negative defense pathways, and this fine-tuning enhances plant fitness and survival.

My study also revealed that NPR1 is directly involved in phytohormone crosstalk. For example, NPR1 targeted to and activated *WRKY46*, *WRKY54*, and *WRKY70*, which are involved in brassinosteroid (BR) biosynthesis (Chen et al., 2017). BR enhances SA-triggered immunity by inhibiting the

BRASSINOSTEROID-INSENSITIVE2 (BIN2)-mediated phosphorylation and destabilization of clade I TGAs (Kim et al., 2022). Thus, NPR1 might reinforce SA-triggered immunity by increasing BR biosynthesis. Genes encoding several WRKYs involved in JA and ethylene (ET) signaling were also among the genes directly targeted and activated by NPR1. SA and JA/ET signaling pathways have been described to have an antagonistic relationship (Pieterse et al., 2009; Li et al., 2019). On the contrary, it has also been reported that SA and JA/ET synergistically regulate SA-responsive genes (De Vos et al., 2006; Hickman et al., 2019) or programmed cell death during ETI (Liu et al., 2016) and that key components in JA/ET pathways positively regulate SA-responsive genes during immunity (Hillmer et al., 2017; Mine et al., 2017). My study showed that NPR1 directly activates genes encoding ethylene response factors (ERFs) that are major transcriptional regulators of ET-responsive genes. Thus, I propose that NPR1 coordinates complex phytohormone signaling networks during SA-triggered transcriptional reprogramming, probably to optimize SA-triggered immunity.

This study uncovered that NPR1 and HAC1 co-targeting at the genome level is involved in *NPR1*- and *HAC1/5*-dependent SA-induced transcriptional reprogramming. My ChIP-seq analyses revealed several hundred NPR1 and HAC1 co-targets. At these co-targeting loci, SA-induced H3Ac levels increased in *NPR1*- and *HAC1/5*-dependent manners, and a subset of the co-targets also showed *NPR1*- and *HAC1/5*-dependent expression upon SA signaling. These results are consistent with a previous study that reported HAC1/5 as epigenetic factors recruited by the NPR1-TGA complex to confer transcriptional coactivator function to NPR1 (Jin et al., 2018). My current study furthers understanding of the cooperative roles of

NPR1 and HAC1/5 at the genome level. Together, these two studies demonstrate that HAC1 is a bona fide epigenetic partner of NPR1 acting at several hundred co-targets upon SA signaling to promote the expression of at least dozens of co-targets. A recent structure-based study proposed an enhanceosome model in which an SA-induced structural change of NPR1 facilitates recruitment of an unknown transcriptional regulator(s) for gene activation (Kumar et al., 2022), consistent with the idea that HAC1 cooperates with NPR1 to regulate SA-induced transcriptional reprogramming. However, it remains unknown how NPR1 induces transcription at *NPR1*-dependent but *HAC1/5*-independent loci during SA-triggered transcriptional reprogramming. Thus, it would be of interest to find new epigenetic partners of NPR1.

I also found that NPR1 and HAC1 co-targeting as well as NPR1 targeting are principally mediated by TGA transcription factors. Consistently, the TGACG sequence was the DNA motif most abundantly found within NPR1 targeting regions, both in the absence or presence of SA. In addition, the TGACG motif was the most abundant even in the co-targeting regions of NPR1 and HAC1 identified upon SA signaling. Further, TGA2, a representative TGA that directly interacts with NPR1 (Zhang et al., 1999; Zhou et al., 2000), bound independently of SA to the NPR1 targets and the NPR1 and HAC1 co-targets containing the TGACG motif. Unexpectedly, TGA2 also bound to NPR1 targets containing the G-box but not the TGACG motif. This suggests that TGA2 binds to TGACG-motif variants or indirectly binds to those NPR1 targets via another transcription factor(s). For this reason, it would be interesting to find another transcription factor(s) mediating the recruitment of the HAC-NPR1-TGA (Jin et al., 2018) or NPR1-TGA complex to

the NPR1 targets containing non-TGACG motifs, especially the G-box.

Dozens of genes were targeted by NPR1 independently of SA treatment, and these SA-independent NPR1 targets were more rapidly and robustly induced by SA compared to SA-dependent NPR1 targets. NPR1 targeting of genes in the basal state probably makes the target chromatin more accessible, allowing drastically increased NPR1 recruitment upon SA signaling. Alternatively, SA binding to pre-targeted NPR1 may lead to an NPR1 conformation efficient for transcriptional activation on site. This feature seems to be related to defense priming, which also accompanies rapid and robust expression of defense genes (Conrath et al., 2011). NPR1 is essential for SA-induced defense priming (Pajerowska-Mukhtar et al., 2013). Therefore, I propose NPR1 pre-targeting as a possible mechanism for defense priming.

In summary, my genome-wide study revealed that the primary role of NPR1 is to directly activate genes encoding DNA-binding factors through SA-dependent targeting. In addition to transcription factor-encoding genes, NPR1 directly activated genes involved in various biological processes required for SA-triggered immunity. Furthermore, NPR1 directly activated positive and negative regulators of SA-triggered immunity and genes involved in phytohormone crosstalk possibly to balance or fine-tune defense responses. A subset of NPR1 targets required HAC1/5 as epigenetic partners, and TGA transcription factors played a major role in recruiting NPR1 and the NPR1-HAC1 complex to genome-wide targets. Furthermore, NPR1 was bound to some targets in the basal state, and this occupancy allowed for more rapid and robust target induction upon SA signaling, reminiscent of defense priming. Thus, my work reveals how NPR1

orchestrates SA-triggered transcriptional reprogramming and how HAC1 and TGAs support NPR1 to elicit SA-induced immune responses at the genome level.

References

Alvarez-Venegas, R., Abdallat, A.A., Guo, M., Alfano, J.R. and Avramova, Z. (2007) Epigenetic control of a transcription factor at the cross section of two antagonistic pathways. *Epigenetics*, 2, 106-113.

An, C., Deng, L., Zhai, H., You, Y., Wu, F., Zhai, Q., Goossens, A. and Li, C. (2022) Regulation of jasmonate signaling by reversible acetylation of TOPLESS in Arabidopsis. *Mol Plant*, 15, 1329-1346.

An, C., Li, L., Zhai, Q., You, Y., Deng, L., Wu, F., Chen, R., Jiang, H., Wang, H., Chen, Q. et al. (2017) Mediator subunit MED25 links the jasmonate receptor to transcriptionally active chromatin. *Proc Natl Acad Sci U S A*, 114, E8930-E8939.

Anders, S., Pyl, P.T. and Huber, W. (2015) HTSeq—a python framework to work with high-throughput sequencing data. *Bioinformatics*, 31, 166-169.

Armijo, G., Salinas, P., Monteoliva, M.I., Seguel, A., García, C., Villarroel-Candia, E., Song, W., van der Krol, A.R., Álvarez, M.E. and Holuigue, L. (2013) A salicylic acid–induced lectin-like protein plays a positive role in the effector-triggered immunity response of Arabidopsis thaliana to Pseudomonas syringae Avr-Rpm1. *Mol Plant Microbe Interact*, 26, 1395-1406.

Attaran, E., Zeier, T.E., Griebel, T. and Zeier, J.r. (2009) Methyl salicylate production and jasmonate signaling are not essential for systemic acquired resistance in Arabidopsis. *Plant Cell*, 21, 954-971.

Axtell, M.J. and Staskawicz, B.J. (2003) Initiation of RPS2-specified disease resistance in Arabidopsis is coupled to the AvrRpt2-directed elimination of RIN4.

Cell, 112, 369-377.

Bailey, T.L., Boden, M., Buske, F.A., Frith, M., Grant, C.E., Clementi, L., Ren, J., Li, W.W. and Noble, W.S. (2009) MEME suite: tools for motif discovery and searching. *Nucleic Acids Res*, 37, W202-W208.

Berr, A., McCallum, E.J., Alioua, A., Heintz, D., Heitz, T. and Shen, W.-H. (2010) Arabidopsis histone methyltransferase SET DOMAIN GROUP8 mediates induction of the jasmonate/ethylene pathway genes in plant defense response to necrotrophic fungi. *Plant Physiol*, 154, 1403-1414.

Berriri, S., Gangappa, S.N. and Kumar, S.V. (2016) SWR1 chromatin-remodeling complex subunits and H2A.Z have non-overlapping functions in immunity and gene regulation in Arabidopsis. *Mol Plant*, 9, 1051-1065.

Bi, G., Su, M., Li, N., Liang, Y., Dang, S., Xu, J., Hu, M., Wang, J., Zou, M., Deng, Y. et al. (2021) The ZAR1 resistosome is a calcium-permeable channel triggering plant immune signaling. *Cell*, 184, 3528-3541.e3512.

Bolger, A.M., Lohse, M. and Usadel, B. (2014) Trimmomatic: a flexible trimmer for Illumina sequence data. *Bioinformatics*, 30, 2114-2120.

Caarls, L., Van der Does, D., Hickman, R., Jansen, W., Verk, M.C.V., Proietti, S., Lorenzo, O., Solano, R., Pieterse, C.M.J. and Van Wees, S.C.M. (2017) Assessing the role of ETHYLENE RESPONSE FACTOR transcriptional repressors in salicylic acid-mediated suppression of jasmonic acid-responsive genes. *Plant Cell Physiol*, 58, 266-278.

Cao, H., Bowling, S.A., Gordon, A.S. and Dong, X. (1994) Characterization of an

Arabidopsis mutant that is nonresponsive to inducers of systemic acquired resistance. *Plant Cell*, 6, 1583-1592.

Cao, H., Glazebrook, J., Clarke, J.D., Volko, S. and Dong, X. (1997) The Arabidopsis NPR1 gene that controls systemic acquired resistance encodes a novel protein containing ankyrin repeats. *Cell*, 88, 57-63.

Cao, Y., Liang, Y., Tanaka, K., Nguyen, C.T., Jedrzejczak, R.P., Joachimiak, A. and Stacey, G. (2014) The kinase LYK5 is a major chitin receptor in Arabidopsis and forms a chitin-induced complex with related kinase CERK1. *eLife*, 3, e03766.

Chanda, B., Xia, Y., Mandal, M.K., Yu, K., Sekine, K.T., Gao, Q.-m., Selote, D., Hu, Y., Stromberg, A., Navarre, D. et al. (2011) Glycerol-3-phosphate is a critical mobile inducer of systemic immunity in plants. *Nature Genet*, 43, 421-427.

Chen, J., Nolan, T.M., Ye, H., Zhang, M., Tong, H., Xin, P., Chu, J., Chu, C., Li, Z. and Yin, Y. (2017) Arabidopsis WRKY46, WRKY54, and WRKY70 transcription factors are involved in brassinosteroid-regulated plant growth and drought responses. *Plant Cell*, 29, 1425-1439.

Chen, X., Li, C., Wang, H. and Guo, Z. (2019) WRKY transcription factors: evolution, binding, and action. *Phytopatho Res*, 1, 13.

Chinchilla, D., Zipfel, C., Robatzek, S., Kemmerling, B., Nürnberger, T., Jones, J.D.G., Felix, G. and Boller, T. (2007) A flagellin-induced complex of the receptor FLS2 and BAK1 initiates plant defence. *Nature*, 448, 497-500.

Chini, A., Fonseca, S., Fernández, G., Adie, B., Chico, J.M., Lorenzo, O., García-Casado, G., López-Vidriero, I., Lozano, F.M., Ponce, M.R. et al. (2007)

The JAZ family of repressors is the missing link in jasmonate signalling. *Nature*, 448, 666-671.

Choi, S.-M., Song, H.-R., Han, S.-K., Han, M., Kim, C.-Y., Park, J., Lee, Y.-H., Jeon, J.-S., Noh, Y.-S. and Noh, B. (2012) HDA19 is required for the repression of salicylic acid biosynthesis and salicylic acid-mediated defense responses in Arabidopsis. *Plant J*, 71, 135-146.

Conrath, U. (2011) Molecular aspects of defence priming. *Trends Plant Sci*, 16, 524-531.

Conrath, U., Beckers, G.J.M., Langenbach, C.J.G. and Jaskiewicz, M.R. (2015) Priming for enhanced defense. *Annu Rev Phytopatho*, 53, 97-119.

D'Urso, A. and Brickner, J.H. (2014) Mechanisms of epigenetic memory. *Trends Genet*, 30, 230-236.

De Vos, M., Van Zaanen, W., Koornneef, A., Korzelius, J.m.P., Dicke, M., Van Loon, L.C. and Pieterse, C.M.J. (2006) Herbivore-induced resistance against microbial pathogens in Arabidopsis. *Plant Physiol*, 142, 352-363.

DeFraia, C.T., Wang, Y., Yao, J. and Mou, Z. (2013) Elongator subunit 3 positively regulates plant immunity through its histone acetyltransferase and radical S-adenosylmethionine domains. *BMC Plant Biol*, 13, 102.

Delaney, T.P., Friedrich, L. and Ryals, J.A. (1995) Arabidopsis signal transduction mutant defective in chemically and biologically induced disease resistance. *Proc Natl Acad Sci U S A*, 92, 6602-6606.

Dennis, G., Sherman, B.T., Hosack, D.A., Yang, J., Gao, W., Lane, H.C. and

Lempicki, R.A. (2003) DAVID: database for annotation, visualization, and integrated discovery. *Genome Biol*, 4, R60.

Després, C., Chubak, C., Rochon, A., Clark, R., Bethune, T., Desveaux, D. and Fobert, P.R. (2003) The Arabidopsis NPR1 disease resistance protein is a novel cofactor that confers redox regulation of DNA binding activity to the basic domain/leucine zipper transcription factor TGA1. *Plant Cell*, 15, 2181-2191.

Ding, Y., Sun, T., Ao, K., Peng, Y., Zhang, Y., Li, X. and Zhang, Y. (2018) Opposite roles of salicylic acid receptors NPR1 and NPR3/NPR4 in transcriptional regulation of plant immunity. *Cell*, 173, 1454-1467.e1415.

Dong, O.X., Tong, M., Bonardi, V., El Kasmi, F., Woloshen, V., Wünsch, L.K., Dangl, J.L. and Li, X. (2016) TNL-mediated immunity in Arabidopsis requires complex regulation of the redundant ADR1 gene family. *New Phytol*, 210, 960-973.

Dowen, R.H., Pelizzola, M., Schmitz, R.J., Lister, R., Dowen, J.M., Nery, J.R., Dixon, J.E. and Ecker, J.R. (2012) Widespread dynamic DNA methylation in response to biotic stress. *Proc Natl Acad Sci U S A*, 109, E2183-E2191.

Dutta, A., Choudhary, P., Caruana, J. and Raina, R. (2017) JMJ27, an Arabidopsis H3K9 histone demethylase, modulates defense against Pseudomonas syringae and flowering time. *Plant J*, 91, 1015-1028.

Feng, F., Yang, F., Rong, W., Wu, X., Zhang, J., Chen, S., He, C. and Zhou, J.-M. (2012) A Xanthomonas uridine 5′-monophosphate transferase inhibits plant immune kinases. *Nature*, 485, 114-118.

Fu, Z.Q. and Dong, X. (2013) Systemic acquired resistance: turning local

infection into global defense. *Annu Rev Plant Biol*, 64, 839-863.

Fu, Z.Q., Yan, S., Saleh, A., Wang, W., Ruble, J., Oka, N., Mohan, R., Spoel, S.H., Tada, Y., Zheng, N. et al. (2012) NPR3 and NPR4 are receptors for the immune signal salicylic acid in plants. *Nature*, 486, 228-232.

Gaffney, T., Friedrich, L., Vernooij, B., Negrotto, D., Nye, G., Uknes, S., Ward, E., Kessmann, H. and Ryals, J. (1993) Requirement of salicylic acid for the induction of systemic acquired resistance. *Science*, 261, 754-756.

Gong, B.-Q., Guo, J., Zhang, N., Yao, X., Wang, H.-B. and Li, J.-F. (2019) Cross-microbial protection via priming a conserved immune co-receptor through juxtamembrane phosphorylation in plants. *Cell Host Microbe*, 26, 810-822.e817.

Guan, L., Denkert, N., Eisa, A., Lehmann, M., Sjuts, I., Weiberg, A., Soll, J., Meinecke, M. and Schwenkert, S. (2019) JASSY, a chloroplast outer membrane protein required for jasmonate biosynthesis. *Proc Natl Acad Sci U S A*, 116, 10568-10575.

Halter, T., Imkampe, J., Blaum, B.S., Stehle, T. and Kemmerling, B. (2014) BIR2 affects complex formation of BAK1 with ligand binding receptors in plant defense. *Plant Signal Behav*, 9, e28944.

Hartmann, M., Zeier, T., Bernsdorff, F., Reichel-Deland, V., Kim, D., Hohmann, M., Scholten, N., Schuck, S., Bräutigam, A., Hölzel, T. et al. (2018) Flavin monooxygenase-generated N-hydroxypipecolic acid is a critical element of plant systemic immunity. *Cell*, 173, 456-469.e416.

Heard, E. and Martienssen, Robert A. (2014) Transgenerational epigenetic

inheritance: myths and mechanisms. *Cell*, 157, 95-109.

Hickman, R., Mendes, M.P., Van Verk, M.C., Van Dijken, A.J.H., Di Sora, J., Denby, K., Pieterse, C.M.J. and Van Wees, S.C.M. (2019) Transcriptional dynamics of the salicylic acid response and its interplay with the jasmonic acid pathway. *bioRxiv*, 742742.

Hillmer, R.A., Tsuda, K., Rallapalli, G., Asai, S., Truman, W., Papke, M.D., Sakakibara, H., Jones, J.D.G., Myers, C.L. and Katagiri, F. (2017) The highly buffered Arabidopsis immune signaling network conceals the functions of its components. *PLOS Genet*, 13, e1006639.

Huang, C., Yan, Y., Zhao, H., Ye, Y. and Cao, Y. (2020) Arabidopsis CPK5 phosphorylates the chitin receptor LYK5 to regulate plant innate immunity. *Front Plant Sci*, 11, 702.

Huang, M., Zhang, Y., Wang, Y., Xie, J., Cheng, J., Fu, Y., Jiang, D., Yu, X. and Li, B. (2022) Active DNA demethylation regulates MAMP-triggered immune priming in Arabidopsis. *J Genet Genomics*, 49, 796-809.

Imkampe, J., Halter, T., Huang, S., Schulze, S., Mazzotta, S., Schmidt, N., Manstretta, R., Postel, S., Wierzba, M., Yang, Y. et al. (2017) The Arabidopsis leucine-rich repeat receptor kinase BIR3 negatively regulates BAK1 receptor complex formation and stabilizes BAK1. *Plant Cell*, 29, 2285-2303.

Innes, R.W. (2011) Activation of plant nod-like receptors: how indirect can it be? *Cell Host Microbe*, 9, 87-89.

Jin, H., Choi, S.-M., Kang, M.-J., Yun, S.-H., Kwon, D.-J., Noh, Y.-S. and Noh,

B. (2018) Salicylic acid-induced transcriptional reprogramming by the HAC–NPR1–TGA histone acetyltransferase complex in Arabidopsis. *Nucleic Acids Res*, 46, 11712-11725.

Ju, C., Yoon, G.M., Shemansky, J.M., Lin, D.Y., Ying, Z.I., Chang, J., Garrett, W.M., Kessenbrock, M., Groth, G., Tucker, M.L. et al. (2012) CTR1 phosphorylates the central regulator EIN2 to control ethylene hormone signaling from the ER membrane to the nucleus in Arabidopsis. *Proc Natl Acad Sci U S A*, 109, 19486-19491.

Kang, J., Hwang, J.-U., Lee, M., Kim, Y.-Y., Assmann, S.M., Martinoia, E. and Lee, Y. (2010) PDR-type ABC transporter mediates cellular uptake of the phytohormone abscisic acid. *Proc Natl Acad Sci U S A*, 107, 2355-2360.

Katagiri F., Thilmony R., and He S.Y. (2002) The Arabidopsis thaliana-Pseudomonas syringae interaction. *Arabidopsis Book*, 1, e0039.

Katsir, L., Schilmiller, A.L., Staswick, P.E., He, S.Y. and Howe, G.A. (2008) COI1 is a critical component of a receptor for jasmonate and the bacterial virulence factor coronatine. *Proc Natl Acad Sci U S A*, 105, 7100-7105.

Kazan, K. and Manners, J.M. (2013) MYC2: the master in action. *Mol Plant*, 6, 686-703.

Kim, M.G., da Cunha, L., McFall, A.J., Belkhadir, Y., DebRoy, S., Dangl, J.L. and Mackey, D. (2005) Two Pseudomonas syringae type III effectors inhibit RIN4-regulated basal defense in Arabidopsis. *Cell*, 121, 749-759.

Kim, S., Piquerez, S.J.M., Ramirez-Prado, J.S., Mastorakis, E., Veluchamy, A.,

Latrasse, D., Manza-Mianza, D., Brik-Chaouche, R., Huang, Y., Rodriguez-Granados, N.Y. et al. (2020) GCN5 modulates salicylic acid homeostasis by regulating H3K14ac levels at the 5′ and 3′ ends of its target genes. *Nucleic Acids Res*, 48, 5953-5966.

Kim, Y.-W., Youn, J.-H., Roh, J., Kim, J.-M., Kim, S.-K. and Kim, T.-W. (2022) Brassinosteroids enhance salicylic acid-mediated immune responses by inhibiting BIN2 phosphorylation of clade I TGA transcription factors in Arabidopsis. *Mol Plant*, 15, 991-1007.

Kourelis, J. and van der Hoorn, R.A.L. (2018) Defended to the nines: 25 years of resistance gene cloning identifies nine mechanisms for R protein function. *Plant Cell*, 30, 285-299.

Kucera, M., Isserlin, R., Arkhangorodsky, A. and Bader, G. (2016) AutoAnnotate: a cytoscape app for summarizing networks with semantic annotations. *F1000Res*, 5, 1717.

Kumar, S., Zavaliev, R., Wu, Q., Zhou, Y., Cheng, J., Dillard, L., Powers, J., Withers, J., Zhao, J., Guan, Z. et al. (2022) Structural basis of NPR1 in activating plant immunity. *Nature*, 605, 561-566.

Langmead, B., Trapnell, C., Pop, M. and Salzberg, S.L. (2009) Ultrafast and memory-efficient alignment of short DNA sequences to the human genome. *Genome Biol*, 10, R25.

Lapin, D., Kovacova, V., Sun, X., Dongus, J.A., Bhandari, D., von Born, P., Bautor, J., Guarneri, N., Rzemieniewski, J., Stuttmann, J. et al. (2019) A coevolved EDS1-SAG101-NRG1 module mediates cell death signaling by TIR-

domain immune receptors. *Plant Cell*, 31, 2430-2455.

Lefevere, H., Bauters, L. and Gheysen, G. (2020) Salicylic acid biosynthesis in plants. *Front Plant Sci*, 11, 338.

Lewis, J.D., Lee, A.H.-Y., Hassan, J.A., Wan, J., Hurley, B., Jhingree, J.R., Wang, P.W., Lo, T., Youn, J.-Y., Guttman, D.S. et al. (2013) The Arabidopsis ZED1 pseudokinase is required for ZAR1-mediated immunity induced by the Pseudomonas syringae type III effector HopZ1a. *Proc Natl Acad Sci U S A*, 110, 18722-18727.

Li, D., Liu, R., Singh, D., Yuan, X., Kachroo, P. and Raina, R. (2020) JMJ14 encoded H3K4 demethylase modulates immune responses by regulating defence gene expression and pipecolic acid levels. *New Phytol*, 225, 2108-2121.

Li, H., Handsaker, B., Wysoker, A., Fennell, T., Ruan, J., Homer, N., Marth, G., Abecasis, G., Durbin, R. and Genome Project Data Processing, S. (2009) The sequence alignment/map format and SAMtools. *Bioinformatics*, 25, 2078-2079.

Li, L., Li, M., Yu, L., Zhou, Z., Liang, X., Liu, Z., Cai, G., Gao, L., Zhang, X., Wang, Y. et al. (2014) The FLS2-associated kinase BIK1 directly phosphorylates the NADPH oxidase RbohD to control plant immunity. *Cell Host Microbe*, 15, 329-338.

Li, N., Han, X., Feng, D., Yuan, D. and Huang, L.-J. (2019) Signaling crosstalk between salicylic acid and ethylene/jasmonate in plant defense: do we understand what they are whispering? *Int J Mol Sci*, 20, 671.

Liu, L., Sonbol, F.-M., Huot, B., Gu, Y., Withers, J., Mwimba, M., Yao, J., He,

S.Y. and Dong, X. (2016) Salicylic acid receptors activate jasmonic acid signalling through a non-canonical pathway to promote effector-triggered immunity. *Nature Commun*, 7, 13099.

Liu, N., Xu, Y., Li, Q., Cao, Y., Yang, D., Liu, S., Wang, X., Mi, Y., Liu, Y., Ding, C. et al. (2022) A lncRNA fine-tunes salicylic acid biosynthesis to balance plant immunity and growth. *Cell Host Microbe*, 30, 1124-1138.e1128.

Livak, K.J. and Schmittgen, T.D. (2001) Analysis of relative gene expression data using real-time quantitative PCR and the 2−ΔΔCT method. *Methods*, 25, 402-408.

Li, W., Ma, M., Feng, Y., Li, H., Wang, Y., Ma, Y., Li, M., An, F. and Guo, H. (2015) EIN2-directed translational regulation of ethylene signaling in Arabidopsis. *Cell*, 163, 670-683.

López, A., Ramírez, V., García-Andrade, J., Flors, V. and Vera, P. (2011) The RNA silencing enzyme RNA polymerase V is required for plant immunity. *PLOS Genet*, 7, e1002434.

López Sánchez, A., Stassen, J.H.M., Furci, L., Smith, L.M. and Ton, J. (2016) The role of DNA (de)methylation in immune responsiveness of Arabidopsis. *Plant J*, 88, 361-374.

Love, M.I., Huber, W. and Anders, S. (2014) Moderated estimation of fold change and dispersion for RNA-seq data with DESeq2. *Genome Biol*, 15, 550.

Luna, E., Bruce, T.J.A., Roberts, M.R., Flors, V. and Ton, J. (2011) Next-generation systemic acquired resistance. *Plant Physiol*, 158, 844-853.

Macho, Alberto P. and Zipfel, C. (2014) Plant PRRs and the activation of innate immune signaling. *Mol Cell*, 54, 263-272.

Mackey, D., Holt, B.F., Wiig, A. and Dangl, J.L. (2002) RIN4 Interacts with Pseudomonas syringae type III effector molecules and is required for RPM1-mediated resistance in Arabidopsis. *Cell*, 108, 743-754.

March-Diaz, R., Garcia-Dominguez, M., Lozano-Juste, J., Leon, J., Florencio, F.J. and Reyes, J.C. (2008) Histone H2A.Z and homologues of components of the SWR1 complex are required to control immunity in Arabidopsis. *Plant J*, 53, 475-487.

Martín-Trillo, M. and Cubas, P. (2010) TCP genes: a family snapshot ten years later. *Trends Plant Sci*, 15, 31-39.

Merchante, C., Brumos, J., Yun, J., Hu, Q., Spencer, Kristina R., Enríquez, P., Binder, Brad M., Heber, S., Stepanova, Anna N. and Alonso, Jose M. (2015) Gene-specific translation regulation mediated by the hormone-signaling molecule EIN2. *Cell*, 163, 684-697.

Merico, D., Isserlin, R., Stueker, O., Emili, A. and Bader, G.D. (2010) Enrichment map: a network-based method for gene-set enrichment visualization and interpretation. *PLOS ONE*, 5, e13984.

Mine, A., Nobori, T., Salazar-Rondon, M.C., Winkelmüller, T.M., Anver, S., Becker, D. and Tsuda, K. (2017) An incoherent feed-forward loop mediates robustness and tunability in a plant immune network. *EMBO rep*, 18, 464-476.

Mou, Z., Fan, W. and Dong, X. (2003) Inducers of plant systemic acquired

resistance regulate NPR1 function through redox changes. *Cell*, 113, 935-944.

Mur, L.A.J., Kenton, P., Atzorn, R., Miersch, O. and Wasternack, C. (2006) The outcomes of concentration-specific interactions between salicylate and jasmonate signaling include synergy, antagonism, and oxidative stress leading to cell death. *Plant Physiol*, 140, 249-262.

Návarová, H., Bernsdorff, F., Döring, A.-C. and Zeier, J. (2012) Pipecolic acid, an endogenous mediator of defense amplification and priming, is a critical regulator of inducible plant immunity. *Plant Cell*, 24, 5123-5141.

Nawrath, C., Heck, S., Parinthawong, N. and Métraux, J.-P. (2002) EDS5, an essential component of salicylic acid–dependent signaling for disease resistance in Arabidopsis, is a member of the MATE transporter family. *Plant Cell*, 14, 275-286.

Ngou, B.P.M., Ahn, H.-K., Ding, P. and Jones, J.D.G. (2021) Mutual potentiation of plant immunity by cell-surface and intracellular receptors. *Nature*, 592, 110-115.

Nomoto, M., Skelly, M.J., Itaya, T., Mori, T., Suzuki, T., Matsushita, T., Tokizawa, M., Kuwata, K., Mori, H., Yamamoto, Y.Y. et al. (2021) Suppression of MYC transcription activators by the immune cofactor NPR1 fine-tunes plant immune responses. *Cell Rep*, 37, 110125.

Pajerowska-Mukhtar, K.M., Emerine, D.K. and Mukhtar, M.S. (2013) Tell me more: roles of NPRs in plant immunity. *Trends Plant Sci*, 18, 402-411.

Palma, K., Thorgrimsen, S., Malinovsky, F.G., Fiil, B.K., Nielsen, H.B., Brodersen, P., Hofius, D., Petersen, M. and Mundy, J. (2010) Autoimmunity in Arabidopsis acd11 is mediated by epigenetic regulation of an immune receptor.

PLOS Pathog, 6, e1001137.

Park, S.-W., Kaimoyo, E., Kumar, D., Mosher, S. and Klessig, D.F. (2007) Methyl salicylate is a critical mobile signal for plant systemic acquired resistance. *Science*, 318, 113-116.

Pauwels, L., Barbero, G.F., Geerinck, J., Tilleman, S., Grunewald, W., Pérez, A.C., Chico, J.M., Bossche, R.V., Sewell, J., Gil, E. et al. (2010) NINJA connects the co-repressor TOPLESS to jasmonate signalling. *Nature*, 464, 788-791.

Pavet, V., Quintero, C., Cecchini, N.M., Rosa, A.L. and Alvarez, M.E. (2006) Arabidopsis displays centromeric DNA hypomethylation and cytological alterations of heterochromatin upon attack by Pseudomonas syringae. *Mol Plant Microbe Interact*, 19, 577-587.

Perez, M.F. and Lehner, B. (2019) Intergenerational and transgenerational epigenetic inheritance in animals. *Nat Cell Biol*, 21, 143-151.

Pieterse, C.M.J., Leon-Reyes, A., Van der Ent, S. and Van Wees, S.C.M. (2009) Networking by small-molecule hormones in plant immunity. *Nat Chem Biol*, 5, 308-316.

Potuschak, T., Lechner, E., Parmentier, Y., Yanagisawa, S., Grava, S., Koncz, C. and Genschik, P. (2003) EIN3-dependent regulation of plant ethylene hormone signaling by two Arabidopsis F box proteins: EBF1 and EBF2. *Cell*, 115, 679-689.

Pruitt, R.N., Locci, F., Wanke, F., Zhang, L., Saile, S.C., Joe, A., Karelina, D., Hua, C., Fröhlich, K., Wan, W.-L. et al. (2021) The EDS1–PAD4–ADR1 node mediates Arabidopsis pattern-triggered immunity. *Nature*, 598, 495-499.

Qiao, H., Shen, Z., Huang, S.-s.C., Schmitz, R.J., Urich, M.A., Briggs, S.P. and Ecker, J.R. (2012) Processing and subcellular trafficking of ER-tethered EIN2 control response to ethylene gas. *Science*, 338, 390-393.

Quinlan, A.R. and Hall, I.M. (2010) BEDTools: a flexible suite of utilities for comparing genomic features. *Bioinformatics*, 26, 841-842.

Rasmann, S., De Vos, M., Casteel, C.L., Tian, D., Halitschke, R., Sun, J.Y., Agrawal, A.A., Felton, G.W. and Jander, G. (2012) Herbivory in the previous generation primes plants for enhanced insect resistance. *Plant Physiol*, 158, 854-863.

Rietz, S., Stamm, A., Malonek, S., Wagner, S., Becker, D., Medina-Escobar, N., Corina Vlot, A., Feys, B.J., Niefind, K. and Parker, J.E. (2011) Different roles of enhanced disease susceptibility1 (EDS1) bound to and dissociated from phytoalexin deficient4 (PAD4) in Arabidopsis immunity. *New Phytol*, 191, 107-119.

Ryals, J., Lawton, K.A., Delaney, T.P., Friedrich, L., Kessmann, H., Neuenschwander, U., Uknes, S., Vernooij, B. and Weymann, K. (1995) Signal transduction in systemic acquired resistance. *Proc Natl Acad Sci U S A*, 92, 4202-4205.

Saleh, A., Alvarez-Venegas, R. and Avramova, Z. (2008) An efficient chromatin immunoprecipitation (ChIP) protocol for studying histone modifications in Arabidopsis plants. *Nat Protoc*, 3, 1018-1025.

Saleh, A., Withers, J., Mohan, R., Marqués, J., Gu, Y., Yan, S., Zavaliev, R., Nomoto, M., Tada, Y. and Dong, X. (2015) Posttranslational modifications of the master transcriptional regulator NPR1 enable dynamic but tight control of plant

immune responses. *Cell Host Microbe*, 18, 169-182.

Sarris, Panagiotis F., Duxbury, Z., Huh, Sung U., Ma, Y., Segonzac, C., Sklenar, J., Derbyshire, P., Cevik, V., Rallapalli, G., Saucet, Simon B. et al. (2015) A plant immune receptor detects pathogen effectors that target WRKY transcription factors. *Cell*, 161, 1089-1100.

Schaller, F., Biesgen, C., Mussig, C., Altmann, T. and Weiler, E.W. (2000) 12-oxophytodienoate reductase 3 (OPR3) is the isoenzyme involved in jasmonate biosynthesis. *Planta*, 210, 979-984.

Seo, J.S., Diloknawarit, P., Park, B.S. and Chua, N.H. (2019) ELF18-INDUCED LONG NONCODING RNA 1 evicts fibrillarin from mediator subunit to enhance PATHOGENESIS-RELATED GENE 1 (PR1) expression. *New Phytol*, 221, 2067-2079.

Seo, J.S., Sun, H.-X., Park, B.S., Huang, C.-H., Yeh, S.-D., Jung, C. and Chua, N.-H. (2017) ELF18-INDUCED LONG-NONCODING RNA associates with mediator to enhance expression of innate immune response genes in Arabidopsis. *Plant Cell*, 29, 1024-1038.

Shah, J., Tsui, F. and Klessig, D.F. (1997) Characterization of a salicylic acid-insensitive mutant (sai1) of Arabidopsis thaliana, identified in a selective screen utilizing the SA-inducible expression of the tms2 gene. *Mol Plant Microbe Interact*, 10, 69-78.

Shearer, H.L., Wang, L., DeLong, C., Despres, C. and Fobert, P.R. (2009) NPR1 enhances the DNA binding activity of the Arabidopsis bZIP transcription factor TGA7. *Botany*, 87, 561-570.

Simon, C., Langlois-Meurinne, M., Didierlaurent, L., Chaouch, S., Bellvert, F., Massoud, K., Garmier, M., Thareau, V., Comte, G., Noctor, G. et al. (2014) The secondary metabolism glycosyltransferases UGT73B3 and UGT73B5 are components of redox status in resistance of Arabidopsis to Pseudomonas syringae pv. tomato. *Plant Cell Environ*, 37, 1114-1129.

Singh, P., Yekondi, S., Chen, P.-W., Tsai, C.-H., Yu, C.-W., Wu, K. and Zimmerli, L. (2014) Environmental History Modulates Arabidopsis pattern-triggered immunity in a HISTONE ACETYLTRANSFERASE1–dependent manner. *Plant Cell*, 26, 2676-2688.

Slaughter, A., Daniel, X., Flors, V., Luna, E., Hohn, B. and Mauch-Mani, B. (2012) Descendants of primed arabidopsis plants exhibit resistance to biotic stress. *Plant Physiol*, 158, 835-843.

Song, S., Huang, H., Gao, H., Wang, J., Wu, D., Liu, X., Yang, S., Zhai, Q., Li, C., Qi, T. et al. (2014) Interaction between MYC2 and ETHYLENE INSENSITIVE3 modulates antagonism between jasmonate and ethylene signaling in Arabidopsis. *Plant Cell*, 26, 263-279.

Spoel, S.H., Mou, Z., Tada, Y., Spivey, N.W., Genschik, P. and Dong, X. (2009) Proteasome-mediated turnover of the transcription coactivator NPR1 plays dual roles in regulating plant immunity. *Cell*, 137, 860-872.

Stassen, J.H.M., López, A., Jain, R., Pascual-Pardo, D., Luna, E., Smith, L.M. and Ton, J. (2018) The relationship between transgenerational acquired resistance and global DNA methylation in Arabidopsis. *Sci Rep*, 8, 14761.

Stegmann, M., Monaghan, J., Smakowska-Luzan, E., Rovenich, H., Lehner, A.,

Holton, N., Belkhadir, Y. and Zipfel, C. (2017) The receptor kinase FER is a RALF-regulated scaffold controlling plant immune signaling. *Science*, 355, 287-289.

Sun, X., Lapin, D., Feehan, J.M., Stolze, S.C., Kramer, K., Dongus, J.A., Rzemieniewski, J., Blanvillain-Baufumé, S., Harzen, A., Bautor, J. et al. (2021) Pathogen effector recognition-dependent association of NRG1 with EDS1 and SAG101 in TNL receptor immunity. *Nature Commun*, 12, 3335.

Thines, B., Katsir, L., Melotto, M., Niu, Y., Mandaokar, A., Liu, G., Nomura, K., He, S.Y., Howe, G.A. and Browse, J. (2007) JAZ repressor proteins are targets of the SCF^{COI1} complex during jasmonate signalling. *Nature*, 448, 661-665.

Tian, W., Hou, C., Ren, Z., Wang, C., Zhao, F., Dahlbeck, D., Hu, S., Zhang, L., Niu, Q., Li, L. et al. (2019) A calmodulin-gated calcium channel links pathogen patterns to plant immunity. *Nature*, 572, 131-135.

Torrens-Spence, M.P., Bobokalonova, A., Carballo, V., Glinkerman, C.M., Pluskal, T., Shen, A. and Weng, J.-K. (2019) PBS3 and EPS1 complete salicylic acid biosynthesis from isochorismate in Arabidopsis. *Mol Plant*, 12, 1577-1586.

Torres, M.A., Dangl, J.L. and Jones, J.D.G. (2002) Arabidopsis gp91phox homologues AtrbohD and AtrbohF are required for accumulation of reactive oxygen intermediates in the plant defense response. *Proc Natl Acad Sci U S A*, 99, 517-522.

van der Hoorn, R.A.L. and Kamoun, S. (2008) From guard to decoy: a new model for perception of plant pathogen effectors. *Plant Cell*, 20, 2009-2017.

Vernooij, B., Friedrich, L., Morse, A., Reist, R., Kolditz-Jawhar, R., Ward, E., Uknes, S., Kessmann, H. and Ryals, J. (1994) Salicylic acid is not the translocated signal responsible for inducing systemic acquired resistance but is required in signal transduction. *Plant Cell*, 6, 959-965.

Walley, J.W., Rowe, H.C., Xiao, Y., Chehab, E.W., Kliebenstein, D.J., Wagner, D. and Dehesh, K. (2008) The chromatin remodeler SPLAYED regulates specific stress signaling pathways. *PLoS Pathog*, 4, e1000237.

Wang, C., El-Shetehy, M., Shine, M.B., Yu, K., Navarre, D., Wendehenne, D., Kachroo, A. and Kachroo, P. (2014) Free radicals mediate systemic acquired resistance. *Cell Rep*, 7, 348-355.

Wang, C., Liu, R., Lim, G.-H., de Lorenzo, L., Yu, K., Zhang, K., Hunt, A.G., Kachroo, A. and Kachroo, P. (2018) Pipecolic acid confers systemic immunity by regulating free radicals. *Sci Adv*, 4, eaar4509.

Wang, D., Amornsiripanitch, N. and Dong, X. (2006) A genomic approach to identify regulatory nodes in the transcriptional network of systemic acquired resistance in plants. *PLOS Pathog*, 2, e123.

Wang, G., Roux, B., Feng, F., Guy, E., Li, L., Li, N., Zhang, X., Lautier, M., Jardinaud, M.-F., Chabannes, M. et al. (2015) The decoy substrate of a pathogen effector and a pseudokinase specify pathogen-induced modified-self recognition and immunity in plants. *Cell Host Microbe*, 18, 285-295.

Wang, J., Hu, M., Wang, J., Qi, J., Han, Z., Wang, G., Qi, Y., Wang, H.-W., Zhou, J.-M. and Chai, J. (2019) Reconstitution and structure of a plant NLR resistosome conferring immunity. *Science*, 364, eaav5870.

Wang, Y., Hu, Q., Wu, Z., Wang, H., Han, S., Jin, Y., Zhou, J., Zhang, Z., Jiang, J., Shen, Y. et al. (2017) HISTONE DEACETYLASE 6 represses pathogen defence responses in Arabidopsis thaliana. *Plant Cell Environ*, 40, 2972-2986.

Wani, S.H., Anand, S., Singh, B., Bohra, A. and Joshi, R. (2021) WRKY transcription factors and plant defense responses: latest discoveries and future prospects. *Plant Cell Rep*, 40, 1071-1085.

Weigel, R.R., Pfitzner, U.M. and Gatz, C. (2005) Interaction of NIMIN1 with NPR1 modulates PR gene expression in Arabidopsis. *Plant Cell*, 17, 1279-1291.

Wildermuth, M.C., Dewdney, J., Wu, G. and Ausubel, F.M. (2001) Isochorismate synthase is required to synthesize salicylic acid for plant defence. *Nature*, 414, 562-565.

Wu, K., Zhang, L., Zhou, C., Yu, C.-W. and Chaikam, V. (2008) HDA6 is required for jasmonate response, senescence and flowering in Arabidopsis. *J Exp Bot*, 59, 225-234.

Wu, Y., Zhang, D., Chu, Jee Y., Boyle, P., Wang, Y., Brindle, Ian D., De Luca, V. and Després, C. (2012) The Arabidopsis NPR1 protein is a receptor for the plant defense hormone salicylic acid. *Cell Rep*, 1, 639-647.

Xia, S., Cheng, Y.T., Huang, S., Win, J., Soards, A., Jinn, T.-L., Jones, J.D.G., Kamoun, S., Chen, S., Zhang, Y. et al. (2013) Regulation of transcription of nucleotide-binding leucine-rich repeat-encoding genes SNC1 and RPP4 via H3K4 trimethylation. *Plant Physiol*, 162, 1694-1705.

Xin, X.F., Kvitko, B. and He, S.Y. (2018) Pseudomonas syringae: what it takes to

be a pathogen. *Nat Rev Microbiol*, 16, 316-328.

Xin, X.-F., Nomura, K., Aung, K., Velásquez, A.C., Yao, J., Boutrot, F., Chang, J.H., Zipfel, C. and He, S.Y. (2016) Bacteria establish an aqueous living space in plants crucial for virulence. *Nature*, 539, 524-529.

Yalpani, N., Silverman, P., Wilson, T.M., Kleier, D.A. and Raskin, I. (1991) Salicylic acid is a systemic signal and an inducer of pathogenesis-related proteins in virus-infected tobacco. *Plant Cell*, 3, 809-818.

Yan, J., Zhang, C., Gu, M., Bai, Z., Zhang, W., Qi, T., Cheng, Z., Peng, W., Luo, H., Nan, F. et al. (2009) The Arabidopsis CORONATINE INSENSITIVE1 protein is a jasmonate receptor. *Plant Cell*, 21, 2220-2236.

Yu, A., Lepère, G., Jay, F., Wang, J., Bapaume, L., Wang, Y., Abraham, A.-L., Penterman, J., Fischer, R.L., Voinnet, O. et al. (2013b) Dynamics and biological relevance of DNA demethylation in Arabidopsis antibacterial defense. *Proc Natl Acad Sci U S A*, 110, 2389-2394.

Yu, G., Wang, L.-G. and He, Q.-Y. (2015) ChIPseeker: an R/Bioconductor package for ChIP peak annotation, comparison and visualization. *Bioinformatics*, 31, 2382-2383.

Yu, K., Soares, Juliana M., Mandal, Mihir K., Wang, C., Chanda, B., Gifford, Andrew N., Fowler, Joanna S., Navarre, D., Kachroo, A. and Kachroo, P. (2013a) A feedback regulatory loop between G3P and lipid transfer proteins DIR1 and AZI1 mediates azelaic-acid-induced systemic immunity. *Cell Rep*, 3, 1266-1278.

Yuan, M., Jiang, Z., Bi, G., Nomura, K., Liu, M., Wang, Y., Cai, B., Zhou, J.-M., He, S.Y. and Xin, X.-F. (2021) Pattern-recognition receptors are required for NLR-mediated plant immunity. *Nature*, 592, 105-109.

Yun, S.-H., Noh, B. and Noh, Y.-S. (2022) Negative evidence on the transgenerational inheritance of defense priming in Arabidopsis thaliana. *BMB rep*, 55, 342-347.

Zhang, X., Ménard, R., Li, Y., Coruzzi, G.M., Heitz, T., Shen, W.-H. and Berr, A. (2020) Arabidopsis SDG8 potentiates the sustainable transcriptional induction of the pathogenesis-related genes PR1 and PR2 during plant defense response. *Front Plant Sci*, 11, 277.

Zhang, Y., Fan, W., Kinkema, M., Li, X. and Dong, X. (1999) Interaction of NPR1 with basic leucine zipper protein transcription factors that bind sequences required for salicylic acid induction of the PR-1 gene. *Proc Natl Acad Sci U S A*, 96, 6523-6528.

Zhang, Y., Liu, T., Meyer, C.A., Eeckhoute, J., Johnson, D.S., Bernstein, B.E., Nusbaum, C., Myers, R.M., Brown, M., Li, W. et al. (2008) Model-based Analysis of ChIP-Seq (MACS). *Genome Biol*, 9, R137.

Zhang, Y., Xu, S., Ding, P., Wang, D., Cheng, Y.T., He, J., Gao, M., Xu, F., Li, Y., Zhu, Z. et al. (2010) Control of salicylic acid synthesis and systemic acquired resistance by two members of a plant-specific family of transcription factors. *Proc Natl Acad Sci U S A*, 107, 18220-18225.

Zhou, C., Zhang, L., Duan, J., Miki, B. and Wu, K. (2005) HISTONE DEACETYLASE19 is involved in jasmonic acid and ethylene signaling of

pathogen response in Arabidopsis. *Plant Cell*, 17, 1196-1204.

Zhou, J., Wang, X., He, Y., Sang, T., Wang, P., Dai, S., Zhang, S. and Meng, X. (2020) Differential phosphorylation of the transcription factor WRKY33 by the protein kinases CPK5/CPK6 and MPK3/MPK6 cooperatively regulates camalexin biosynthesis in Arabidopsis. *Plant Cell*, 32, 2621-2638.

Zhou, J.-M., Trifa, Y., Silva, H., Pontier, D., Lam, E., Shah, J. and Klessig, D.F. (2000) NPR1 differentially interacts with members of the TGA/OBF family of transcription factors that bind an element of the PR-1 gene required for induction by salicylic acid. *Mol Plant Microbe Interact*, 13, 191-202.

Zhu, Z., An, F., Feng, Y., Li, P., Xue, L., A, M., Jiang, Z., Kim, J.-M., To, T.K., Li, W. et al. (2011) Derepression of ethylene-stabilized transcription factors (EIN3/EIL1) mediates jasmonate and ethylene signaling synergy in Arabidopsis. *Proc Natl Acad Sci U S A*, 108, 12539-12544.

국문 초록

고착 생활을 하는 식물은 일생 동안 끊임없이 병원균들에 의한 공격에 노출된다. 식물은 다양한 식물성 병원균들로부터 스스로를 방어하기 위하여 정교한 선천 면역(innate immunity)과 유도 면역(induced immunity)을 발달시켜 왔다. 식물에 침입한 병원균이 세포막 수용체 또는 세포 내 수용체에 의해 인식되면 국소 면역(local immunity)이 유발된다. 식물은 국소 면역을 활성화시킬 뿐만 아니라 전신 면역(systemic immunity)을 확립하는데, 전신 면역은 오래 지속되면서도 식물에 감염된 병원균 외 다른 병원균들에 대한 저항성을 부여한다. 살리실산(salicylic acid)은 국소 면역과 전신 면역을 모두 조절하는 식물 호르몬 중 하나이다. 살리실산은 병원균이 감염된 국소 조직에서 전사 재프로그래밍(transcriptional reprogramming)을 유도하고, 이를 통하여 활물영양성 병원균(biotrophic pathogen)과 반활물영양성 병원균(hemibiotrophic pathogen)에 대한 면역이 유발된다. 식물이 병원균에 감염된 이후 살리실산의 양은 병원균 감염에 노출되지 않은 원위 조직 내에서도 증가하며, 이를 통해 전신 획득 저항성(systemic acquired resistance)이 확립된다. 전신 획득 저항성이 확립될 경우 식물은 이차 감염 시 보다 신속하고 강력한 면역 반응을 유도할 수 있는 준비 상태가 되는데, 이러한 현상을 defense priming이라고 한다. 살리실산에 의해 유도된 전사 재프로그래밍과 면역

관련 유전자들의 priming 과정에는 후성유전학적 메커니즘(epigenetic mechanism)이 관여하는데, 후성유전학적 메커니즘은 염색질 구조와 염색질에 대한 전사 인자들의 접근성을 조절한다. 많은 연구 결과들이 식물 면역에서 후성유전학적 조절이 중요함을 보여주고 있다.

본 연구에서는 애기장대 면역의 전사 및 후성유전학적 조절에 관한 두 가지 주제를 다룬다. 첫 번째 연구에서는 defense priming의 transgenerational epigenetic inheritance에 대한 반증을 제시하였다. 과거에 부모 식물의 defense priming이 자손에게 유전될 수 있다는 사실이 관찰된 바 있다. 본 연구에서는 defense priming의 transgenerational epigenetic inheritance를 가능하게 하는 후성유전학적 메커니즘을 규명하는 것을 목적으로 수립하였고, 먼저 애기장대에서 transgenerational defense priming 여부를 엄밀한 기준에서 재평가하였다. Defense priming이 진정한 transgenerational epigenetic inheritance를 통하여 부모 세대에서 자손 세대로 전달되는지 명확하게 하기 위해서, 영양 생장(vegetative growth) 또는 생식 생장(reproductive growth) 단계에 있는 부모 식물을 세균성 병원체에 반복적으로 감염시켰다. 부모 세대의 식물들이 병원균에 감염되는 기간 동안 생식 세포(gametes)를 형성하였는지 여부와 관계없이, 자손 세대에서 세균성 병원체에 대한 식물들의 저항성은 향상되지 않았다. 병원체로부터 주어지는 스트레스의 수준에 변화를 주기 위해서 병원균을 서로 다른 방법으로 부모 식물에 감염시킨 경우에도 동일한 결과들이 확인되었다. 이러한 결과는 애기장대에서

defense priming의 transgenerational epigenetic inheritance가 가능하다고 밝힌 이전의 연구 결과들과 상반된다. 따라서 식물에서 transgenerational defense priming 여부는 철저하게 재평가되어야 한다.

두 번째 연구에서는 살리실산에 의해 유발되는 면역에서 NONEXPRESSER OF PATHOGENESIS-RELATED GENES1 (NPR1)이 수행하는 역할을 전장 유전체 수준에서 연구하였고, 그 결과들을 개괄적으로 제시하였다. 살리실산은 전사 재프로그래밍을 통해서 면역을 유발한다. NPR1은 살리실산 수용체 및 transcriptional co-activator로 작용하므로, 살리실산에 의해 유도되는 전사 재프로그래밍은 대부분 NPR1에 의해서 조절이 되는데, 이는 NPR1이 살리실산에 의해 유발되는 면역의 핵심 조절자임을 의미한다. 본 연구에서는 살리실산 신호에 특이적인 NPR1의 직접 타겟 유전자들을 전장 유전체 수준에서 발굴하였으며, *NPR1* 의존적으로 발현이 조절되는 NPR1 타겟 유전자들과 연관된 생물학적, 분자적 기능들이 무엇인지 분석하였다. 살리실산 신호에 의존적으로 이루어지는 NPR1 타겟팅은 주로 다양한 전사 인자들을 암호화하는 유전자들의 전사 활성화를 유도하였고, 이를 통하여 전사 cascades(transcriptional cascades)가 유발됨으로써 전사 재프로그래밍이 발생하였다. 더 나아가 본 연구에서는 NPR1과 NPR1의 결합 파트너인 HISTONE ACETYLTRANSFERASE OF THE CBP FAMILY1 (HAC1) 및 TGACG-모티프에 결합하는 전사 인자들(TGACG-motif binding

transcription factors; TGAs)의 협력적 작용을 전장 유전체 수준에서 연구하였다. HAC1 타겟 유전자군 및 살리실산 신호의 존재 하에서 NPR1과 HAC1이 공통적으로 타겟팅되는 유전자군을 발굴하였으며, NPR1과 HAC1이 공통 타겟 유전자군에 속한 일부 유전자들을 대상으로 살리실산에 의해 유도되는 히스톤 H3 아세틸화(H3Ac) 및 유전자 발현의 증가를 조절함을 밝혀내었다. 또한 NPR1이 타겟팅되는 유전체 내 영역들 가운데 가장 많이 존재하는 DNA 서열이 TGACG 모티프임을 발견하였으며, TGA2가 실제로 TGACG 모티프를 가진 NPR1 타겟팅 영역에 결합함을 증명하였다. 이는 전장 유전체 수준에서 NPR1 타겟팅이 주로 TGAs에 의해 매개됨을 의미한다. 마지막으로 본 연구에서는 기저 상태에서 NPR1이 미리 타겟팅되어 있는 유전자들의 발현이 살리실산 신호가 주어질 경우에만 NPR1이 타겟팅되는 유전자들의 발현에 비해서 살리실산 신호가 활성화된 이후 더 신속하고, 크게 증가함을 발견하였다. 결론적으로, 이 연구는 살리실산 신호가 활성화되었을 시 전사 재프로그래밍을 유도하기 위해서 NPR1이 수행하는 역할과 NPR1, HAC1 및 TGAs의 협력적 작용을 전체적인 관점에서 보여준다.

주요어 : Defense priming, Transgenerational epigenetic inheritance, 살리실산-유도 전사 재프로그래밍, NPR1, HAC1, TGAs

학 번 : 2013-20307